



# HHS Public Access

Author manuscript

*Chem Rev.* Author manuscript; available in PMC 2024 May 24.

Published in final edited form as:

*Chem Rev.* 2023 May 24; 123(10): 6612–6667. doi:10.1021/acs.chemrev.2c00649.

## Next Generation Gold Drugs and Probes: Chemistry and Biomedical Applications

**R. Tyler Mertens,**

Department of Chemistry, University of Kentucky, Lexington, Kentucky 40506, United States

**Sailajah Gukathasan,**

Department of Chemistry, University of Kentucky, Lexington, Kentucky 40506, United States

**Adedamola S. Arojojoye,**

Department of Chemistry, University of Kentucky, Lexington, Kentucky 40506, United States

**Chibuzor Olelewe,**

Department of Chemistry, University of Kentucky, Lexington, Kentucky 40506, United States

**Samuel G. Awuah**

Department of Chemistry, University of Kentucky, Lexington, Kentucky 40506, United States

Department of Pharmaceutical Sciences, College of Pharmacy, University of Kentucky, Lexington, Kentucky 40536, United States

University of Kentucky Markey Cancer Center, Lexington, Kentucky 40536, United States

### Abstract

The gold drugs, gold sodium thiomalate (Myocrisin), aurothioglucose (Solganal), and the orally administered auranofin (Ridaura), are utilized in modern medicine for the treatment of inflammatory arthritis including rheumatoid and juvenile arthritis; however, new gold agents have been slow to enter the clinic. Repurposing of auranofin in different disease indications such as cancer, parasitic, and microbial infections in the clinic has provided impetus for the development of new gold complexes for biomedical applications based on unique mechanistic insights differentiated from auranofin. Various chemical methods for the preparation of physiologically stable gold complexes and associated mechanisms have been explored in biomedicine such as therapeutics or chemical probes. In this Review, we discuss the chemistry of next generation gold drugs, which encompasses oxidation states, geometry, ligands, coordination, and organometallic compounds for infectious diseases, cancer, inflammation, and as tools for chemical biology

---

**Corresponding Author: Samuel G. Awuah** – Department of Chemistry, University of Kentucky, Lexington, Kentucky 40506, United States; Department of Pharmaceutical Sciences, College of Pharmacy, University of Kentucky, Lexington, Kentucky 40536, United States; University of Kentucky Markey Cancer Center, Lexington, Kentucky 40536, United States; awuah@uky.edu.

Author Contributions

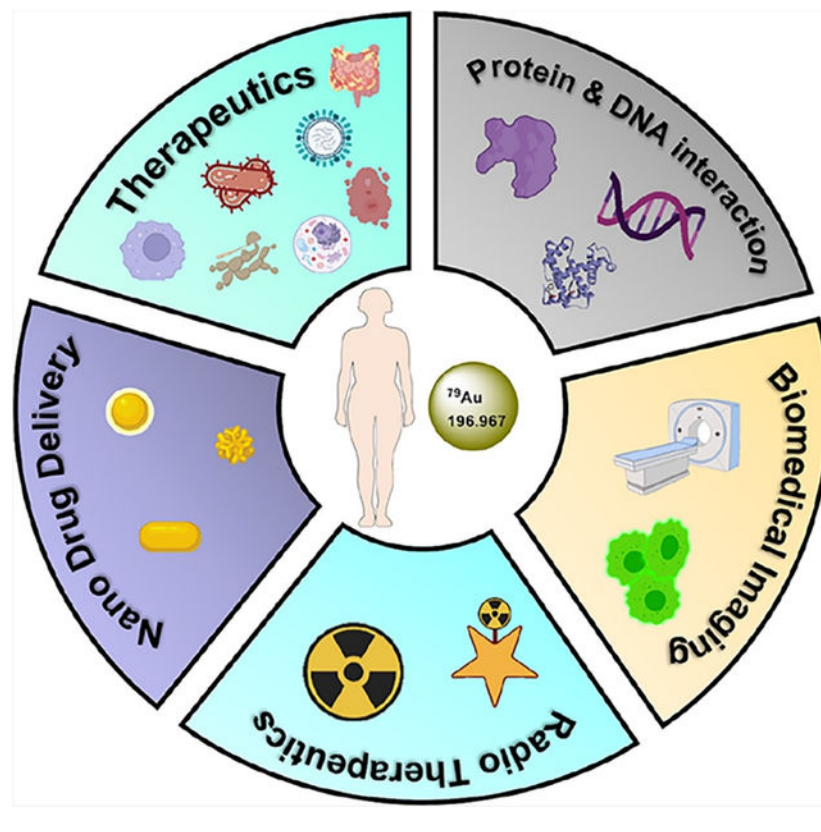
CRedit: **Randall Tyler Mertens** conceptualization, writing-original draft, writing-review & editing; **Sailajah Gukathasan** conceptualization, formal analysis, software, writing-original draft, writing-review & editing; **Adedamola S. Arojojoye** formal analysis, software, writing-original draft, writing-review & editing; **Chibuzor Olelewe** formal analysis, software, writing-review & editing.

The authors declare the following competing financial interest(s): Samuel G. Awuah has patents pending to University of Kentucky Research Foundation.

Complete contact information is available at: <https://pubs.acs.org/10.1021/acs.chemrev.2c00649>

via gold–protein interactions. We will focus on the development of gold agents in biomedicine within the past decade. The Review provides readers with an accessible overview of the utility, development, and mechanism of action of gold-based small molecules to establish context and basis for the thriving resurgence of gold in medicine.

## Graphical Abstract



## 1. INTRODUCTION

Gold (Au)-containing compounds represent an attractive class of therapeutic agents and probes in chemical biology. The clinically approved Au agents for the treatment of rheumatoid arthritis and the rich history of Au in medicine, spanning several millennia, continue to ignite new research avenues toward the development of biologically relevant Au-based compounds. Major developments of Au-based therapeutic agents were reviewed in this Journal in 1999 by Frank Shaw,<sup>1</sup> who highlighted key milestones achieved by the development of Au agents. Other significant contributions summarizing specific areas of Au-based biological reagents or mode of action have also been reported.<sup>1–11</sup> Over the past two decades, essential aspects of the mechanism of action and new therapeutic Au compounds for different diseases have been unraveled, which will be the focus of this Chemical Review.

Au is characterized by unique chemical and physical properties that influence its reactivity and biocompatibility. Unusual relativistic effects of Au distinguish it from other transition

metals including neighboring Group 11 Cu and Ag atoms.<sup>12,13</sup> Consequently, Au possesses high ionization potential of ~2 eV due to a large 6s-orbital contraction.<sup>14,15</sup> This direct relativistic contraction effect is orchestrated by relativistic perturbation operators that impact the regions of the nucleus and simultaneously affect the density of *s*-electrons within the valence shell, leading to an increase in the square of the nuclear charge (*Z*). Although *s*-contraction and stabilization factors lead to an increased first ionization potential (IP) and electron affinity (EA) for all Group 11 elements, relativistic effects substantially elevate the overall electronegativity (i.e.,  $\lambda\text{IP} + \lambda\text{EA}$ ) of Au close to that of iodine (EN = 2.2).<sup>15</sup> Au is therefore an electronegative transition metal and often referred to as a pseudohalide. The relativistic effects described have implications on atomic, molecular, bonding, and electrochemical behavior of Au that result in its broad utility in biology and medicine. For a more focused work on the relativistic effects of Au in catalysis<sup>16</sup> and materials, readers may refer to ref 17.

Over the course of history, dating back to ancient Egypt,<sup>18,19</sup> the medicinal value of Au has gained enormous traction, evolved in its synthetic development, and biological utility (Figure 1).<sup>20–24</sup> Advanced gold-containing prescriptions in Zixue dan and Zhibao dan exhibit activity to treat high body temperature and measles within the Han and Qing Dynasty of China.<sup>23</sup>

Arnald of Villanova's discovery of the *Aurum potabile* recipe to treat melancholy, although imaginary, shed light on gold therapy in the 1300s.<sup>25</sup> Further use of this concoction continued through the 17th century, as many proclaimed alchemists fancied the use of *Aurum potabile*.<sup>26–28</sup> One such medical skeptic, Paracelsus, prescribed this gold-based mixture again for the use of melancholy, as it "made one's heart happy".<sup>29</sup> As the 17th century approached, many medical iconoclasts became skeptical of chemically prepared medicines and touted the use of gold for medicinal applications as dangerous. Nevertheless, gold entered the "*Pharmacopeia Londinensis*" drug compendia in the 17th century.<sup>30,31</sup> Keeley's proposition to cure alcoholism by gold therapy was not effective. Using sodium salt of gold chloride for the treatment of syphilis advanced development of gold-based therapeutics beyond alchemy in the late 19th century.<sup>32</sup> Rational gold therapy came to light with the demonstration of antibacterial activity of gold cyanide  $\text{K}[\text{Au}(\text{CN})_2]$  by the German Robert Koch in 1895. Further, Forestier's discovery that gold complexes exhibit antiarthritic activity brought renewed interest in gold medicine.<sup>33–36</sup> All these scientific innovations led to the development of gold thiolate compounds that were developed along with myochrysin, allochrysin, solganal, and sanochrysin (Chart 1).<sup>1,37–42</sup> Since then, numerous developments in synthetic strategies have been employed to establish novel gold complexes for a plethora of disease treatments.<sup>1,4,5,22,43–49</sup>

For improved chrysotherapy (the use of gold salt for treatment of diseases) that is specific for rheumatoid arthritis (RA), Sutton and co-workers first reported the synthesis of 2,3,4,6-tetra-*O*-acetyl-1-thio- $\beta$ -D-glucopyranosato-*S*-(triethylphosphine) gold (auranofin) in 1972.<sup>50,51</sup> The efficacious antiarthritic properties and the oral administration of auranofin led to its approval in 1985 by the FDA.<sup>10,52,53</sup> Despite its current use as a second-line therapy for RA, the well-established safety profile in humans makes auranofin a useful candidate for other common and rare diseases in the context of drug repurposing.<sup>54–58</sup>

Drug repurposing leverages new knowledge from unraveled molecular basis of diseases and FDA approved medication for translational therapeutic benefit.<sup>59</sup> Auranofin is a viable drug for repurposing due to its ability to potentiate thiol-related redox homeostasis and lower inflammation. Recent clinical trials outline 14 studies that involve auranofin for the treatment of different diseases including HIV, cancer, pain syndrome, Giardia Protozoa, tuberculosis, and combination therapy for rheumatoid arthritis.<sup>10,36,50,53,60–62</sup> These studies cover different clinical phases and across multiple continents (Figure 2). In addition to emphasizing the wide range of therapeutic benefits, auranofin offers decreased costs for discovery of novel medicine, a faster pace of drug discovery and development, and lower attrition rate. Inspired by auranofin's success, gold-based drug discovery has garnered enormous attention with important contributions, but challenges remain. In this Review, we present recent developments of gold-based therapeutics and probes, mechanisms-of-action, and challenges that need to be addressed as well as innovative chemical strategies to circumvent these challenges toward a fuller biomedical potential.

## 2. SCOPE OF REVIEW AND ORGANIZATION

The high proliferation of gold-based reagents has led to important biomedical discoveries with diverse mechanisms and those yet to be unraveled. Our discussion will begin with a brief assessment of the mechanism-of-action of gold agents for disease treatment. The goal is to articulate fundamental mechanistic insights for in-depth descriptions during this Review. Au(I) complexes such as auranofin are soft and polarizable with affinity for soft nucleophilic amino acid side chains in proteins. Therefore, stable, and irreversible adducts are a result of Au(I)–protein interactions. We expand this discussion to other gold complexes that interact with proteins to form gold–protein adducts that offer structural and biophysical insights into gold–protein interactions and can lead to understanding cellular mechanisms for disease treatment. Attempts to tune gold compounds to target DNA and DNA-related processes are also expounded. This section is followed by target identification strategies to address potential biological target(s) of gold complexes. We then discuss the impact of gold agents on molecular imaging, radiodiagnostics, and radiotherapy, followed by therapeutic gold compounds that elucidates approved drugs, targeted agents, and mechanisms. We will cover Au(I) complexes and their utility as potential drugs in different diseases. Here, idiosyncratic mechanisms that result in treatment *in vitro* and preclinical models will be addressed. The burgeoning field of Au(III) for disease treatment will also be discussed along with potential biological targets that have been elucidated to date. Finally, we will address targeting modalities and nanodelivery approaches of biologically active gold compounds.

## 3. MECHANISM OF ACTION

The main mechanism of gold action has been a subject of scrutiny over many decades by scientists of multidisciplinary backgrounds. Recent advances in Cryo-electron microscopy, crystallography, bioorthogonal chemistry, affinity labeling, and chemical proteomics have led to target identification and an unbiased mode of action,<sup>63–69</sup> which is sometimes enigmatic. The polarized character of Au(I) complexes renders them highly thio- and selenophilic. Thus, enzymes with cysteine and selenocysteine residues within the active site are



favorable targets for gold ligation. Readers may refer to other comprehensive reviews and perspectives on gold–sulfur interactions.<sup>70–73</sup>

An earlier report on the uptake of auranofin used the everted sac model of intestinal absorption. Auranofin was incubated with the everted sac, and the gold concentration in the sac after 2 h of incubation was found to be about 20% of the incubation media showing that gold passes through the intestinal wall, although this study suggests that it is the deacetylated form of auranofin that passes through the wall and not auranofin itself.<sup>74</sup> Another study indicates that rather than through a transmucosal absorption, auranofin is absorbed via the enteric cell surface.<sup>75</sup> The entry of auranofin in cells is by interaction with the phospholipid bilayer largely through a passive uptake profile.<sup>76</sup> Active transport by interrogating ion channels and membrane proteins remains a possibility but unexplored. Snyder et al. proposed a ligand exchange shuttle mechanism that is different from the traditional active or passive transport for uptake of auranofin and other gold-based complexes. This model proposes that uptake is dependent on ligand selectivity for thiol groups based on their relative affinities, lipophilicity, charge, and steric factors.<sup>77</sup> Within the cell, auranofin interacts with oxidoreductases (redox enzymes) including thioredoxin reductase (TrxR) and trypanothione reductase through substitution by cysteine or selenocysteine amino acid residues within the enzyme active site.<sup>78,79</sup> Structural evidence by protein X-ray crystallography demonstrates that the linear geometry of auranofin allows for the displacement of the thioglucose and triethylphosphine moieties by the nucleophilic sulfhydryl groups (Figure 3).<sup>80–83</sup> Whereas active site cysteines have been the generally accepted binding site for auranofin to confer its inhibitory activity to TrxR function, X-ray structures of *Entamoeba histolytica* TrxR (EhTrxR) reveal a noncatalytic Au(I) binding site at Cys<sup>286</sup> with low affinity with no interaction with active site Cys<sup>140</sup>–Cys<sup>143</sup> redox center.<sup>80</sup> This is indicative of a resolute disulfide bond formation that precludes Au(I) binding even in the presence of reducing agents. Conceivably, reactivity of cysteines at the active sites of TrxR differs based on molecular weight, proximity of cysteines for disulfide formation, and the size of the catalytic motif, CXXC for EhTrxR.<sup>80</sup> These structural insights point to mechanistic differences in the inhibition of TrxR by auranofin and other linear Au(I) complexes.

Given the essential role of redox homeostasis in physiological and pathophysiological conditions, modulating redox enzymes such as TrxR via the formation of stable and irreversible adducts has enormous consequences for several cellular processes and regulating intracellular reactive oxygen species (ROS).<sup>84–86</sup> In cells that overexpress TrxR, such as parasites, cancer cells, and memory T cells, inhibition of the redox enzyme resulting in oxidative stress and eventually apoptotic cell death is therapeutically beneficial.

The discovery of relatively stable Au(III) complexes for biological application has allowed for variable ligand modification of the  $d^8$  Au(III) system, which often takes on a square planar geometry.<sup>87–92</sup> Recent advances in omics technology, spectroscopy, and chemical biology are revolutionizing the target identification toolbox to support Au(III) mechanism of action.<sup>93,94</sup> It has become obvious that proteins, which are the largest component of biomolecular systems in biology, are the primary target of gold-based drugs.<sup>95,96</sup> With a few exceptions to be discussed, Au(III) complexes target proteins beyond TrxR.<sup>93,94,97–99</sup>

Au(III) complexes are relatively harder than Au(I) complexes, and ligand tuning has direct effects on biological target as well as mechanism. Passive diffusion across the plasma membrane remains the dominant transport pathway for Au(III) systems. The pathway of intracellular uptake of Au(III) complexes can be characterized more broadly under ATP-independent endocytosis and micropinocytosis processes. Active transport mechanisms of Au(III) complexes are yet to be unraveled in detail. Once in cells, Au(III) can remain intact until it reaches its biological target or can be reduced by biological nucleophiles such as glutathione (L-GSH), ascorbate to Au(I) for biological action in a prodrug format.<sup>100–102</sup> Au(III) complexes with distinct structural scaffolds induce different mechanisms of action in cells. Au(III) porphyrins target the mitochondrial heat shock protein 60,<sup>103,104</sup> whereas Au(III) mesoporphyrin IX target cysteine thiol containing proteins, thioredoxin, deubiquitinase, and heat shock protein 90 via an arylation of the meso carbon and sulfur atom of cysteine in a C–S bond formation (Chart 2).<sup>105</sup> The proteasome, endoplasmic reticulum, and mitochondria are attractive targets of Au(III) complexes, providing a broad range of mechanisms of Au(III) action.<sup>89,93,100–102,106–109</sup> The peculiar mechanistic detail will be discussed in the context of diseases within the ensuing sections of this Review.

### 3.1. Structural Basis for Gold–Protein Complexes

Significant progress has been achieved over the past two decades in elucidating gold–protein interactions, ranging from EXAFS, Mossbauer, NMR, and ESI-MS to X-ray crystallography data.<sup>71,73,110–117</sup> New crystallographic information is beginning to shift our understanding of the affinity of gold for nitrogen ligands juxtaposed to the conventional sulfur and selenium ligands. Here we offer selected examples. A detailed structural analysis of gold–protein adducts was reviewed by Messori et al.<sup>118</sup> Using X-ray crystallography, gold adducts at distinct histone sites of nucleosome core particles (NCP) using auranofin can be elucidated.<sup>119</sup> The NCP-gold adduct reveals two-symmetry-related locations, Au1 and Au1' along the 2-fold axis of the nucleosome and with good proximal distance from the central base. Whereas the sugar thiolate groups were substituted by the histone ligand through the histidine delta nitrogen side chains, the triethyl phosphine groups make hydrophobic interactions with surrounding H3 residues. It must be noted that the requirement for NCP-gold adduct formation is the presence of both RAPTA-T and auranofin in the NCP treatments that allows for RAPTA-T adducts to promote reactivity of the H3/H3' H113 sites (Figure 4).<sup>119</sup> This study adds to the knowledge of Au-histidine binding but more importantly reveals an allosteric phenomenon upon drug binding to the nucleosome acidic patch, which is a chromatin binding hotspot and may be relevant for *in vivo* genomic regulation and histone posttranslational modifications.<sup>119</sup>

Metallo- $\beta$ -lactamases (MBL) and mobilized colistin resistance (MCR) expressing Gram-negative bacteria pose a major threat to human health due their role in antibiotic resistance. To resensitize carbapenem- and colistin-resistant bacteria to antibiotics, auranofin was identified as a dual inhibitor of MBLs and MCRs.<sup>120</sup> Enzyme activity shows that auranofin inhibits the clinically relevant New Delhi metallo- $\beta$ -lactamase 1 (NDM-1) and MCR-1 catalysis to boost antibiotic action. Structural insights revealed that Au(I) binds NDM-1 (PDB: 6LHE) in the active site by Zn(II) displacement with two Au ions. One ion, Au<sup>282</sup> tetrahedrally coordinates Cys208, His250, Asp124 and water molecule (w<sup>291</sup>), and Au<sup>283</sup>

tetrahedrally coordinates His122, His 120, His 189, and a water molecule ( $w^{410}$ ) (Figure 5). The Au–Au contacts possess a distance of  $\sim 3.8$  Å. A remote Au ion located at the interface of two protein monomers was found to coordinate Asp223, Glu152, water molecule, and a Glu227 from a neighboring NDM-1 molecule in a distorted tetrahedral geometry.

Furthermore, the Au-bound MCR-1-S crystal structure (PDB: 6LI6) demonstrates Au ion displacement of Zn(II) in the catalytic site by coordinating to Glu246, Asp465, His466, and TPO285 in a distorted geometry (Figure 6). Two other Au ions coordinate to His252 or His 424 and  $PEt_3$  group or water molecule in a linear/quasi-linear geometry, respectively. Interestingly, the displacement of metal ions, e.g., Zn within the catalytic core of enzymes by Au, is a common phenomenon exhibited for enzyme inhibition.<sup>120</sup>

Despite the incredible information obtained from X-ray crystallography to elucidate gold–protein interactions, the ability to design ligands to predict gold complex reactivity, Au compound recognition, and potential binding sites in proteins using computational aided drug design (CADD) still require dynamic evolution of transition metal parametrization in computational software as well as extensive experimentation to obtain guiding rules. Whereas this is an existential bottleneck, it presents opportunities for inorganic chemists, structural biologists, and computational chemists to work together in addressing the issue to advance the field. We predict that the modern era of artificial intelligence (AI) will facilitate the rapid identification of Au-based ligands with affinity for specific proteins.

### 3.2. DNA-Targeting Gold Compounds

DNA is a formidable molecular target for many drugs approved by the Food and Drug Administration (FDA), primarily for the treatment of cancer.<sup>121–126</sup> Despite the nonspecific cytotoxic character of traditional chemotherapeutics, modern drug discovery has promoted selective agents that target DNA and associated DNA processes. Alkylating agents nondiscriminately interact with DNA and often covalently in the form of cross-links. Cisplatin, the platinum(II) antitumor drug that shares isoelectronic similarity with Au(III), was the first transition metal-based drug to be approved for the treatment of cancer. Following the serendipitous finding by Rosenberg and colleagues during an investigation of the effect of electric field on bacteria cell division,<sup>127,128</sup> extensive work into the mechanism of cisplatin and next generation Pt(II) drugs, carboplatin and oxaliplatin, demonstrate formation of Pt–DNA cross-links as lethal complexes that lead to apoptosis.<sup>129–134</sup> These metal agents have been remarkably transformative in the clinic against several cancers including testicular, bladder, lung, ovarian, breast, cervical, and brain tumors.<sup>61,135–137</sup> However, toxic side effects and drug resistance are limiting concerns.<sup>138–140</sup> Another class of agents target protein–DNA complexes with somewhat precise sequence selectivity. Agents designed to target the minor and major grooves of DNA such as polyamides and triplex forming compounds showed promise as chemotherapeutic agents. Compounds targeting secondary structures such as G-quadruplexes were particularly valuable in interrogating telomeres and transcriptional elements.<sup>2</sup>

**3.2.1. Au(I) Complexes Targets Calf Thymus-DNA.**—Gold(I) complexes with thiosemicarbazones ligands have been reported to interact with DNA (Chart 3). The

complexes interact with calf thymus DNA (ctDNA) when incubated at different concentrations with changes in electronic transitions observed with UV–vis between 250–400 nm. The binding constant of gold complexes to ct-DNA was calculated to be within  $6.26 \times 10^4$ – $4.42 \times 10^6 \text{ M}^{-1}$ , indicating strong binding. Furthermore, competitive binding assay between the complexes at different concentration from 0–100  $\mu\text{M}$  and ethidium bromide/ctDNA was used to confirm binding. Emission fluorescence shows a decrease in emission intensity and displacement of the ethidium/DNA adduct after the addition of the gold(I) complex. This is due to competition between the gold(I) derivative and ethidium bromide for binding to the DNA groove.<sup>141</sup>

**3.2.2. Au(III) Complexes as DNA Intercalator.**—Nuclear enzymes such as the monomeric human Topoisomerase IB (TOP1) and Topoisomerase II $\alpha$  (TOP2 $\alpha$ ) are crucial regulators of DNA topology for the orchestration of important cellular processes including DNA replication, gene transcription, and cell division.<sup>142,143</sup> These enzymes function by inducing transient single-strand (type I) or double-strand (type II) breaks in the DNA helical structure. Despite the relatively short half-life of these enzyme–DNA complexes *in vivo*, they represent a viable molecular target in cancer drug discovery.<sup>144</sup>

There are two classifications of compounds targeting TOP1. First, compounds known as interfacial poisons (IFPs) interfere with enzyme–DNA complexes to prevent plausible religation of DNA. This is achieved by a noncatalytic binding of DNA–intercalating IFPs at nicked sites enzyme–DNA cleavage complexes, thereby poisoning the TOP1 enzyme. Camptothecin and indenoisoquinolines represent important examples of this class.<sup>145–148</sup> Second, catalytic inhibitor compounds (CICs) block two crucial catalytic steps through (i) competitive inhibitor binding to Top1 or competitive binding to DNA and (ii) step 2 catalytic inhibitors (Figure 7). CICs generally convey reduced genotoxicity but are uncommon,<sup>149,150</sup> thus raising the need for novel compounds. Au(III) compounds generally inhibit TOP1 catalytically; however, it is critical to note that inhibition of supercoiled DNA relaxation by TOP1 is not the only parameter to delineate CICs from IFPs. A novel class of pyrrole-containing Au(III) macrocycles was identified as CICs of human TOP1 and TOP2 $\alpha$  (Figure 7). The  $d^8$  complexes exist in a square planar geometry with an aromatic quinoxaline backbone that facilitate DNA intercalation with binding affinities in the low micromolar range using standard competitive displacement of DNA intercalator, ethidium bromide assay. These Au(III) macrocycles exhibit cytotoxic potency across National Cancer Institute (NCI, USA)-60 human cancer cell lines.<sup>151</sup> The Au(III) ion plays a critical role in DNA intercalation and concomitant inhibition of TopI and TopII $\alpha$  using purified DNA and enzyme.

**3.2.2.1. Au(III) Macrocycles.**: Macrocyclic Au(III) compounds containing pyrrolic fragments have demonstrated CIC and DNA intercalating properties. Studies with *meso*-tetraarylporphyrins (Chart 4) revealed significant interaction with duplex DNA and an intrinsic binding constant of  $K_b = 2.79 + 0.34 \times 10^6 \text{ dm}^3 \text{ mol}^{-1}$  with calf thymus DNA.<sup>152</sup> A series of tetraarylporphyrin Au(III) complexes were prepared, bearing different substituents on the *meso*-aryl ring including glycosyl and methoxyphenyl groups. The complexes bind to DNA in absorption titration assays in the range  $4.9 \times 10^5$ – $4.1 \times 10^6 \text{ dm}^3 \text{ mol}^{-1}$  and act

as intercalators of DNA. Inhibition of Top1 by these compounds is by inducing supercoiled DNA relaxation. Additionally, in a polymerase chain reaction stop assay, Au(III) porphyrins inhibit amplification of DNA substrates with G-quadruplex structures.<sup>153</sup>

**3.2.2.2. Au(III)-N-Heterocyclic Carbenes.:** Another class of stable organometallic Au(III) compounds of the type,  $[\text{Au}_n(\text{R}-\hat{\text{C}}\text{N}\hat{\text{C}})_n(\text{NHC})]^{n+}$  (Chart 5) were synthesized and displayed interaction with DNA as well as *in vitro* and *in vivo* anticancer activity.<sup>154,155</sup> The complexes interact with DNA with a binding constant of  $4.5 \times 10^5 - 5.3 \pm 0.8 \times 10^5 \text{ dm}^3 \text{ mol}^{-1}$  at 298 K toward ctDNA. Further characterization reveals retardation of 123-bp DNA ladder mobility in gel-mobility-shift-assay. The complex inhibits Top1-mediated DNA relaxation at lower concentrations than the well characterized CPT. Detailed studies show that the complex is a catalytic inhibitor that inhibits the topoisomerase I cleavage reaction by preventing DNA substrate binding.

**3.2.2.3. Gold(III) Pyridyl and Isoquinolyl Complexes.:** Although guiding principles for the design of gold-based agents to target DNA-associated elements appear elusive, the use of nitrogen-containing heterocycles with sufficient planarity fosters interaction with DNA and inhibition of Top1 and Top2 enzymes. The synthesis of pyridyl- and isoquinolylamido complexes of Au(III) contributes to our understanding of the affinity of gold complexes to DNA and consequent inhibition of topoisomerase (Chart 6).<sup>156</sup> We briefly noted, with regard to the discussion above, that cationic Au(III) porphyrins revealed interaction with DNA, thus variation of multidentate amido complexes of cationic character may potentially act as cytotoxic DNA intercalators. Pyridyl or isoquinolyl ligands of the type H<sub>2</sub>L<sub>n</sub> react with Au(III) salts to afford neutral pyridyl or isoquinolyl amido-dichloro gold(III) complexes. Perhaps the use of a base in the reaction may lead to the formation of cationic tetradentate AN<sub>2</sub>N'<sub>2</sub> trischelates of gold toward cytotoxic complexes consistent with cationic Au(III) porphyrins. The Au(III) pyridyl- and isoquinolylamido chelates are square planar in character with the cis-Cl ions coordinated amido chelating moiety in a trans fashion. The soft, polarizable nature of gold<sup>157</sup> facilitates covalent interaction with soft thiol or selenothiol nucleophiles compared to nitrogen nucleophiles under biological conditions. This limits DNA alkylation by gold complexes at the nucleophilic <sup>7</sup>N-guanine of DNA. Thus, N-donor ligands promote overall gold complex stability and their planarity dictate DNA intercalation.

**3.2.2.4. Gold(III) Biscarbene Complexes.:** Another class of DNA targeted gold(III) complexes consist of bis(carbene) pincer type ligand supported by a carbazole framework for gold chelation (Chart 7). The complex follows the prototypical  $[\text{Au}^{\text{III}}(\text{CNC})\text{Cl}]^+$  archetype with distinct aromatic planarity and redox stability. Although these gold(III) pincer complexes form adducts with *L*-glutathione, their DNA binding affinity is a magnitude larger than the well-characterized DNA intercalator psoralen at a  $K_A$  of  $3.7(3) \times 10^4 \text{ M}^{-1}$  when ctDNA (37 °C, pH 7.4 Tris-HCl buffer) is used. It is possible that these complexes target DNA 3-way junctions, B- and Z-DNA forms. Theoretical insights show hydrophobic p-type interaction of T and A bases as well as phosphate O–Au interaction underlying B-form DNA binding and Z-DNA binding, respectively.<sup>158</sup>



#### 4. TARGET IDENTIFICATION OF GOLD COMPLEXES

Proteins are the main targets of gold-derived bioactive compounds;<sup>159–161</sup> however, unbiased, system-wide approaches to examine protein activity and function remain underexplored in metal-based drug discovery. New molecular biology methods combined with recent developments in sequencing and mass spectrometry-based proteomics have contributed to deciphering biological target modulation by gold complexes and associated disease phenotypes (Figure 8). In this section, we discuss recent advances in chemical biology and omics technologies that are and could revolutionize the chemical and analytical toolbox available to drive gold-based drug/probe discovery. We also shed light on the application of these analytical technologies to identify potential targets of gold complexes and mechanism of action.

Classical proteomic tools are available to profile gold complexes in cells. The pipeline involves 2-D gel electrophoresis for protein separation of lysed treated or untreated cells on an SDS-PAGE gel followed by gel staining and imaging, electrophoretic spot excision, mass spectrometry and protein identification, bioinformatic functional analysis to characterize differentially expressed genes or proteins, and validation by 2-D Western blot of selected targets and subsequent functional assays. This approach was used to characterize the potential mechanism of the organometallic Au(III) antiproliferative agent, Aubipy<sub>c</sub>, in ovarian cancer cells (A2780 and A2780 CDDP) following a 24 h incubation with the Au complex at a 10  $\mu$ M concentration.<sup>162,163</sup> Inhibition of proteins in the glycolytic pathway including GAPDH, ENO1, PKM, PGK1, ALDOC, and LDHB by Aubipy<sub>c</sub> demonstrates a promising approach for gold mechanism of action despite limitations of laborious sample preparation, high throughput, and batch-to-batch variability (Figure 9).<sup>163</sup>

Au probe-based target deconvolution is emerging as an attractive technique for target identification of bioactive Au compounds. The strategy is based on derivatization of the Au compound with affinity tags such as biotin for affinity enrichment or reactive group to facilitate immobilization to a solid support such as Sepharose beads. Combining affinity enrichment with mass spectrometry-based proteomics provides improved sensitivity, resolution, and specificity for profiling the whole cellular proteome. For details on mass spectrometry methods in drug discovery, readers may refer to recent reviews that may be applicable to gold-derived bioactive complexes.<sup>164–167</sup> The described target identification approach is well-known as compound-centric chemoproteomics.<sup>168</sup> Specificity can be largely enhanced by derivatizing Au compounds with reactive handles such as diazirines, aromatic azides, and benzophenones that covalently modify protein targets through photoaffinity labeling.<sup>93,104,169–172</sup> Modular probe development using click chemistry tools can streamline synthetic efforts, whereas providing versatility with regards to tools for analyzing Au complex localization, target identification and mechanism of action.

Implementing competition-binding experiments using the parent or unmodified Au agent is a robust way to verify candidate pull down targets when using the Au probe-based target deconvolution method for Au target identification with integrated scientific rigor.

Cellular thermal shift assay (CETSA)<sup>173</sup> can be used as a profiling tool for gold-based drug discovery when coupled with proteome-wide MS. Current use of CETSA in the context of gold-derived complexes has been limited to validating identified targets by assessing thermal protein stability changes via Western blot. This is achieved by incubating cells with a desired Au agent or vehicle, followed by cell lysis and heat across a range of temperatures. After centrifugation, the soluble fractions are subjected to gel electrophoresis and incubation with intended protein target antibodies. Direct Au complex-target engagement induces thermal stability changes to deconvolute protein targets. A major advantage with CETSA is that it does not require functionalized bioactive Au complexes, which can be difficult to develop. We posit that combining quantitative MS and CETSA in gold-based thermal proteome profiling will be a powerful analytical strategy to decipher the MoA of Au drug candidates or chemical probes. The ability to integrate 2D thermal proteome profiling will merge temperature dependent and isothermal ligand concentration-dependent studies to address prevailing false negatives associated with CETSA-MS.

The use of a clickable photoaffinity probe of a Au(III)-porphyrin complex enabled the isolation of protein binding partners, notably, heat-shock protein 60 (Hsp60). Synthesis of the probe followed tethering a hexaethylene glycol linker, clickable alkyne tag and a benzophenone photoaffinity tag to the meso-phenyl rings of the porphyrin ligand of the Au(III)-porphyrin complex (Chart 8). Photoaffinity labeling was performed by incubating cancer cells with Au(III) Probe-1 followed by UV irradiation, after which click reaction with azide-conjugated biotin was carried out. Competition experiments using the parent Au(III)-porphyrin complex showed a diminished signal of the photoaffinity-labeled protein. Subsequent click reaction using azide-conjugated Cy5 in cell lysates followed by 2D gel electrophoresis, fluorescence scanning, and MALDI-TOF/TOF MS revealed Hsp60 as the potential target. Using quantitative proteomics by stable isotope labeling by amino acids in cell culture (SILAC) and subsequent affinity isolation of biotinylated proteins and LC-MS/MS analysis using orbitrap confirmed Hsp60 identification. Additional validation of Hsp60 as the target of Au(III)-porphyrin complex was confirmed by CETSA.<sup>103</sup>

Leveraging the reactivity of the meso-carbon of mesoporphyrin IX, Che and co-workers described the formation of C–S bond formation as a covalent modification strategy to target thiol containing proteins in cancer cells. The use of Au(III) mesoporphyrin IX dimethyl ester facilitates nucleophilic aromatic substitution with cysteine thiols such as thioredoxin. Other targets such as peroxiredoxin III (PRDX3) and deubiquitinase, UCHL3 were identified via thermal proteome profiling mass spectrometry and CETSA. This study highlights the value of new orthogonal approaches for target identification.<sup>174</sup>

Recently, Awuah et al. used azide–alkyne functionalization of in Au(III) complex for post-treatment click modification to enable localization and mechanism of action studies (Figure 10). Post-treatment fluorescent labeling is achieved by the initial exposure of cancer cells to alkyne functionalized P-chirogenic Au(III) followed by the biorthogonal Cu(I)-catalyzed azide–alkyne cycloaddition (CuAAC) reaction using an azide-tagged FITC fluorophore. Co-localization studies using Mito Tracker red demonstrate predominant mitochondria localization.<sup>175</sup>

Another class of stable Au(III) complexes used as anticancer agents includes the tridentate  $\hat{C}N\hat{C}$ ,  $\hat{C}N^{\wedge}N$ , or  $N\hat{C}^{\wedge}N$  carbon donor pincer or NHC ligands.<sup>176</sup> Mechanistic studies of these complexes have largely been accelerated by the use of photoaffinity, fluorescent, and affinity labeling probes of the parent Au complexes (Chart 9) that allow for pull downs, chemoproteomics, and fluorescence imaging toward protein target engagement.<sup>176</sup>

The use of activity-based protein profiling (ABPP) to identify binding sites of Au complexes within the proteome is a suitable methodology to identify new druggable targets, uncover elusive targets, decipher new mechanisms, and generate broad reactive protein maps in different living species. Isotopic tandem orthogonal proteolysis-ABPP (isoTOP-ABPP) uses an amino acid residue specific (e.g., cysteine) reactive small-molecule electrophilic compound to covalently modify and enrich selective residues within the whole proteome using a chemoproteomic approach.<sup>177–179</sup> A low-pH isoTOP-ABPP platform was developed to screen selenoprotein-targeted inhibitors in a comparative analysis with iodoacetamide electrophilic probe. Auranofin treatment of mammalian cells revealed strong sensitivity of auranofin to Sec residues of Txnr1, Gpx4, MsrB1, and Seleno under IA-labeling conditions and analyzed by MS.<sup>179</sup> Recently, the ligandable cysteines in *Staphylococcus aureus* was profiled with an organogold(III) complex using isoDTB-ABPP (isotopically labeled desthiobiotin azide-activity-based protein profiling) platform (Figure 11), which differs from the traditional ABPP by using isotopically labeled (light and heavy) desthiobiotin azide tags and is compatible with IA competition.<sup>180</sup> The unique C–S bond via cysteine arylation mediated by  $[\hat{C}N]$ -cyclometalated Au(III) allows for an expanded or uncovered ligandable cysteines within the proteome. Overall, 108 cysteines were modified by the  $[\hat{C}N]$ -cyclometalated Au(III); interestingly, 59 cysteines were not liganded by previously screened organic electrophilic probes. Indicating a broader reactivity and scope of ligand ability by Au-mediated cysteine arylation.<sup>180</sup>

High-throughput screening with yeast deletions and gene knockdown systems including RNA interference (RNAi) and short-hairpin RNA (shRNA) to study drug–target interactions was pivotal in advancing chemical genetics.<sup>181–186</sup> The discovery of CRISPR-Cas9 has emerged as a powerful tool to edit the mammalian genome with ease and is useful for biological target identification, unravel mechanism of action, and resistant pathways to chemical agents.<sup>187–189</sup> The application of CRISPR-Cas9 screens in metallodrug target identification will be transformative. In a proof-of-concept study, Vulpe and Awuah et al. used a targeted pooled CRISPR approach known as TOXCRISPR to elucidate the targets of a chiral gold(I) anticancer agent, **JHK-21** (Figure 12).<sup>190</sup> **JHK-21** largely target mitochondrial oxidative processes. In addition, ABCC1 (a gene encoding MRP1 chemical exporter) knockout sensitizes cells to **JHK-21** and the loss of SPRED2, which negatively regulates the Ras-ERK pathway confers resistance to cells exposed to **JHK-21**.<sup>190</sup> This work paves the way for a systematic study to identify drug targets in mammalian cells of gold-containing compounds using CRISPR-Cas9 screening.

## 5. GOLD COMPLEXES FOR BIOMEDICAL IMAGING AND SENSING

Au complex localization in cells or whole animals reveals insights into its mechanism of action. The use of fluorescent, luminescent, and radiolabeled Au probes can be used

to monitor the location of compounds in real time. Tuning the luminescence of gold complexes requires stringent conditions. Thermodynamically, the high redox potential of gold [ $E^\circ(\text{Au(III/I)}) = 1.41 \text{ V}$ ]<sup>191</sup> renders it difficult to oxidize, leading to much elevated energy of radiative metal-to-ligand charge transfer (MLCT) states and low-lying HOMO levels compared to other third row transition metals such as Ir or Pt. Consequently, the photochemistry and photophysics of gold complexes are often detrimentally overwhelmed by energetically low-lying states with metal-centered (d-d) and/or ligand-to-metal charge transfer (LMCT) character that can be easily populated. Additionally, population of the excited state of structurally distorted d-d ligand field in Au(III) systems can lead to quenching via nonradiative decay processes.<sup>192</sup> This can be circumvented by incorporating strong  $\sigma$ -donating ligands to elevate the energy of the ligand field state toward luminescent Au(III) complexes in solution and at room temperature beyond solid state or low temperature.<sup>193,194</sup> In two-coordinate Au(I) complexes with filled  $d^{10}$  configuration, nonradiative decay can be avoided. However, examples are dominated by complexes with aurophilic interactions of metal–metal states. Two-coordinate, mononuclear Au(I) emitters with emission from MLCT states make up an attractive endeavor for biological applications.<sup>195–197</sup> So far, efforts to develop emissive gold complexes have adopted intuitive strategies via unique mechanisms including gold–gold interactions in solution or solid state as well as in multinuclear/heteronuclear systems. Multiple strategies employed to implement Au complex imaging in cells or whole animals are discussed.

It is worth noting that the use of gold(I) alkynyls in phosphorescence has been widely explored in materials research, which is beyond the scope of this Review. The development of phosphorescent gold complexes with decreased background fluorescence in biological medium has gained traction. We refer readers to comprehensive reviews on luminescent metal-based complexes including gold.<sup>198–203,194</sup> In this section, we focus on luminescent gold complexes used in cell imaging and sensing biomacromolecules such as DNA and proteins.

## 5.1. Au(I) Complexes for Luminescent Cell Imaging

Enhancing sigma donor character at the gold center, extended conjugation, gold–gold interaction, or multinuclear systems are a few strategies that facilitate single or triplet excited state transitions toward phosphorescence. The use of carbon donors such as NHCs and alkynyl ligands provides ready access to Au(I) complexes exhibiting phosphorescence in the solid state or in solution. Early demonstration of Au(I) cell imaging, made possible by the dinuclear Au(I) complex,  $[\text{Au}_2\text{L}_2]^{2+}$ , bearing the bidentate cyclophane NHC ligand.<sup>204</sup> The combination of Au–Au interaction<sup>204–206</sup> and NHC ligand leads to a red-shifted luminescence profile that enables phosphorescence imaging in living cells and is useful for biodistribution by fluorescence microscopy. This class of Au(I) luminescent agents defines lysosomal localization in cells.

**5.1.1. Au(I) Conjugated Fluorophores.**—The preparation of luminescent Au(I) phosphine naphthalimide complexes enables cellular imaging, nuclei accumulation, and demonstrates antiproliferative activity, inhibition of angiogenesis in zebra fish embryo, whereas it maintains homogeneous biodistribution in zebra fish embryos

by fluorescence microscopy.<sup>207</sup> The reaction of mercaptanaphthalic anhydride with 2-(dimethylamino)ethylamine in ethanol under refluxing conditions affords the *N*-(*N*',*N*'-dimethylaminoethyl)-1,8-naphthalimide-4-thiolate ligand and upon metalation with trialkyl/triphenyl phosphine Au(I) chloride analogs leads to luminescent naphthalimide gold(I) phosphine complexes.<sup>208</sup>

Expansion of luminescent naphthalimide Au(I) complexes introduced the alkynyl moiety with tunable photophysical properties and intracellular localization based on the naphthalimide substituent (Figure 13).

Multinuclear Au(I) alkynyl phosphanes represent an interesting class of luminescent gold complexes both in the solid state or in solution.<sup>209</sup> Initial efforts to synthesize water-soluble Au(I) acetylides began with the treatment of [AuCl(PR<sub>3</sub>')] where PR<sub>3</sub>' correspond to water-soluble phosphanes such as PTA and DAPTA with terminal alkynes in the presence of KOH in methanol to afford mononuclear phosphane Au(I) acetylides.<sup>210</sup> In addition, dinuclear alkynyl Au(I) compounds can be prepared from bis-alkyne starting materials and employing PTA and DAPTA ligands. The use of propargyl amine leads to the formation of trinuclear Au(I) complexes under similar reaction conditions using a base and water-soluble phosphane ligands. These Au(I) alkynyl derivatives display luminescence in the solid state at room temperature with excitation maxima in the range of 356–428 and emissions between 486 and 555 nm. The photophysical character of Au(I) alkynyl phosphanes is attributed to intraligand electronic transitions, gold-centered transitions, Au–P to alkyne transitions, and often Au–Au interactions to alkyne transitions. Au-PR<sub>3</sub>' may serve as a directing moiety to enhance the emission from the triplet states of the alkynyl luminophores.<sup>211–218</sup> It must be noted for design purposes that the choice of phosphane ligands can influence bathochromic shift in the emission spectra of Au(I) alkynyl phosphane complexes due to p–p\*(C≡C) or σ(Au–P) → π\*(C≡C) transitions.

Anthraquinones have been used as relevant antibiotics and antitumor agents.<sup>219,220</sup> Functionalization of hydroxy anthraquinones with propargyl bromide generates planar, conjugated ligands to form C(sp)–Au bonds, leading to complexes that are luminescent. A key optical advantage in the context of metal complexes is the added emissive property from the anthraquinone chromophore in the visible region. Mononuclear and dinuclear Au(I) complexes bearing alkynyl-substituted anthraquinones can be used in cells as fluorescent imaging probes toward mechanism of action studies via cellular localization.<sup>221</sup> Specifically, in MCF7 cells, both mono and dimetallic Au(I) anthraquinones exhibit bright fluorescence within 530–580 nm emission following a 405 nm excitation (Figure 14).

To visualize the cellular distribution and intracellular targets of Au(I) therapeutics, incorporation of established fluorophores such as acridine,<sup>222,223</sup> coumarin,<sup>224–226</sup> and borondipyromethene (BODIPY)<sup>227</sup> into the structural framework of Au(I) complexes makes it possible. The development of fluorescent BODIPY–Au(I) trackable probes for bioimaging over the past ten years has grown from cell imaging to whole animal imaging. We discuss in this section the modifications that have catapulted the translational application of BODIPY–Au(I) trackable probes (Chart 10). Initial work began with tracking Au complexes in live cells; this was quickly followed by research based on targeting cancer cells with sugar



ligands for the glucose transporters (GLUTs) or the bombesin receptors overexpressed in cancer cells. The relatively short visible light emission of these constructs led to failed preclinical evaluation, creating opportunities to explore far-red or NIR conjugates.

The goal to use trackable Au(I) agents in whole animals has been hamstrung by visible light emission probes. To overcome this limitation, near-infrared emitting agents for deep tissue penetration are required. Recently, Bode and Goze et al. added three NIR aza-BODIPY dinuclear Au(I) complexes to the trackable Au toolbox.<sup>228</sup> These complexes expand the guiding principles for designing fluorescent Au(I) complexes through the incorporation of (i) NIR dyes with emission maxima >700 nm and decent fluorescence quantum yields (~25–36%) in *in vitro* and *in vivo* optical imaging; (ii) water-solubilizing groups and disruptors of solution aggregation; and (iii) dinuclear Au(I) agents for therapeutic impact. Generally, the design possesses theranostic potential *in vivo*. Specifically, in a CT-26 colon murine mouse model, a pronounced anticancer activity was observed when azaBDP-Au1 was administered (Figure 15).

**5.1.2. Au(I) Conjugated Metal Luminophores.**—Improving the optical characteristics of trackable Au complexes offers opportunities for the use of luminescent metal complexes as luminophores including Ru, Re, and Ir with longer emissive lifetimes and high quantum yields of luminescence. Thus, Re(I)/Au(I),<sup>203,229–232</sup> Ru(II)/Au(I),<sup>233</sup> and Ir(III)/Au(I)<sup>201,234</sup> heterometallic complexes have been synthesized as trackable probes for cell imaging. First, the use of rhenium(I) tricarbonyl [Re(CO)<sub>3</sub>] scaffold in biomedicine is attractive due to its low spin  $d^6$  electron configuration, octahedral geometry for variable coordination, kinetic inertness as a result of strong-field ligands, and photophysical properties that allow for excited triplet state transitions. Leveraging the impressive chemical properties of Re with cytotoxic Au complexes leads to theranostic agents and provides a framework to assess the mechanism of action of Au anticancer complexes. The use of polypyridyl ligands, NHC, phosphine, and alkynyl functionality enable tethering of Au(I) to Re(I) without compromising the luminescent properties of Re(I). It is important to note that there are several components to designing cell-permeable heteronuclear multimetallic Re(I)/Au(I) complexes including linker lengths and ligand types. Gimeno's group has pioneered this field with different variations of luminescent Re(I)/Au(I) complexes for cell imaging and cancer therapy. Starting with *fac*-[Re(bipy)(CO)<sub>3</sub>(CF<sub>3</sub>SO<sub>3</sub>)], the displacement of the triflate ligand with Au(I) alkynylpyridine, Au(I) alkynylimidazole, or imidazole substituted Au(I) gave rise to heteronuclear Re–Au luminescent complexes.<sup>230</sup> Strikingly, the complex localized in the nucleolus, when compared to the Re(I) species, which localized to the cytoplasm. The use of ditopic P,N-donor ligand that double as linkers lead to different Re(I)/Au(I) heteronuclear complexes of the type, *fac*-[Re-(bipy)(CO)<sub>3</sub>(LAuCl)]<sup>+</sup> (**Re–Au-5** and **Re–Au-7**) and [(*fac*-[Re(bipy)(CO)<sub>3</sub>(L)])<sub>2</sub>Au]<sup>3+</sup> (**Re–Au-6** and **Re–Au-8**) with red-shifted emission profiles up to 605 nm attributed to a triplet metal-to-ligand charge transfer (Re( $d\pi$ ) → bipy( $\pi^*$ )) transition (Chart 11).<sup>229</sup> The quantum yield of fluorescence of these complexes is up to 12.5% in polar solvents. Fluorescence microscopy reveals a nonuniform cytoplasmic distribution as well as nuclear accumulation. These agents do not display potent antiproliferative activity with IC50s in the range of 35–76  $\mu$ M when tested in A549 cells.

Analogs of luminescent Re(I)/Au(I) complexes bearing pyridyl N-heterocyclic carbene ligands on Re have been synthesized (**Re–Au–9–11**) to improve (photo)cytotoxicity in cancer cells (as low as 2.66  $\mu\text{M}$ ).<sup>232</sup> The emission of these complexes is slightly blue-shifted in the range of 377–514 nm, which could be associated with a mixed MLCT from the  $(\text{Re}(\text{d}\pi) \rightarrow \text{NHC}(\pi^*))$ , LLCT imidazolyl/pyridyl to the NHC ligand, and ligand centered transitions. The cellular distribution of these agents reveals cytoplasm localization by fluorescence microscopy.

The incorporation of dinuclear Au(I) into Re(I)/Au(I) conjugates has the potential to enhance red-shifting to about 680 nm and maintain potent anticancer activity to 1  $\mu\text{M}$  in HeLa cells.<sup>231</sup> The design is manifested via a bis-alkynyl framework for Au-NHC metalation that is located on the N<sup>^</sup>N-bidentate ligand coordinated to the Re center. The emission profile of these complexes demonstrates a characteristic broad band between 565 and 680 nm, which can be assigned to <sup>3</sup>MLCT transition from the  $\text{d}\pi(\text{Re}) \rightarrow \pi^*$ - (diimine).<sup>235</sup>

Recently, the synthesis and antiproliferative activity of a new class of luminescent Au–Re complexes containing fused imidazo[4,5-*f*]-1,10-phenanthroline core were explored (Chart 12).<sup>236</sup> The heterobimetallic  $\text{Re}^{\text{I}}/\text{Au}^{\text{I}}$  and trimetallic  $\text{Re}^{\text{I}}/\text{Au}^{\text{I}}/\text{Re}^{\text{I}}$  *fac*-[ReCl(CO)<sub>3</sub>(N<sup>^</sup>N<sup>^</sup>C<sup>^</sup>AuR)]<sup>0/+</sup> and [(*fac*-[ReCl(CO)<sub>3</sub>(N<sup>^</sup>N<sup>^</sup>C<sup>^</sup>)]<sub>2</sub>Au)<sup>+</sup>, where R is an iodide phenylacetylene, dodecanethiol, or 2,3,4,6-tetra-*O*-acetyl-1-thio- $\beta$ -D-glucopyranose display long wavelength emission profiles in the range 641–673 nm following a 398 nm excitation. Despite the excellent photophysical profile, these complexes are not cytotoxic against cancer cells.

Second, the synthesis of luminescent heterobimetallic Au(I)–Ru(II) complexes bearing heteroditopic bipyridine-NHC ligands (Chart 13) has prospects for studying cellular distribution, uptake mechanisms, and impact on cytotoxicity against cancer cells, *Leishmania infantum*, and *Plasmodium falciparum*.<sup>233,237</sup> The use of Ru(bipy)<sub>3</sub> and Ru(bipy)<sub>2</sub>(dipy) as luminophores and Au(I) bearing 1-thio- $\beta$ -D-glucose 2,3,4,6-tetraacetate allows for the generation of auranofin-like imaging agents to study GLUT-1 transporters and distribution in cancer cells. Tuning the gold fragment of Au(I)–Ru(II) complexes for improved stability and cytotoxicity can take advantage of strong electron donation in NHC ligands. Emission spectra of luminescent Au(I)–Ru(II) complexes are in the range of 615–630 nm with a luminescence quantum yield in water of 0.020–0.026. Whereas these photophysical properties are attractive, they are far from ideal. Challenges including longer emission wavelength, poor aqueous solubility, and bulky luminophores that obscure precise intracellular localization of desired metallodrugs exist.

Third, phosphorescent iridium complexes possess excellent optical properties and have found utility in several areas of biomedical, material, energy, and catalytic research.<sup>238–241</sup> Harnessing the remarkable photophysical properties of Ir, including high phosphorescent quantum yield, large Stokes shift, and long emission lifetimes and the cytotoxic potential of Au represent a synergistic tool for theranostics. The use of emissive cyclometalated Ir(III) complexes conjugated to Au(I) fragments does not alter the photophysical properties of Ir. The high sensitivity of cancer cells to such complexes could be attributed to the

Au(I) unit. Additionally, intracellular accumulation of these luminescent conjugates via fluorescence microscopy is often characterized by lysosomal and mitochondrial localization. Access to  $[\text{Ir}(\text{ppy})_2(\text{dppm})]\text{PF}_6$  as a precursor to Au–Ir complexes can be obtained in a single step by reacting dppm and  $[[\text{Ir}(\text{ppy})_2(\mu\text{-Cl})]_2]$  in anhydrous and degassed methanol for 12 h. Metalation with Au(I) bearing ancillary ligands such as chloride, thiocytosine, and triphenylphosphine can then be carried to obtain luminescent Au(I)–Ir(III) complexes (Chart 14).<sup>201</sup> Further, the development of Au–Ir bimetallic peptide conjugates has been explored using an enkephalin analog, Tyr-Gly-Gly-Phe-Leu, and a propargyl-substituted derivative, Tyr-Gly-Pgl-Phe-Leu, demonstrating a strong proof-of-principle agents for theranostic bimetallic peptide bioconjugates.<sup>234</sup> Significant work is required to advance these phosphorescent heteronuclear complexes for preclinical studies.

## 5.2. Bioimaging and Sensing of Au(III) Complexes

Optimized probes can be used for cellular imaging. The use of  $\pi$ -extended C-deprotonated  $[\hat{\text{C}}\text{N}\hat{\text{C}}]$  ligands readily afford organogold(III) complexes that display long-lived emissive excited states as biosensors for proteins and DNA with lifetimes and emission quantum yields of up to 282  $\mu\text{s}$  (Figure 16). This fluorogenic strategy capitalizes on the low  $5dx^2-y^2$  orbital of the Au(III) metal center, which gives the overall Au(III)-NHC complex a nonemissive character in solution but upon reduction to Au(I) by biological reductants and the concomitant release of the fluorescent pincer ligand a strong emission is observed.<sup>242</sup> Other amphiphilic Au(III) complexes that self-assemble into micelles with good biocompatibility, high *in vivo* permeability and retention, and *in vitro* phototoxicity have been developed.<sup>243</sup>

Derivatives of cationic Au(III) complexes containing highly emissive tridentate  $\text{N}^+\text{N}^+\text{N}^+$  ligands ( $\text{H}_2\text{N}^+\text{N}^+\text{N}^+$  ligands, 2,6-bis(imidazol-2-yl)pyridine ( $\text{H}_2\text{IPI}$ ), and 2,6-bis(benzimidazol-2-yl)pyridine ( $\text{H}_2\text{BPB}$ )) and supported by NHC ligands generate fluorogenic probes (Figure 17).<sup>101</sup> These Au(III) complexes act as fluorescent thiol “switch-on” probes following reduction of Au(III) to Au(I) by thiols including glutathione. The strategy employed takes advantage of the ability of low energy Au(III)  $5dx^2-y^2$  orbital to quench intraligand emission; however, reduction activates the high emissive character of the ligands.

Transition metal hydrides represent an interesting class of compounds with utility in catalysis and materials.<sup>244</sup> Following the first evidence of Au hydrides<sup>245</sup> by Andrews et al.,<sup>246–249</sup> these complexes were considered unstable until the first isolable Au(I) hydride bearing an NHC ancillary ligand in 2008<sup>250</sup> and AuH stabilized by Xanthphosphole ligand.<sup>250,251</sup> Ever since, Bochmann and co-workers pioneered the development of Au(III) hydrides of the structural type  $[(\hat{\text{C}}\text{N}\hat{\text{C}})\text{AuH}]$  with the hydride ligand trans to the N-donors<sup>252,253</sup> and subsequent applications in catalytic water–gas shift reactions.<sup>252,253</sup> Variations of this class of complexes possess emission properties with sufficient biological stability. It is possible that the Au–H bond gains susceptibility to photolability due to trans effect at which stage allows the excited state contribution to be dominated by intraligand phenyl to pyridyl transition mixed with a minor metal to ligand charge transfer transition. Further, photoinduced thiol reactivity by incubating  $[(\hat{\text{C}}\text{N}\hat{\text{C}})\text{AuH}]$  (100  $\mu\text{M}$ ) with NAC (10

mM) in aqueous solution (H<sub>2</sub>O:20% DMF, v/v) and subsequent irradiation with 365 nm light generates ligated [Au(III)( $\hat{C}N\hat{C}$ )S<sub>(NAC)</sub>] in >90% conversion in just 30 min (Figure 18).<sup>254</sup>

## 6. RADIOACTIVE AU COMPLEXES FOR RADIOTHERAPY AND BIODISTRIBUTION

Incorporation of <sup>198</sup>Au and <sup>199</sup>Au into the radiopharmaceutical toolbox has been largely unexplored until the past decade, largely due to synthetic complexity and stability associated with high valent Au(III) complexes. Development of radioactive <sup>198</sup>Au and <sup>199</sup>Au uncovers an important new class of radiopharmaceuticals for the treatment of cancer and diagnostics. <sup>198</sup>Au and <sup>199</sup>Au are radioactive  $\beta$  and  $\gamma$  emitters with strong penetrating power. <sup>198</sup>Au isotope has a  $t_{1/2} = 2.7$  days,  $E_{\beta} = 0.97$  and  $E_{\gamma} = 411$  keV and <sup>199</sup>Au isotope has a  $t_{1/2} = 3.14$  days,  $E_{\beta} = 0.46$  and  $E_{\gamma} = 158$  and 208 keV. The high energy  $\gamma$  photons make these Au isotopes suitable for imaging and detection by single-photon imaging instruments. Additionally, their half-lives are optimal for production, shipping, and administration. Beyond the use of colloidal gold radionuclide <sup>198</sup>Au colloids, which was reported by Sheppard et al. and received US approval in 1950 as an antineoplastic and liver imaging agent,<sup>255</sup> few gold-derived monomeric radionuclide complexes have been developed.<sup>256–259</sup> <sup>198</sup>Au and <sup>199</sup>Au radionuclides of Au(III) bis-thiosemicarbazones bearing diversified dithiosemicarbazone ligands were synthesized and their radiochemistry characterized.<sup>257</sup> In particular, the radionuclide with (1*Z*,1'*Z*)-*N,N''*''-((2*E*,3*E*)-pentane-2,3-diylidene)bis(*N*-ethylcarbamohydrazonothioic acid) ligand, <sup>198</sup>Au-TSC was synthesized with >90% radiochemical yield with good stability in phosphate-buffered saline (PBS) and mouse/human serum stability. The biodistribution of <sup>198</sup>Au-TSC demonstrates a >50% accumulation in the bloodstream and 39% ID/g lung distribution in 4 h following administration. It must be noted that ligand systems must be carefully chosen to circumvent existing problems associated with the rapid reduction of Au(III) complexes.

Additionally, the <sup>198</sup>Au radiolabeled Au(III) bis(pyrrolide-imine) Schiff base complex was synthesized with a high radiochemical purity of >95% and 73% yield (Chart 15).<sup>258</sup> The high energy  $\gamma$  radiation of <sup>198</sup>Au allowed for biodistribution of the complex in Sprague–Dawley rats using gamma capture, giving insights into blood accumulation of the hydrophilic complex and its retention in tissue as evidenced by  $t_{1/2}$  of 24 h in the heart and lung and excretion via the kidneys.<sup>258</sup> Whereas these studies are of promise, the inability to use the described radiolabeled complexes to evaluate Au(III) to Au(I) reduction of drugs in animal models present limitations that require alternate radiolabeling approaches. The use of iodine (<sup>124</sup>I) radionuclide labeled Au(III) carbene complexes take advantage of the positron emission capability of <sup>124</sup>I to monitor the speciation of **Au-I-124** *ex vivo* and *in vivo* using whole body imaging by positron emission tomography (PET) and Au concentration in different organs by ICP-MS (Figure 19).<sup>259</sup>

## 7. THERAPEUTIC GOLD COMPLEXES

### 7.1. Approved Gold Drugs

We would like to draw readers attention to the clinical use and development of gold agents (Table 1) as a prelude to the exciting new discoveries of gold-derived compounds for therapeutic application in different disease indications. The antituberculosis effect of potassium gold cyanide by Koch spurred several therapeutic trials of cationic gold complexes across Europe in humans.<sup>260,261</sup> The German pharmacologist Adolf Feldt introduced sodium (4-amino-2-mercaptobenzoato(2-)-*O,S*) aurate (Krysolgan) in 1917 for the treatment of tuberculosis and aurothioglucose (Solganol), which inhibited streptococcal infections in humans.<sup>260–263</sup> In 1845, Fordos and Gelis synthesized sodium aurothiosulfate (Sanocrysin)<sup>264</sup> for the first time and its preparation later refined and characterized by McCluskey and Eichelberger in 1926 as an Au(I) complex.<sup>265</sup> Despite Mollgaard's mischaracterization of sanocrysin as a Au(III) dimethyl complex, the chemotherapeutic investigation of sanocrysin in the context of pulmonary tuberculosis was favorable. Several independent studies by physicians and scientists from Sweden, Denmark, Germany, and France published findings of the use of cationic gold complexes in polyarthritis and rheumatoid arthritis.<sup>266</sup> Seminal work by Jacques Forestier in 1932 that utilized sodium aurothiopropionol sulfonate (Allochrysin) proved effective against infective and rheumatoid arthritis with cases that eliminated symptoms and signs of disease progression toward clinical cure.<sup>35</sup>

Following the introduction of sanocrysin in 1924 by Mollgard as a chemotherapeutic agent, the first clinical use of sanocrysin in humans was fostered by Knud Secher for the treatment of pulmonary tuberculosis in Denmark.<sup>266</sup> Secher reported that 114 patients were *tubercle bacilli*-symptom free and proposed a mechanism that suggests the release of toxins in air-passages after sanocrysin administration to fight the infection.<sup>266–268</sup> Other studies around Europe contested the Mollgard–Secher theory based on unsatisfactory therapeutic effect of sanocrysin in treating tuberculosis. The lack of a formidable experimental basis of sanocrysin's mode of action dampened enthusiasm for its use.<sup>269–272</sup> However, several clinicians continued its use to treat tuberculosis and other indications.

Aurotioprol acid is a racemic gold(I) salt, first prepared by Lumiere and marketed by Solvay under the trade name allochrysin for the treatment of rheumatoid arthritis.<sup>36,273</sup> This drug exists as a polymeric complex with a chiral 2-hydroxy-3-sulfidopropane-1-sulfanto ligand. It is administered via intramuscular injection and currently marketed outside the United States. In several clinical trials dating back to the 1940s allochrysin showed superior patient response to placebo as a disease modifying drug.<sup>274</sup>

Sodium aurothiomalate exists as a 50 mg injection solution with nitrogen, phenylmercuric nitrate, and water. Sanofi markets this drug under the trade name myocrisin as disease modifying agent for the management of progressive rheumatoid arthritis and juvenile chronic arthritis and administered via deep intramuscular injection. There is widespread use of myocrisin in Australia and New Zealand, where it was approved in 1969. Myocrisin was discontinued in the United Kingdom due to shortage of the Active Pharmaceutical Ingredient (API) and not due to safety concerns in June 2019.<sup>275</sup> In The Netherlands, myocrisin was



established as an alternative to aurothioglucose (Solganol) in 2001. Out of 120 patients with rheumatoid arthritis, 79% overall survival rate was recorded after 12 months. Maximum therapeutic benefit is gained in the early stages of disease. In advanced stages of the disease, where cartilage and bone damage have occurred, myocrysin is capable of management. Weekly injections of 10 mg to 50 mg of active gold until sodium aurothiomalate reaches 1 g is the general rheumatoid arthritis therapeutic dose.<sup>276</sup>

Krysolgan, also referred to as sodium (4-amino-2-mercaptobenzoato(2-)-*O,S*) aurate is a polymeric water-soluble complex introduced by Adolf Feldt for the treatment of tuberculosis and leprosy.<sup>277</sup> In 1926, the use of Krysolgan in a patient with sarcoid lesions demonstrated a positive outcome including softened large nodules, flaccid skin area and disappearance of nodules following 14 injections of the drug up to 1.5 g dose.<sup>278</sup> Application of Krysolgan in treating Lupus Erythematosus quickly emerged.<sup>279</sup> Increasing toxicity, lack of potency, and lack of a defined mode of action, led to the discontinuation of Krysolgan as first-line therapy.<sup>280</sup>

Aurothioglucose can be viewed as a sugar derived Au(I) polymeric salt, which is often administered by intramuscular injection or intragluteally and marketed as Solganol. The American Medical Association designated Solganol for the treatment of rheumatoid arthritis, particularly for patients that have been unresponsive to conventional therapy. Although the mechanism is not fully elucidated, a general mode of action is that the gold agent accumulates in macrophages and consequently inhibits lysosomal enzymes as well as phagocytosis.<sup>276,281</sup>

Auranofin is a monomeric gold drug approved by any public health agency. It is an oral antiarthritic alkylphosphine gold(I) drug bearing a tetra-*O*-acetyl-1-thio- $\beta$ -D-glucopyranose ligand. The search for new antiarthritic agents with improved efficacy led Sutton and the research team at Smith Kline and French laboratories, Philadelphia to synthesize a series of trialkyl-phosphine gold complexes in 1972.<sup>51</sup> In the structure–activity relationship study that evaluated therapeutic responsiveness by the adjuvant arthritis rat model and bioavailability by measuring Au plasma levels, the triethylphosphine gold (AuPEt<sub>3</sub>) class was found to be most effective.<sup>51</sup> Following the structural elucidation of auranofin using different spectroscopic techniques and X-ray crystallography, detailed pharmacokinetic and pharmacological profiling, and clinical trials, auranofin was approved by the US FDA in 1985 for the treatment of rheumatoid arthritis. Auranofin is marketed as Ridaura by Sebel Ireland Ltd. as a 3 mg capsule for oral administration. Recent repurposing efforts in identifying new drugs for different disease indications have positioned auranofin as an attractive drug for cancer, microbial, and viral infections beyond arthritis. We discuss the current landscape of auranofin in clinical trials around the world.

## 7.2. Current State of Gold Drugs in Clinical Trials

The ability for auranofin to perturb redox homeostasis by inhibiting thiol and selenocysteine rich oxidoreductases offers a broad mechanism to target for several diseases that have oxidative stress and inflammatory underpinnings such as cancer, microbial infections, and neurodegeneration.<sup>10,55,282–290</sup> Despite the relegation of auranofin as a first line treatment

for rheumatoid arthritis, there are several clinical trials that have been conducted and other ongoing trials to repurpose the gold drug to treat other diseases as summarized in Table 2.

Investigation into the use of auranofin as an adjunctive host directed tuberculosis therapy (TB HDT) is in phase II clinical trials. This study examines the safety and preliminary efficacy of auranofin and other drugs including everolimus, vitamin D3, and CC-11050. TB treatment is long and often prevents patient medication compliance. Additionally, TB disease burden leads to acute lung inflammation. Thus, new treatment options that shorten TB treatment and prevent permanent lung damage is of clinical need.

An observational study sponsored by Hoffman-La Roche conducted in 11 countries of 1239 enrolled participants aimed at assessing the antiarthritic biologic, rituximab, and alternative tumor necrosis factor (TNF) inhibitors in patients with rheumatoid arthritis and an inadequate response to a single previous TNF-inhibitor. The study recruited participants with previous nonbiologic disease-modifying antirheumatic drugs therapy including auranofin, aurothioglucose, allochrysin, and gold. Disease activity score-erythrocyte sedimentation rate (DAS28-ESR) is used as a measure of disease activity in rheumatoid arthritis and is calculated from the number of swollen joint count, tender joint count (TJC, 28 joints count) and ESR (millimeters per hour [mm/h]) with a higher score indicating more disease activity. This will be applied to the study over a 14-year period. In a recent study by Pfizer to examine patients initiating Xeljanz (tofitinib, Janus kinase inhibitor) for the treatment of moderate to severe active rheumatoid arthritis in combination with oral methotrexate (MTX), patient enrollment comprised those who have received Au treatment in the form of auranofin, aurothioglucose, or sodium gold thiomalate during a 1–5.2 years period before the index date. These observational models position Au drugs for potential combination therapy in the effective treatment of active rheumatoid arthritis in patients.

The use of auranofin to deplete latent viral reservoir in patients with HIV infection was supported by the hypothesis that antiretroviral therapy suppress HIV viral load and further reduction of viral load may lead to disease cure. In 2014, vaccine and gene therapy institute in collaboration with the University of Miami sponsored an interventional trial to investigate the reduction of HIV viral reservoir by oral auranofin (3–6 mg). This study was later withdrawn. Researchers in Sao Paulo launched a clinical trial toward HIV cure by studying a combination therapy involving Maraviroc and/or dolutegravir, dendritic cell vaccination, class III histone deacetylases (HDACs), surtuin-1, and auranofin to decrease the ratio of long-lived central memory/transitional memory (T<sub>CM</sub>) CD4<sup>+</sup> T-cells.<sup>291,292</sup> Although results are not yet available, a positive outcome will result in an efficacious combination treatment regimen for HIV sterilizing cure.

Auranofin was granted an orphan drug status for the treatment of amebiasis. Amebiasis is a parasitic disease caused by the one-celled protozoon called *Entamoeba histolytica*. To monitor the safety of auranofin after 7 days of daily oral administration, the National Institute of Allergy and Infectious Diseases (NIAID) completed a Phase I open label study to evaluate the pharmacokinetics of auranofin following a daily dose of 6 mg oral dose for 7 days to healthy individuals. In a separate phase IIa study, the NIAID designed a comparative

study to evaluate placebo to once daily doses of 6 mg auranofin for the treatment of amebiasis or giardiasis (a diarrheal infection caused by the parasite *Giardia duodenalis*).

Chemotherapy remains the first line treatment for many cancers, but patients develop resistance to drug treatment and can die as a result. There is an unmet medical need to develop novel therapies for chemotherapy-resistant disease. The previous regulatory approval of auranofin established it as a reasonably safe and effective drug for rheumatoid arthritis. Thus, making auranofin attractive for the treatment of cancers. The University of Kansas Medical Center, NIH, and the Leukemia and Lymphoma Society identified auranofin as a selective inhibitor of the rare blood cancer, CLL. A phase I/II interventional trial was initiated at three sites following an IND clearance from the FDA. Due to diminished unmet need because of four promising therapies for CLL, the auranofin study was abrogated. The University of Ulm, Germany sponsored and proof of concept interventional clinical trials that combines Temozolomide with other approved drugs including auranofin for treatment of recurrent glioblastoma. The Mayo Clinic through its multiple locations in collaboration with the National Cancer Institute initiated several clinical trials to evaluate efficacy and overall tumors response rate of auranofin and sirolimus combination in treating serous and recurrent ovarian cancer. In the context of nonsmall cell lung cancer (NSCLC), phases I and II studies are currently recruiting patients to establish the maximum tolerated dose of auranofin when given in combination with sirolimus after a round of platinum-based chemotherapy as well as the potential to inhibit lung cancer growth.

### 7.3. Next Generation Gold Therapeutic Complexes

Ongoing research efforts to generate Au-derived compounds that are safe, efficacious, and selective have led to building unique molecular scaffolds with features akin to the FDA approved auranofin. New Au complexes have led to the discovery of novel mechanisms, potency, and precise target engagement. We describe such developments in subsequent sections of this Review. Here we discuss efforts to create novel and efficacious Au(I) and Au(III) compounds for different disease indications. Due to the broad utility of Au agents for disease treatment we have organized this section by disease indication and provided recent advances in gold-based therapeutic development for each disease category. We claim that the discussion of individual compounds is beyond the scope of this Review.

**7.3.1. Antifungal Gold Complexes.**—Only three types of antifungal drugs exist for treatment, namely the azoles, which inhibit the primary fungal sterol, ergosterol; polyenes, which interact with the membranes of sterols; and 5-fluorocytosine, which is an inhibitor of macromolecular synthesis.<sup>305</sup> The growing threat of fungal resistance to these drugs poses a major health crisis and further affirms the desperate need for new drugs with different mechanism of action. The current excitement surrounding auranofin as antimicrobial agent provides impetus for the development of Au-derived antifungal agents. Seminal work by Garneau-Tsodikova and Awuah et al. demonstrated that chiral and achiral forms of linear and square-planar Au(I) complexes (Chart 16) display broad-spectrum activity and potent antifungal effects strains of the multidrug resistant fungus, *Candida auris*.<sup>306</sup> The reaction of Au(I)Cl(THT) with phosphine ligands in chloroform at room temperature give rise to dinuclear Au(I)-phosphines with a linear geometry as well as

distorted tetrahedral (based on the  $\tau_4$  parameter)<sup>307</sup> counterparts, which can be separated by column chromatography to obtain highly pure complexes. Notably, the distorted tetrahedral complexes bearing chiral 1,2-bis[(2*R*,5*R*)-2,5-dimethylphospholano]benzene or 1,2-bis[(2*S*,5*S*)-2,5-dimethylphospholano]benzene display excellent antifungal activity with MIC < 1.95  $\mu\text{g}/\text{mL}$ . Notably, AuFun-4 and AuFun-6 prevent biofilm formation and decrease metabolic activity of fungal biofilms.

Incorporating Au(III) into clinically approved antifungal azoles have been achieved via metalation of the imidazole (Chart 17).<sup>308</sup> These Au(III) complexes display antifungal activity in multiple *Candida* strains including *albicans*, *glabrata*, *kusei*, and *auris* in the submicromolar range. An asexual fungus, *Microsporium canis*, is highly prevalent worldwide that has high relapse rates and treatment failures could benefit from more efficacious antifungal agents such as gold-based antifungals.

A major drawback in antifungal metallodrug discovery is the lack of target discovery and a clear mechanism of fungal inhibition. The ability to harness some of the target identification strategies expounded in the earlier sections of this Review in the context of fungus has the potential to revolutionize gold-based antifungal discovery from oral agents to topical formulations.

**7.3.2. Antibacterial Gold Complexes.**—The continuous rise of antibiotic resistance possesses a major health threat to society with increasing treatment challenges.<sup>309–311</sup> Bacteria multidrug resistance mechanism against antibiotics arise through the production of enzymes that degrade antibiotics, overexpression of efflux pumps that drive antibiotics out of the bacterium, and alteration of target proteins through mutation.<sup>311,312</sup> Most of the new set of antibacterial drugs are derivatives of existing drugs and have also shown resistance to some strains of bacteria, hence the search for more efficacious drugs. Auranofin and other gold-based complexes have been studied as potential antibacterial agents. In a report by Cassetta et al., auranofin was shown to be potent against *Staphylococcus* spp. in a concentration dependent manner.<sup>313</sup> Auranofin also showed moderate bactericidal activity in *Staphylococcus aureus* and *Pseudomonas aeruginosa* biofilms.<sup>314,315</sup> Despite auranofin's potency against Gram-positive bacteria, its activity against Gram-negative bacteria has been suboptimal. The outer membrane of Gram-negative bacteria may create a barrier that prevents auranofin permeability. To mitigate this drawback, coadministration of auranofin with polymyxin B and E, antibiotics used for Gram-negative bacteria, has been shown as an effective way to improve auranofin activity.<sup>287</sup>

Wu et al. carried out structure activity relationship (SAR) on auranofin by modulating the thiol and phosphine ligands to create auranofin-like molecules. Forty compounds were screened for their activity against the notorious ESKAPE bacteria (*Enterococcus faecium*, *Staphylococcus aureus*, *Klebsiella pneumoniae*, *Acinetobacter baumannii*, *Pseudomonas aeruginosa*, and *Enterobacter cloacae*) and noted that compounds with trimethylphosphine ligands have improved activity against Gram-negative bacteria (Table 3). Their study also revealed that the thiol ligand is necessary for the bactericidal activity of both Gram-positive and Gram-negative bacteria.<sup>316</sup> Other reports from this lab have also shown that auranofin

and its derivatives are active against *Helicobacter pylori* and bacteria from the *Burkholderia* genus.<sup>317,318</sup>

Another study has also shown that auranofin inhibited, in a concentration-dependent manner, the growth of *Helicobacter pylori* TrxR (Gram-negative bacteria) and showed synergistic or additive effect with known *H. pylori* antibiotics such as amoxicillin or metronidazole and clarithromycin. Also, when the phosphane ligand on auranofin was replaced by N-heterocyclic carbene as shown in Figure 20, stability and inhibitory activity of the complexes were not altered greatly, and they show reduced *in vitro* toxicity.<sup>319</sup>

Schmidt et al. evaluated the activity of eight Au(I)-NHC complexes against ESKAPE bacteria, the bactericidal activity of the complexes **Au(I)-NHC 1–8** (Chart 18) was in the lower micromolar range for Gram-positive bacteria and Gram-negative bacteria showed resistance to drug treatment, this results compared to earlier works suggest that the nature of the NHC used can be a factor in determining the activity of this class of compound and the lack of glutathione in many Gram-positive bacteria resulted in greater dependence on the thioredoxin/thioredoxin reductase system.<sup>320</sup> Thus, sensitizing such cells to these gold compounds that inhibit TrxR. Pyrazine functionalized Au(I)-NHC complexes have also been studied as potential antibiotics. These stable neutral (**Au-NHC 9**) and cationic (**Au-NHC 10**) complexes inhibit biofilm formation, and are potent against pathogens that showed resistance to antibiotics with MIC of 2–16  $\mu\text{g}/\text{mL}$ , and are nontoxic to the red blood cells with docking studies suggesting affinity for the Dap-type peptidoglycan thereby inhibiting the synthesis of cell wall.<sup>321</sup> Another report incorporating derivatives of estrogen, ethinylestradiol (**Au-NHC 12**) and ethisterone (**Au-NHC 13**) to carbenes was shown to have lower *in vitro* antibacterial activity compared to the precursor carbenes in both *S.aureus* and *E. coli* strain and the complexes were nontoxic in an *in vivo* experiment.<sup>322</sup>

Bussing et al. also reported Au(I)-NHC complexes and their Au(III) counterpart and examined their antibacterial and thioredoxin inhibition (Chart 19). The oxidation state of the gold complexes did not affect the cytotoxicity as both classes of compounds are similar in activity with higher bactericidal activity in Gram-positive bacteria (*E. faecium*, methicillin-resistant *S. aureus*, MRSA) compared to Gram-negative bacteria (*A. baumannii*, *E. coli*, *K. pneumoniae*, *P. aeruginosa*) studied. Using an enzymatic assay, the inhibition of thioredoxin was studied in isolated *E. coli* TrxR. All complexes inhibited TrxR with an  $\text{IC}_{50}$  of 0.2–0.6  $\mu\text{M}$  suggesting its mechanism of action to be inhibition of thioredoxin.<sup>323</sup>

Recent studies on Au(I) selenium NHC complexes by Chen et al. showed potent antibacterial activity on multidrug-resistant bacterial strains both *in vitro* and *in vivo* comparable to auranofin. The antibacterial mechanism of action of these Au(I) selenium complexes were related to cellular DNA degradation and irreversible inhibition of the bacterial TrxR via targeting the redox-active motif.<sup>324</sup>

Cationic Au(I) benzothiazoles (Chart 20) complexes have been shown to inhibit the spread of *A. baumannii* in skin and soft tissue infection (SSTI) model experiment. The inhibition of *A. baumannii*, a Gram-negative bacterium by **Au-BTZ 1** and **Au-BTZ 2** compared to neutral

AuCl(PPh<sub>3</sub>) was attributed to the ability of the cationic complexes to move through the cell wall and interfere with biological processes in the cell.<sup>325</sup>

Alkynyl gold(I) complex is another class of compound that has been studied for their bactericidal activity (Chart 21). Novel alkynyl chromone or flavone complexes bearing Au(I)PPh<sub>3</sub> were synthesized in good yields and compared with Au(I)PPh<sub>3</sub> against both Gram-positive and Gram-negative bacteria strains. The complexes exhibited high bactericidal activity with a MIC between 1 and 4 µg/mL for **Au-chromone-1** and **Au-chromone-2** comparable to Au(I) TPP in strains of Gram-positive bacteria *S. aureus* but were not effective in Gram-negative bacteria *E. coli*.<sup>326</sup>

Pintus et al. synthesized Au(III) dithiolate complexes (Chart 22) and evaluated their antimicrobial activity against 10 strains of Gram-positive and Gram-negative bacteria using the agar diffusion method. The compounds were selective in their action as it inhibited growth from the 2 strains of *Staphylococcus* tested, this could be because of permeable cell surface structure of cocci Gram-positive bacteria compared to other strains examined. The difference in metabolism of *Staphylococcus* compared to *Streptococcus* strains may account for the disparity in sensitivity of **Au(III)-dithiolate-1** to both strains. **Au(III)-dithiolate-1** also interfered with biofilm formation in strains *Staphylococcus* at a concentration of 3.125 µg/mL.<sup>327</sup> Fontinha and co-workers (Chart 22) further synthesized and tested 6 Au(III) bis(dithiolate) and evaluated their antibacterial and anticancer activity. Antibacterial activity of *S. aureus* Newman, and *E. coli* was determined using the microdilution method. Only **Au(III)-dithiolate-2** inhibited the growth of *S. aureus* Newman with MIC value of 12.5 µg/mL, while other compounds had MIC values greater than 125 µg/mL indicating no inhibition. Although the MICs of these Au(III) dithiolate complexes are higher than auranofin, they provide a new structural class in expanding the library of Au(III) antibacterial agents.<sup>328</sup>

To understand the mechanism of action of Au(III) complexes, Chakraborty et al. synthesized several cyclometalated Au(III) complexes. All complexes studied were inactive against *E. coli* and *B. subtilis* bacteria strains except **Au(III)C<sup>N</sup>-Cl<sub>2</sub>** and **[Au(III)C<sup>N</sup>NS]PF<sub>6</sub>** (Chart 23) that inhibited *B. subtilis* colonies comparable to kanamycin, a potent antibiotic. Further experiment to decipher the mode of action of **Au(III)C<sup>N</sup>-Cl<sub>2</sub>** on *B. subtilis* reveals that the compound has no effect on bacterial membrane permeability, membrane potential and there was no generation of reactive oxygen species, but a decrease in overall energy levels of the cells. RNA sequencing result shows that several metal transporters, oxidoreductases, and proteases were upregulated while genes involved in cell wall formation and ABC transporter genes were downregulated. Overall, a multimodal mechanism of action was proposed involving various cellular stress response pathways.<sup>329</sup>

**7.3.3. Antileishmanial Gold Complexes.**—The disease burden imposed by leishmania parasites remains a major public health concern, particularly in the tropics. Current treatment approaches for visceral and cutaneous forms of leishmaniasis include miltefosine, pentamidine, paromomycin, amphotericin B, and the antimonates (urea stibamine, sodium stibogluconate, meglumine antimoniate). Whereas these agents have been employed for decades, effectiveness is a challenge in several cases, prompting



resistance and requiring higher doses of drugs. New agents such as auranofin display strong leishmanicidal activity, thus uncovering an untapped chemical space for gold complexes in the treatment of leishmaniasis. The premise for the use of Au(I) complexes is derived from the established interaction of Au(I) with the thioredoxin machinery in humans that is akin to the trypanothione system in leishmania parasites for redox homeostasis.<sup>330</sup> Establishment of auranofin as an antileishmanial agent was through a high-throughput screening campaign to identify novel antileishmanial chemotypes using a library of 2,157 bioactive compounds. Auranofin showed prominent growth inhibition of *L. amazonensis* promastigote and dose–response assays with EC50 comparable to the established antileishmanial drug, amphotericin B (Chart 24). In a Balb/c mouse model inoculated with 10<sup>6</sup> metacyclic *L. major* promastigotes, auranofin dosed 20 mg/kg/d × 10 d, or liposomal amphotericin B at 12.5 mg/kg/d × 10 d, showed comparable lesion suppression. These impressive results expanded. An expanded structural study of the gold pharmacophore against leishmaniasis provides impetus for antileishmanial drug discovery.<sup>331</sup> For a discussion into the potential mechanisms and biological targets of leishmaniasis, we refer readers to a recent review by Abbehausen et al.<sup>332</sup>

Structure–activity relationship studies using neutral Au(I) complexes of the type Cl–Au–L, where L represent different monodentate phosphine ligands of electronic and steric variability, significant modulation of antileishmanial activity was observed.<sup>331</sup> As shown in Table 4, water-soluble phosphines showed attenuated antileishmanial response, implicating lipophilicity as an important descriptor.

Benzimidazole-ligated Au(I) and Au(III) complexes (Chart 25) represent another class of antileishmanial agents with activity against promastigotes of *L. amazonensis*, *L. braziliensis*, and *L. major*.<sup>333</sup> The condensation of o-phenylenediamine with benzaldehyde or p-anisaldehyde generated ligands in respectable yields for Au(I) or Au(III) metalation. Although the antileishmanial effects of these complexes are modest in the range of (1–54 μM), it provides a framework to expand this class of compounds.

Gold-derived antileishmanial complexes bearing NHC ligands have shown encouraging results. The NHC ligands enable the formation of Au–C bonds for stabilization and demonstrates potential for diversification. Beginning with the synthesis of imidazolium salts, metalation to form carbene Au complexes could be either through transmetalation with Ag or direct metalation with Au in the presence of a base. Both monofunctionalized carbene and bis-carbene Au complexes have been achieved through the process (Chart 26).<sup>334,335</sup> The antileishmanial activity of Au(I)-NHC complexes are in the sub micromolar range in promastigotes of *L. major* or *L. infantum* and *Leishmania* intracellular amastigotes. Notably, mononuclear neutral Au(I)-NHC complexes with asymmetric imidazole substitution achieve nanomolar inhibitory concentrations in *L. infantum* axenic amastigotes with selectivity index of >40.<sup>336</sup> Encouraging results demonstrated the ease of functionalizing NHCs and the broad tunable characteristics imparted on biological response by NHC ligands make them attractive for exploration in leishmaniasis drug discovery. Recently Nolan et al. reported Au(III) bis-carbene complexes that act as potent inhibitors of α-glucosidase and β-glucuronidase and antileishmanial activity of 0.11–1.62 μM in *Leishmania major* promastigotes.

A new class of Au(I)-oxadiazole complexes (Chart 27) with antileishmanial activity was synthesized by the reaction of Au(PEt<sub>3</sub>)Cl or Au(PPh<sub>3</sub>)Cl and 5-phenyl-1,3,4-oxadiazole-2-thione ligands.<sup>337</sup> The aromatic ring of the ligand accommodates different substituent groups, ranging from gluconolactone,<sup>338</sup> electron withdrawing NO<sub>2</sub>, F, and Cl groups to electron donating, OCH<sub>3</sub> groups that affect the electronic character of the complex and contribute to diversity. The antileishmanial activity did not discriminate against chemical modification.

In a more elaborate study with translational potential, Monte-Neto and co-workers synthesized a new class of adamantane substituted oxadiazole or thiazolidine Au(I) phosphines as antileishmanial agents.<sup>339</sup> The complexes inhibit thioredoxin reductase in mammalian cells and trypanothione reductase in parasites, eliciting potent antileishmanial activity in the low micromolar range across multiple leishmania species via oxidative stress. *In vivo* efficacy demonstrates that combination of the Au agents with Miltefosine reduces lesions by up to 65% and parasitic load of up to 80% by luminescence measurements (Figure 21). Taken together, these studies set the stage for clinical development of **AdT Et** as a monotherapy or in combination with existing drugs for the elimination of leishmaniasis.

**7.3.4. Anticancer Gold Complexes.**—Several research groups have capitalized on the hopeful clinical development of auranofin for cancer therapy to develop new Au(I) and Au(III) anticancer complexes with the goal of uncovering novel mechanisms and targets, improve *in vivo* potency and minimize potential side effects. We describe such endeavors in subsequent sections of this Review. It is important to note that perturbations made to Au(I) and Au(III) scaffolds through ligand modification remain at their peak. Here, we discuss efforts to create novel gold complexes that are structurally distinct and have potential for targeted therapy. Given that recent reviews on gold in biology have focused on the anticancer action, we pivot this section to recent developments toward new anticancer scaffold and targeting strategies to achieve highly efficacious Au agents. Specifically, we have chosen to focus on organelle-specific targeting, tumor targeting using ligands or antibodies, and immunochemotherapy involving gold complexes.

**7.3.4.1. Mitochondrial Targeting of Gold Complexes.:** Mitochondria is commonly referred to as the powerhouse of the cell due to its abundant production of ATP through the redox driven oxidative phosphorylation process.<sup>340–344</sup> In addition to being an energy hub, mitochondria are involved in anabolic and catabolic biological processes that facilitate cell signaling, differentiation, immune signaling, growth and cell death pathways.<sup>95,345–351</sup> The mitochondria structure is defined by an outer membrane, which protects the protein-rich matrix of the organelle and the inner mitochondria membrane that is home to the electron transport chain responsible for mitochondria respiration. Intrinsic functions of the organelle include mitochondrial respiration/bioenergetics, dynamics (fusion/fission), morphology, fatty acid oxidation, and superoxide-mediated signaling to mention a few. Increasing evidence implicates mitochondria dysfunction in cancer, representing a viable target. Although many examples of gold complexes that modulate mitochondria function are known, uncovering direct targets beyond thioredoxin have been underexplored.

Early reports by Berners Price demonstrated that cationic Au(I) analogs bearing bis-phosphine or bis-carbene ligands could induce mitochondrial dysfunction through mitochondrial uncoupling activity and the disruption of thioredoxin system.<sup>95,352,353</sup> Recent developments in omics technology have contributed to gold drug discovery in ways that uncover new mitochondrial pathways or targets. The negative inner membrane potential of the mitochondria serves as a driving force for the accumulation of lipophilic cationic structures. This phenomenon has been well studied and selective mitochondria targeting via cationic ligands has been recently reviewed.<sup>109</sup> The Lewis acidic character of gold as earlier described coupled with the lipophilic ligands can often generate cationic Au complexes with degrees of lipophilicity  $>2$ . This structural feature makes such complexes innately attracted to the redox active mitochondria. Awuah and co-workers have exploited this feature to uncover novel mitochondria pathways impacted by rationally designed Au(I) and Au(III) complexes.

An interesting discovery of Au complexes that perturb mitochondria structure offers new tools and potential therapeutics for the treatment of diseases.<sup>336,354</sup> Phosphine and arsine supported Au(I) complexes ligated by N<sup>^</sup>N-bidentate ligands afford unsymmetrical cationic structures in three-coordinate geometry, referred to as AuTri (Figure 22).<sup>355,356</sup> The different Au–N bonds of the metal center to the bidentate ligand dictates the asymmetry. The rational was to rely on the labile Au–N bond for binding to macromolecules under physiological conditions. Using transmission emission tomography (TEM), the AuTri compounds induced distortions of the mitochondria structure with concomitant time-dependent depletion of mitochondria membrane proteins including, OPA1, MFN1, MFF, and TOM20 by Western blot. A global proteomics study of AuTri-9 treated in comparison to untreated breast cancer cells showed that differentially expressed proteins were largely mitochondria membrane proteins. Overall, this work highlights the potential to identify new Au complexes that target novel biological targets and further supports the report that disruption of mitochondrial structure proteins may overcome cancer drug resistance.

Derivatives of Au(III) dithiocarbamate (AuDTC) have been prepared with strong proteasome inhibition and anticancer activity against breast and prostate cancer.<sup>357–360</sup> These complexes possessed dibromido ligands and peptide ligands ligated to the Au center via a thiolate moiety. Modifications to AuDTC by incorporating  $\hat{C}N$ -cyclometalated ligands and tuning the ancillary ligands with different dialkyl dithiocarbamate ligands generate highly potent Au(III) complexes with selective mitochondria targeting (Chart 28).<sup>361</sup> Using transcriptomics, bioenergetics, and function mitochondrial assays the lead AuDTC complex displayed cancer cell selective inhibition of mitochondrial respiration. The impact of ligand tuning cannot be underestimated in the design of Au(III) anticancer agents, particularly in the context of mechanism of action and potency.

A new class of organogold(III) complexes was synthesized by the reaction of  $\hat{C}N$ -cyclometalated Au(III) complexes with bis-phosphine ligands under mild conditions, herein referred to as AuPhos (Chart 29).<sup>362</sup> The geometry of the complexes could be square planar or square pyramidal depending on the ligand. Whereas the varying geometry is an interesting finding, more work is required to provide guiding principles and insights into the structural phenomenon. Interestingly, AuPhos modulates mitochondria activity with high

potency across the NCI-60 panel and *in vivo* tumor inhibition in the aggressive 4T1 TNBC mouse model. Combined transcriptomics and proteomics reveal the mitochondrial electron transport chain as a potential target for the lead AuPhos-89 complex.<sup>362</sup> A chiral form of AuPhos, using the chiral QuinoxP ligand gave rise to AuPhos-19<sup>363</sup> which induces ATF4 activation and inhibits mitochondria respiration acutely with potent *in vivo* activity.<sup>175</sup> A careful examination of the speciation of this class of compounds supports stability under physiological conditions with minor Au(I) species and concomitant reductively eliminated aryl(C)–S bond formation under reducing glutathione conditions. Expanding the chemical library of AuPhos has enormous potential for therapeutic discovery.

Independent studies by Ang and Awuah developed Au(III)-metformin complexes, herein **3met** or **auraformin** (Chart 30) with significant efficacy against TNBC.<sup>364,365</sup> Coordination of the N-donor ligands from the FDA approved metformin to the  $\hat{C}N$ -cyclometalated Au(III) center afford square planar prodrugs with superior potency to metformin up to 6000-fold. **Auraformin-1** (Chart 30) reportedly accumulates significantly in the mitochondria of MDA-MB-468 cells to efficiently impair mitochondria respiration and depolarize the mitochondria membrane. Similarly, the **3met** (**Auraformin-2**) was reported to disrupt energy metabolism in MDA-MB-231 cells and induce ER stress and autophagy.<sup>365</sup> *In vivo* efficacy of **3met** (**Auraformin-2**) was demonstrated in athymic nude mice with orthotopic implantation of MDA-MB231 cells in the mammary fat pad. Significant tumor reduction was noted at 15 mg/kg after 3 weeks. The promising *in vivo* activity of this class of compounds establishes a platform for translational application in the treatment of aggressive cancer.

**7.3.4.2. Gold Conjugated Cancer Targeting Ligands.:** Direct interaction of anticancer agents with tumors can be greatly enriched by selective targeting of overexpressing proteins or receptors in cancer that often act as biomarkers. Gold complexes conjugated to cell adhesion molecules (e.g., integrins), epidermal growth factor receptors, G-protein coupled receptors (e.g., bombesin), hormone receptors and glucose transporters have been explored (Chart 31).<sup>366</sup> The use of cancer targeting ligands and peptides, either linear or cyclic have been demonstrated *in vitro*. For example, integrins overexpressed in multiple solid tumors such as breast cancer are heterodimeric transmembrane receptors composed of an  $\alpha$ - and  $\beta$ - subunit noncovalently associated with each other. Conjugation of RGD peptides to Au(III) $\hat{C}N$ -Cl<sub>2</sub> complexes via a dithiolate moiety led to Au(III)-RGD constructs **A** and **A'** with improved efficacy in breast cancer.<sup>367</sup> Additionally, the conjugation of pyrazine supported pincer Au(III) complex [Au(bbfpz)(acbim)]<sup>+</sup> (bbfpz = 2,6-bis(4-(*tert*-butyl)phenyl)-pyrazine; acbim = 1-methyl-3-(4-(6-aminoethyl)-carboxamido)benzylbenzimidazol-2-ylidene) to a derivative of 17 $\alpha$ -ethinylestradiol afforded Au(III)-ER conjugates, **B** with potent cytotoxicity and uptake in ER(+) breast cancer cells than ER(-) cells.<sup>368</sup> Moreover, linear Au(I) complexes can be tethered to EGFR inhibitors such as erlotinib, **C** to improve anticancer action by ~68-fold in EGFR positive breast cancer, MDA-MB-231.<sup>369</sup> Conjugating the human epidermal growth factor receptor (HER2) antibody, Trastuzumab or otherwise known as Herceptin to Au(PPh<sub>3</sub>)(DPTP) (DPTP = 2,5-dioxopyrrolidinyl-3-(1-*H*-1,2,3-triazol-4-yl)propanoate) or Au-(PPh<sub>3</sub>)(MBANHS) (MBANHS = 4-mercapto-benzylmaleimido propionamide) via *N*-hydroxysuccinimide or maleimide groups respectively achieved constructs **D** and **E** with

enhanced cytotoxicity in breast cancer cells expressing HER2 compared to the parent Au(I) complexes.<sup>370</sup> Au(III) biotin complexes **F** have also been developed to target cancers that overexpress biotin receptors (BR). Selectivity of these constructs were achieved in BR(+) MCF7 compared to BR(-) HCT-116 cells.<sup>368</sup> Despite the promising results of these targeting constructs, the lack of validation in isogenic cell lines or *in vivo* is a major bottleneck.

**7.3.4.3. Immunogenic Cell Death (ICD) Induction by Gold Complexes.:** Other metal complexes and several gold complexes have been shown to induce immune-potentiating effects.<sup>371,372</sup> Gold(I) compounds not only act on tumor cells and immune cells directly, but also affect the expression of cell adhesion molecules on endothelial cells.<sup>373</sup> Despite chemotherapy commonly increasing the risk of secondary infections via myelosuppression and lymphocytopenia, indicating that it may lead to immune suppression, an appropriate combination of cytotoxic chemotherapy and immunotherapy may exert a highly synergistic anticancer activity.<sup>373–375</sup> Innate immunity forms the first line of defense in the human immune system. For example, NK cells are natural immune effector cells with a direct killing function that plays a key role in the clearance of tumor cells. Metal drugs have been shown to upregulate signals on cancer cells that are perceptible to the NK cell compartment, such as the Nkp30 ligand B7-H6F.<sup>376</sup> Gold compounds such as [Au(C-C-2-NC<sub>5</sub>H<sub>4</sub>)(PTA)] induce colorectal carcinoma cell death via ROS-mediated necroptosis by activating TNF- $\alpha$  and NF- $\kappa$ B signaling and also have been shown to exert an immunosuppressive role by inhibiting IKK kinase activation and promoting cell apoptosis.<sup>377–379</sup> Au(I) can oxidize inside phagocyte lysosomal compartments, resulting in Au(III), which plays the role of a major hapten that acts synergistically in innate immunity.<sup>380</sup> Elie et al. investigated the antimetastatic effects of gold compounds in renal cancer cells and revealed strong inhibition of several cytokines (IL17A, IL-8, IL-6, and IL-5) by gold compounds.<sup>377–379,381</sup> Various studies have shown that gold compounds can elicit an innate immune response, which can be ascribed to the triggering of TLR3 rather than TLR4.<sup>382</sup> Additionally, to innate immunity, adaptive immunity presents another unique angle to approach gold-based immunotherapy. Although not thoroughly researched, a seminal study suggested that gold compounds contribute to the frequent development of adaptive immunity by directly triggering TLR3 and increasing the expression of downstream mediators.<sup>383</sup>

Immunogenic cell death is a form of cell death that can stimulate the immune response to antideath cell antigens, especially those derived from tumor cells.<sup>384</sup> Gold compounds in combination with CRISPR/Cas9-mediated disruption of PD-L1 and mild hyperthermia induce the activation of immunogenic cell death.<sup>384,385</sup> Additionally, gold compounds eliminate primary tumors and induce immunogenic cell death via the release of damage-associated molecular patterns (DAMPs), activation of effector cells, and induction of dendritic cell maturation. These phenomena, in a coordinated manner, eventually evoke systematic anticancer immune responses.<sup>386,387</sup>

Recently, Sessler and Arambula et al. reported Au(I) bis N-heterocyclic carbene (NHC) that induce ICD *in vitro* and *in vivo* (Figure 23).<sup>387</sup> A potential mechanism for this phenomenon is the inhibition of thioredoxin system and promotion of ER stress to promote type II ICD as evidenced by CRT translocation and the release of ATP and HMGB1. Further,

Balb/c mice were subcutaneous injected with CT26 cells pretreated with Au-ICD (5, 10, and 100  $\mu$ M) and subsequently challenged with na>ve, live CT26 cells on the other flank. Strikingly, delayed or no tumors developed on the challenged in a manner consistent with the concentration of Au-ICD dosed. Demonstrably, gold compounds can induce ICD *in vivo* and have potential for cancer vaccine development.

**7.3.4.4. Gold Compounds Targeting Cancer Stem Cells.:** Eradication of cancer stem cells (CSCs) represents a difficult challenge in the effective treatment of cancer patients. Given the capacity of CSCs for self-renewal, differentiation and secondary tumor formation, CSCs can evade conventional chemotherapy regimen and drive tumor relapse in treated patients.<sup>388,389</sup> Current standard of care chemotherapy agents for treatment of patients and many reported organometallic complexes are ineffective in removing CSCs.<sup>390</sup> Hence, the need for improved treatment options effective against both bulk tumor cells as well as CSCs.

Zou et al. reported binucleargold(I) complex with mixed bridging diphosphine and bis(*N*-heterocyclic carbene) ligands that inhibited self-renewal ability in HeLa and U-87 MG human glioblastoma cells *in vivo* with 79% tumor volume inhibition in nude mice bearing HeLa xenografts.<sup>391</sup> Roesch et al. synthesized 6-membered phosphorus heterocycles Au(I) compounds and examined their anticancer activity in both glioblastoma cancer cells (GCC) and glioblastoma stem-like cells (GSC). The compounds were potent in GCC and demonstrated observable decrease in wound closure in glioblastoma stem-like cells.<sup>392</sup>

Suntharalingam and co-workers developed gold(I) complexes bearing nonsteroidal anti-inflammatory drugs (NSAID) to target breast cancer stem-cells (Figure 24).<sup>393</sup> Lead complex containing indomethacin moiety showed greater inhibitory effect (80-fold) against breast CSCs than the bulk breast cancer cell population. An inquiry into the mechanism of action of the lead complex revealed cytoplasmic accumulation of the complex, inhibition of cyclooxygenase-2 (COX-2) and increased levels of intracellular ROS. *In vivo* efficacy for the gold(I)-indomethacin complex was demonstrated in 4T1 tumor-bearing mice; tumor was significantly reduced without affecting mice body weight. This work further demonstrates that targeting CSCs is an effective strategy for cancer treatment.<sup>393</sup>

Sun et al. also reported a gold(III) *meso*-tetraphenylporphyrin complex that inhibit formation of spheroids from single cell suspension in U-87 glioblastoma cancer cells. The porphyrin complex demonstrated potent *in vitro* and *in vivo* toxicity in a panel of cancer cells and high physiological stability in glutathione and serum albumen. Furthermore, there was a reduction in NANOG expression (stemness marker), while deregulating 16 microRNAs linked to glioblastoma stem cell function.<sup>394</sup>

**7.3.5. Antiviral Gold Complexes.—**Given the timing of the review coinciding with the latter half of the pandemic, it is important to highlight the potential antiviral properties of a few gold complexes. The current outbreak of SARS-CoV-2 has resulted in an unprecedented health crisis with the number of infected well into the millions.<sup>395</sup> The lack of an effective antiviral drug for the treatment has triggered a major surge in drug-development, specifically transition metal complexes given their success in the past. The urgent development of an effective therapeutic is an utmost priority for medicinal chemists across the globe.



Despite the long-standing history of gold complexes in medicine, it was without question that chemists would turn to gold-based complexes by either (a) repurposing old drug candidates and (b) developing new innovative scaffolds. The application of gold complexes as antiviral drugs has not been studied very intensively, although some promising results suggest a possible future use as human immunodeficiency virus (HIV) therapeutics.<sup>41,396,397</sup> Gil-Moles et al. reported a pilot study in which select gold complexes were investigated to determine their activity against two coronavirus targets (spike protein, papain like protease, and PLpro) (Figure 25).<sup>159</sup>

An enzymatic FRET assay was used to determine the antiviral activity of gold compounds against PLpro from SARS-CoV-1 and SARS-CoV-2. The  $IC_{50}$  for Au-1, Au-2, and Au-5 against PLpro from SARS-CoV-1 was determined to be within the range of 5–7  $\mu\text{M}$ . This range is similar to the inhibitory concentration of Disulfiram, which was used as a reference for comparison. The gold complexes Au-3 and Au-4 showed less antiviral effect with an  $IC_{50}$  of 14  $\mu\text{M}$ , while Auranofin had the least inhibitory effect with with  $IC_{50}$  of 25.5  $\mu\text{M}$  as represented in Table 5.<sup>159</sup>

A recent review profiled inhibition of SARS-CoV-2 by structurally diverse metal complexes including 36 gold(I)/(III) complexes.<sup>398</sup> Inhibition of SARS-CoV-2 can occur either by the interaction of spike protein with the ACE2 receptor or by the papain-like protease PLpro. For instance, chloroauric acid showed a moderate inhibition (about 47% inhibitory activity) while the other gold compounds were poorly active or inactive.<sup>398</sup>

Also, structure–activity relationship studies reveals a preference for complexes with good leaving groups (e.g., chloride) compared to complexes with firmly coordinated ligands such as dicarbene gold complexes of the type  $[(\text{NHC})_2\text{Au}]^+$ , which were inactive. Gold(III) dithiocarbamate glycoconjugates showed strong selectivity against SARS-CoV-2 PLpro.<sup>398</sup> The gold complexes studied showed strong toxicity against Caco-2 cell line except for four complexes which were then selected and tested for SARS-CoV-2 antiviral assay, with the  $[\text{Au}(\text{I})\text{-NHC}]$  complex showing excellent activity at micromolar range.

Auranofin has also been shown to inhibit SARS-CoV-2 replication in human cells (Huh7 cells) at a low concentration ( $EC_{50}$  1.4  $\mu\text{M}$ )<sup>52</sup> with about 95% reduction in the viral RNA at 48 h after infection. Treatment with auranofin showed a reduction of SARS-CoV-2-induced cytokines expression levels in human cells. These results indicate that auranofin could be potent to limit SARS-CoV-2 infection and associated lung injury due to its antiviral, anti-inflammatory and antireactive oxygen species (ROS) properties. Further *in vivo* study is required to establish the safety and efficacy of auranofin for the management of SARS-CoV-2 associated disease.<sup>399,400</sup>

Furthermore, highly active antiretroviral therapy (HAART) has caused decreased death rate from acquired immune deficiency syndrome due to human immunodeficiency virus.<sup>401</sup> However, acquired drug resistance has hindered the success of current HAART, therefore the need for improved therapeutics.<sup>402–404</sup> In addition, reports exist on gold-based inhibitors of reverse transcriptase (RT), protease (PR) and viral entry of host cells.<sup>339,405–409</sup>

Taken together, the antiviral properties of gold complexes prove to be a critical field of study for medicinal chemists to tackle as approaches to develop therapeutics remains to be confined to simply repurposing old drugs such as auranofin. Given the success auranofin has had and promising characteristics, it is up to current day medicinal chemists to explore more innovative avenues in developing new gold-based therapeutics for antiviral therapies.

**7.3.6. Gold in Inflammatory Bowel Diseases.**—Gold compounds (in this case auranofin) have been shown to decrease the expression of inflammatory cytokines (IL-1 $\beta$ , IL-6 and TNF) in rheumatoid arthritis patients as well as inhibits the expression of nuclear factor kappa beta (NF- $\kappa$ B) which has been associated with chronic inflammatory diseases e.g., IBD.<sup>378,410–413</sup> Given this finding, to date there have been scarce attempts at purposing gold-based complexes for IBD therapy.

In 2012, seminal work by Travnicek et al. reported the synthesis of a class of AuPPh<sub>3</sub> complexes with anti-inflammatory activity (Chart 32).<sup>414</sup> These complexes exhibited a strong ability to reduce the production of pro-inflammatory cytokines such as TNF- $\alpha$ , IL-1 $\beta$ , and HMGB1 without effecting secretion of anti-inflammatory cytokines from LPS activated macrophages. The complexes significantly influenced the formation of edema induced by polysaccharide carrageenan *in vivo*. Notably, these compounds were significantly less toxic than auranofin in culture.

Several Au(I) complexes bearing *O*-substituted 9-deazahypoxanthine derivatives (**1–5**; Chart 33) have been reported for their antitumor and anti-inflammatory activity. The compounds show potent anticancer activity in a panel of cancer cell lines (MCF7, HOS, A549, G361, A2780, A2780R, 22Rv1, and THP-1) with IC<sub>50</sub>s in the range of 0.6–22.8  $\mu$ M. In addition, the complexes show no cross-resistance to cisplatin and are more efficacious than cisplatin in the cell lines tested. The complexes show significant selectivity for cancer cells compared to normal HEP220 cell lines. Furthermore, results from the anti-inflammatory activity of **1–5** (Chart 33) revealed that the complexes significantly decreased the production of TNF- $\alpha$  and IL-1 $\beta$ , attenuating the production of pro-inflammatory cytokines by blocking NF- $\kappa$ B signaling and inhibiting I $\kappa$ B degradation similar to auranofin. Also, *in vivo* anti-inflammatory activity of **2** (Chart 33) in a carrageenan-induced hind paw edema model reveals a pronounced antiedematous effect comparable to the FDA approved Indomethacin.<sup>415</sup>

Another recent report by Bodio et al. developed BODIPY tagged gold(I)-imidazole bimetallic complexes (as seen in section 5.1.1), which exhibited anti-inflammatory effects.<sup>227</sup> Although these complexes were designed with anticancer therapies in mind the researchers discovered that BDP-Au7 is far less toxic: viability of PBMC is slightly superior to 60% at 10  $\mu$ M. Interestingly, at 1  $\mu$ M, BDP-Au7 inhibits more than 30% of the production of IL-1 $\beta$  without displaying any toxicity, and at 3  $\mu$ M, BDP-Au7 inhibits almost all the production of IL-1 $\beta$  with low toxicity.

Recently, work by Wempe et al. utilized a novel gold(III) complex, termed AuPhos developed by Awuah and co-workers for the treatment of ulcerative colitis.<sup>416</sup> Initial pharmacokinetics and biodistribution studies revealed that oral administration of AuPhos

demonstrated high rates of adsorption into the small intestine and colon compared to systemic adsorption while displaying a dose-dependent uptake in IEC mitochondria. *In vivo* studies revealed that mice treated with AuPhos showed lower disease activity index (DAI), histology score, and FITC-dextran compared to vehicle control. Mechanistically, oral administration of AuPhos increased crypt fissioning near the mucosa while simultaneously reducing mRNA expression of pro-inflammatory cytokines.<sup>416</sup> Further studies by the group in a piroxicam-accelerated (Px) knockout mice (an accelerated colitis model) showed that administration of AuPhos led to reduced DAI, weight loss and less crypt ablation and hyperplasia evidenced by HE sectioning.<sup>417</sup> Mice administered with AuPhos had decreased DAI, reduction in weight loss, and resulted in less crypt ablation and hyperplasia evidenced by HE sectioning. RT-qPCR of tissue from Px-IL10 KO mice treated with AuPhos revealed significant increases in mitochondrial complex I genes (Ndufa1, Ndufa4, Ndufb6), complex IV gene (Cox5B), and stem cell markers (Lgr4, Lgr5, and Lrig1), with corresponding decreases in pro-inflammatory markers (IL-1 $\beta$ , MCP1, and RankL).<sup>417,418</sup> These new promising findings suggest that gold complexes can be tuned to modulate bioenergetics and metabolism to prevent inflammation-associated barrier damage when subjected to chronic colitis conditions.

## 8. TARGETING MODALITIES AND NANODELIVERY OF BIOACTIVE GOLD COMPLEXES

Nanobased constructs for the delivery of therapeutic agents have been clinically transformative. The ability to control the size, chemical, magnetic, and biological properties of nanocarriers and their drug cargo make nanoconstructs an excellent platform for drug delivery. Also, their enhanced bioavailability and controlled drug release profiles offer advantages for targeted delivery that minimize toxic side effects or improve efficacy.<sup>419–424</sup> Nanodrug delivery can occur either by active or passive targeting. In active targeting, the surface of the nanocarrier is coated with ligands such as peptides and antibodies that promote recognition of specific receptors or proteins overexpressed at the target site whereas in passive targeting, the physicochemical properties of the nanocarrier such as size, shape, pH, dictate affinity, internalization and enhances permeability and retention (EPR) at target sites.<sup>423,425–427</sup> Development of nanodelivery constructs for gold complexes have been described, employing different nanocarriers, such as liposomes, polymeric, apoferritin, albumen, collagen, and mesoporous silica materials. These have recently been reviewed by different authors,<sup>428–430</sup> thus we refrain from giving a detailed narrative here. Nevertheless, in a review of next generation gold drugs and probes, it is imperative that we provide an overview of the significant scientific and preclinical advances made in the nanodelivery of defined gold-based complexes.

### 8.1. Polymeric Nanoparticles

Au(I)-loaded poly( $\beta$ -amino ester) micelle-like nanoparticles have been reported by Wang et al. This pH-sensitive Au(I) polymeric nanoparticle triggers cancer cell death by autophagy. Evidence for lysosomal accumulation via endocytosis and consequent pH-driven nanoparticle degradation is the likely mechanism of the Au(I) cargo (Figure 26). The

released Au(I) agent subsequently inhibits TrxR activity to increase intracellular ROS, enhance oxidative stress and induce cell death.<sup>431</sup>

The *in vivo* anticancer potency of auranofin is limited by rapid ligand displacement upon interaction with serum albumin in circulation.<sup>432,433</sup> To circumvent this limitation, Stenzel et al. developed micellar analogs of auranofin using glycopolymers-based self-assembled micelles (Figure 27). The reported analogs were cytotoxic to OVCAR-3 ovarian cancer cells (in both serum-containing media and serum-free media) and less liable to deactivation by serum proteins compared to free auranofin, possibly due to the protection offered by the micelle system. However, the micellar analogs accumulate in the lysosomes unlike free auranofin, which interacts with TrxR. This suggests that the micellar nanoconstructs may have a mechanism of action distinct from auranofin.<sup>434</sup>

The triblock polymer, Pluronic F127 in combination with the amphiphilic peptide of the type (C18)<sub>2</sub>-PEG1000-G-CCK8, was used by Fregona and co-workers to form supramolecular aggregates that deliver Au(III) dithiocarbamate to enhance bioavailability. The functionalization of this aggregate system with cholecystokinin octapeptide (CCK8) act as a targeting moiety to improve tumor specificity. The resulting nanoconstruct demonstrated stability in saline solution up to 72 h and the CCK8 targeting moiety contributed to improved cytotoxicity and selectivity between A431 cells and CCK2-R-transfected A431 cells.<sup>435</sup>

Owing to the excellent physiological stability, anticancer activity, and the ability of Au(III) porphyrins (AuP) to form nanostructure, other approaches have also been utilized to deliver Au(III) porphyrin selectively to target cells. Che et al. developed Au(III) porphyrin-PEG conjugates [Au(TPP-COO-PEG<sub>5000</sub>-OCH<sub>3</sub>)]Cl and [Au(TPP-CONH-PEG<sub>5000</sub>-OCH<sub>3</sub>)]Cl that self-assemble into nanostructures.<sup>436</sup> The conjugates feature an ester linkage that is easily hydrolyzed, leading to release of the chemotherapeutic Au(III) porphyrin [Au(TPP-COOH)]+ *in vitro* and *in vivo*. The nanostructures showed selective cytotoxicity in cancer cells ((HeLa, NCI-H460, HCT116, A2780) compared to normal cells. The lead Au(III) porphyrin-PEG conjugate [Au(TPP-COO-PEG<sub>5000</sub>-OCH<sub>3</sub>)]Cl (Au-P-P in Figure 28) significantly inhibited tumor growth in HCT116 xenografts tumor bearing mice.<sup>436</sup> These studies highlight the potential for polymer-based self-assembled nanoparticles to facilitate the delivery of gold-derived therapeutics.

Recently, Kao and Che et al. utilized a multifunctional hydrogel and microparticle system to deliver AuP in a lung cancer xenograft.<sup>437,438</sup> AuP was loaded into polyethylene glycol (PEG)-diacrylate (PEGdA) or an interpenetrating network system (IPN) composed of PEGdA and gelatin conjugated with PEG-cysteine (Gel-PEG-Cys). Results showed that increasing the mole ratio of PEG-400 to AuP from 636:1, 1270:1, 2540:1, 5650:1, 11,300:1, 25,400:1, to 67,800:1 led to the corresponding decrease in size of the AuP-PEG-400 constructs from 12.07 ± 1.40 μm, 5.61 ± 0.91 μm, 4.68 ± 1.28 μm, 3.37 ± 1.95 μm, 2.80 ± 0.36 μm, 1.03 ± 0.71 μm, to 0.23 ± 0.03 μm, respectively. The cumulative release profile of AuP-loaded IPN reached about 65% after 7 days following an initial burst within the first 24 h compared to the AuP-loaded PEGdA that showed about 30% release of AuP after 7 days. Cell cytotoxicity studies showed that AuP-loaded IPN exhibited significantly higher

cytotoxicity in A549 and NCI-H460 lung cancer cells compared to IPN control *in vitro* and inhibited tumor growth in mice.<sup>437</sup>

## 8.2. Lipid-Based Micelles

Sterically stabilized micelles (SSM) of DSPE-PEG2000, and sterically stabilized mixed micelles (SSMM) composed of egg 1- $\alpha$ -phosphatidylcholine (PC) or 1,2-dioleoyl-*sn*-glycero-3-phosphocholine (DOPC) phospholipids (with different DSPE-PEG2000 mol ratio) as delivery systems for Au(III)-dithiocarbamate complexes have been reported. Bombesin peptide derivatives were incorporated into the micelles to improve targeting. The liposomal constructs enabled Au(III) dithiocarbamate stability, selective uptake and anticancer potential in PC-3 cells overexpressing GRP/bombesin receptors (an autocrine growth factor receptor in tumor cells).<sup>439</sup>

## 8.3. Apoferritin Nanoparticles

Some protein-based molecules have been used as drug delivery constructs. These macromolecules are naturally assembled protein subunits of the same protein with reduced toxicity.<sup>440</sup> Ferritin is a blood protein for iron storage.<sup>441,442</sup> Apoferritin can be loaded with different drugs for delivery into target cells. Merlino and co-workers developed Au(III) oxo-apoferritin complex (Apt-Auoxo) (Figure 29).<sup>443</sup> The encapsulation of Auoxo into the ferritin core was confirmed by ICP-MS. Of note, Auoxo is capable binding histidine and cysteine side chains of proteins, which may offer insights into the mode of interaction between Auoxo and apoferritin.<sup>444,445</sup> The Apt-Auoxo nanoparticles showed significant cytotoxicity in cancer cells compared to normal cell.<sup>443</sup>

Recently, apoferritin encapsulated Au(III) thiosemicarbazones were synthesized by Zhang et al. and demonstrates high potency in glioma cancer cells with the ability to cross the blood brain barrier (Figure 30). Apoferritin-AuNPs are taken up via lysosome-mediated endocytosis in U87MG glioma cells with selective accumulation in tumors as well as promising *in vivo* tumor inhibition.<sup>446</sup> Taken together, these are encouraging studies that highlight the potential of apoferritin nanoparticles for efficacious gold-based therapy.

## 8.4. Silica-Based Nanoparticles

Silica-based materials such as mesoporous silica nanocarrier (MSN) have also been used as carriers for bioactive gold compounds. Silica is considered safe by the FDA and has unique properties such as excellent encapsulation efficiency, facile large-scale production, large surface area and adjustable uniform pore size, which makes MSN a good delivery system.<sup>447-451</sup> Che et al. reported AuP (Au-1@MSN(R)), an RGD-functionalized MSN nanoparticle carrying gold(III) porphyrin complex as cargo. The nanoparticle displayed higher anticancer activity and selectivity to normal cells compared to the free Au(III) porphyrin complex and inhibited thioredoxin reductase as a mode of apoptotic cancer cell death.<sup>452</sup>

## 8.5. Peptide-Based Nanoparticles

Peptides are gaining attention as promising nanosized drug delivery systems.<sup>453-455</sup> Among several properties of peptide delivery systems, are that they undergo proteolytic

degradation by proteases overexpressed by recalcitrant TNBC and renal cancer cells.<sup>456,457</sup> Therefore, an interesting approach to increase the potency of cytotoxic gold agents is by utilizing peptide-based nanoparticle delivery systems to improve cancer cell selectivity. Recently, Contel, Ulijn, and colleagues reported the encapsulation of Au(I) N-heterocyclic carbene compounds in amphiphilic decapeptides (Figure 31). Peptide self-assembly of gold compounds, **1** or **2** and subsequent free gold precipitation and centrifugation resulted in the peptide nanostructures, which were characterized by AFM, TEM, FTIR, and zeta potential analysis. Varying encapsulation efficiency of the different peptides at 1 mM and two stock concentrations (10  $\mu$ M or 500  $\mu$ M) of gold compounds **1** or **2** was observed. The combination of compound **1** at 10  $\mu$ M and the AD peptide yielded an encapsulation efficiency of >60%. The gold-loaded nanostructures displayed significant cytotoxicity in MDA-MB-231 and Caki-1 (renal carcinoma) cells with selectivity compared to noncancerous cells, IMR-90 (lung fibroblast). It is assumed that the proteolytic degradation of peptide filament encapsulating the drug facilitate the drug uptake by the cancer cells.<sup>458</sup> Hence, this highlights an interesting approach to improve drug selectivity for cancer cells and consequently its cytotoxic effect.

### 8.6. Noncovalent Self-Assembled Nanoparticles

Gold(III) porphyrins (AuP) display superior anticancer efficacy and with structural modifications can self-assemble to nanostructures without responsive nanocarriers. This noncovalent self-assembly strategy has been previously employed in other Sn-, Zn-, and Gd-based porphyrin systems for photocatalytic and photodynamic therapy applications.<sup>459–461</sup> In applying this approach to gold, an Au(III) tetra-(4-pyridyl) porphyrin (AuTPyP) nanosphere (AuPNS) capable of generating intracellular ROS, and thioredoxin inhibition for synergistic chemo-photothermal therapy of tumors (Figure 32) was recently described by Bai and Shi et al.<sup>462</sup> Full characterization of AuPNS by FTIR, XPS, and TEM support the development of spherical nanostructures with an average diameter of ~65 nm. Further functionalization of AuPNSs with cRGD produced cRGD-AuPNS, which showed improved overall pharmacokinetic behavior than free AuPNSs. Treatment of HeLa tumor-bearing mice with cRGD-AuPNS (10 mg/kg) and light irradiation (635 nm, 0.8W/cm<sup>2</sup>) for 5 min resulted in 100% tumor inhibition rate. The approach represents a new paradigm for efficacious gold-based cancer therapy.

## 9. CONCLUSION AND FUTURE OUTLOOK

This Review highlights research to develop next generation gold-based drugs to treat diseases and chemical probes to interrogate human physiology. As summarized throughout this Review, we articulate the rich history of gold and its relevance throughout medicinal breakthroughs and bring to prominence efforts to elucidate the mechanism of novel gold complexes. As outlined in the Review, a great deal of effort has been invested in repurposing old gold-based drugs as well as the development of novel gold complexes, notably stable Au(III) complexes, which were previously challenging to develop. To energize the scientific and medical communities, we strung together fundamental discoveries of gold chemistry considering its applicability in basic biology such as diagnostics; radiotherapy; and preclinical studies in several disease indications as well as translational clinical trials.



Subsequently, the pursuit of a more mechanistic investigation on how Au(I) and Au(III) complexes function in model systems received a boost from new omics technologies. What was a long-antiquated field in medicinal applications has now emerged as a burgeoning area of scientific rigor. As scientists have revisited the field of gold chemistry in medicine, more compound libraries have been made and have been examined to understand their true mechanism(s) of action. Furthermore, we describe novel mechanistic insights that have been published by experts all over the globe. From DNA targeting to covalent modification of proteins, and metabolic regulation just to highlight a few. Gold-derived complexes display immense potential in modulating diseases and offer new chemical tools for researchers to elucidate elusive biological processes and targets. The long history of gold in humans including FDA approved agents and current clinical trials emboldens the rationale to pursue gold drug/probe discovery. Therefore, it is critical to revisit gold-based therapeutics with a fresh sense of innovation that builds on the progress made thus far. This Review not only highlights the new classes of gold agents synthesized but further touches on the vast number of diseases in which gold has found success within the past decade. Moreover, we detail the application of gold compounds in a plethora of diseases including cancer, bacterial, leishmaniasis, microbial infections, and inflammation (e.g., RA and IBD). We posit that gold-derived agents are of therapeutic value to numerous disease indications.

Though impressive strides have been made, the stability of gold complexes remains a bottleneck toward the development of new libraries and scaffolds. This Review highlights complexes prepared by novel synthetic strategies. We must mention that detailed synthetic methodologies for the preparation of gold complexes are out of the scope of this Review. However, readers are encouraged to visit the articles cited at the end of the Review to peruse creative synthetic strategies outlined as well as a recently reviewed strategies to preparing gold anticancer complexes.<sup>463</sup> Despite the drawbacks, new possibilities have arisen within the past decade to developing next generation gold agents beyond auranofin, the “gold standard.” Progressively, evidence of (i) the importance of gold in medicine, (ii) the success of gold in clinical trials (14 to date), (iii) the determination and creativity of scientists, and (iv) state-of-the-art technologies will propel next generation gold agents into clinical use. Leveraging the development of new gold-based libraries and high-throughput screens has the potential to accelerate first-in-class gold-based drugs/probes.

Overall, this Review highlights how fundamental discoveries of gold chemistry and mechanisms of gold action in biology have become cornerstones for researchers across the globe to unlock tool compounds and therapeutic agents that were unthinkable even 10 years ago. With the advancement of cutting-edge molecular biology tools, omic technologies, and preclinical/translational science, furthering the potential of gold-derived complexes into the clinic has never been more attainable.

## ACKNOWLEDGMENTS

This work and S.G.A. was supported by grant R01CA258421-01 from the National Cancer Institute and NSF Grant No. 2203559. Figure 1 was generated using [BioRender.com](https://BioRender.com).

## Biographies

R. Tyler Mertens was born in Madisonville, Kentucky. He received his B.S. in chemistry from Centre College. He then earned his Ph.D. in 2021 under the advisement of Prof. Samuel G. Awuah at the University of Kentucky where he developed novel gold complexes to target metabolism in cancer. In late 2021, he joined the laboratory of Prof. Roni Nowarski in the Department of Immunology at Harvard Medical School as a postdoctoral fellow where he focuses on understanding mechanisms behind metabolic regulation of inflammation during colitis.

Sailajah Gukathasan received her Ph.D. from the University of Kentucky under the supervision of Prof. Samuel G. Awuah, where her work focused on the unique niche of developing gold-based reagents for protein modifications. She is currently a postdoctoral research fellow in the lab of Prof. Eranthie Weerapana at Boston College. Her research focuses on chemical proteomics. She is originally from the idyllic city of Jaffna, Srilanka, and graduated B.Sc. with honors in chemistry and zoology from the University of Jaffna, Srilanka.

Adedamola S. Arojojoye received his B.Tech degree from Ladoke Akintola University of Technology, and MSc. degree in Chemistry from University of Lagos, Nigeria. Motivated to pursue advanced research, he proceeded to the University of Kentucky for his PhD in Chemistry. He joined Awuah Lab in Fall 2019, and his research focuses on synthetic strategies for stable organogold(I/III) complexes using structurally diverse ligands and understanding their mechanism of cytotoxic action to develop next generation therapeutics.

Chibuzor Olelewe received his BSc degree in Biochemistry from the University of Nigeria. His interest in drug discovery which lies at the interface of Chemistry and Biology motivated him to pursue a graduate degree to acquire the requisite skills needed to be successful in this field of science. As a graduate student in the Awuah lab, he is interested in understanding the mechanism of action of gold-based small molecules designed with potential as chemotherapeutics.

Samuel G. Awuah received a BSc degree in Chemistry from Kwame Nkrumah University of Science and Technology, Ghana, and a PhD from University of Oklahoma. After postdoctoral training at MIT, he accepted a position as an assistant professor of Chemistry and Pharmaceutical Sciences (joint) at the University of Kentucky. His work on gold complexes has contributed to the development of new structural scaffolds to unravel elusive targets such as mitochondrial structure and dynamics to cure diseases. He developed a new protein bioconjugation strategy known as the metal-mediated ligand affinity chemistry that utilizes transition metals such as gold in a proximity guided approach to covalently modify protein targets at their endogenous sites.

## REFERENCES

- (1). Shaw CF Gold-Based Therapeutic Agents. *Chem. Rev.* 1999, 99, 2589–2600. [PubMed: 11749494]

- (2). Barnard PJ; Berners-Price SJ Targeting the Mitochondrial Cell Death Pathway with Gold Compounds. *Coord. Chem. Rev.* 2007, 251, 1889–1902.
- (3). Best SL; Sadler PJ Gold Drugs: Mechanism of Action and Toxicity. *Gold Bull.* 1996, 29, 87–93.
- (4). Dominelli B; Correia JDG; Kühn FE Medicinal Applications of Gold(I/III)-Based Complexes Bearing N-Heterocyclic Carbene and Phosphine Ligands. *J. Organomet. Chem.* 2018, 866, 153–164.
- (5). Glišić B; Djuran MI Gold Complexes as Antimicrobial Agents: An Overview of Different Biological Activities in Relation to the Oxidation State of the Gold Ion and the Ligand Structure. *Dalton Trans.* 2014, 43, 5950–5969. [PubMed: 24598838]
- (6). Yue S; Luo M; Liu H; Wei S Recent Advances of Gold Compounds in Anticancer Immunity. *Front. Chem.* 2020, 8, 543–557. [PubMed: 32695747]
- (7). Zou T; Lum CT; Lok C-N; Zhang J-J; Che C-M Chemical Biology of Anticancer Gold(III) and Gold(I) Complexes. *Chem. Soc. Rev.* 2015, 44, 8786–8801. [PubMed: 25868756]
- (8). Lu Y; Ma X; Chang X; Liang Z; Lv L; Shan M; Lu Q; Wen Z; Gust R; Liu W Recent Development of Gold(I) and Gold(III) Complexes as Therapeutic Agents for Cancer Diseases. *Chem. Soc. Rev.* 2022, 51, 5518–5556. [PubMed: 35699475]
- (9). Fernández-Moreira V; Herrera RP; Gimeno MC Anticancer Properties of Gold Complexes with Biologically Relevant Ligands. *Pure Appl. Chem.* 2019, 91, 247–269.
- (10). Roder C; Thomson MJ Auranofin: Repurposing an Old Drug for a Golden New Age. *Drugs in R&D* 2015, 15, 13–20. [PubMed: 25698589]
- (11). Balfourier A; Kolosnjaj-Tabi J; Luciani N; Carn F; Gazeau F Gold-Based Therapy: From Past to Present. *Proc. Natl. Acad. Sci. U. S. A.* 2020, 117, 22639–22648. [PubMed: 32900936]
- (12). Bartlett N Relativistic Effects and the Chemistry of Gold. *Gold Bull.* 1998, 31, 22–25.
- (13). Schwerdtfeger P; Dolg M; Schwarz WHE; Bowmaker GA; Boyd PDW Relativistic Effects in Gold Chemistry. I. Diatomic Gold Compounds. *J. Chem. Phys.* 1989, 91, 1762–1774.
- (14). Handschuh H; Ganteför G; Bechthold PS; Eberhardt W A Comparison of Photoelectron Spectroscopy and Two-Photon Ionization Spectroscopy: Excited States of Au<sub>2</sub>, Au<sub>3</sub>, and Au<sub>4</sub>. *J. Chem. Phys.* 1994, 100, 7093–7100.
- (15). Pizlo A; Jansen G; Heß BA; von Niessen W Ionization Potential and Electron Affinity of the Au Atom and the Au<sub>n</sub> Molecule by All-Electron Relativistic Configuration Interaction and Propagator Techniques. *J. Chem. Phys.* 1993, 98, 3945–3951.
- (16). Mertens RT; Awuah SG Gold Catalysis: Fundamentals and Recent Developments. *Catalysis by Metal Complexes and Nanomaterials: Fundamentals and Applications* 2019, 1317, 19–55.
- (17). Gorin DJ; Toste FD Relativistic Effects in Homogeneous Gold Catalysis. *Nature* 2007, 446, 395–403. [PubMed: 17377576]
- (18). Guerra MF; Calligaro T Gold Cultural Heritage Objects: A Review of Studies of Provenance and Manufacturing Technologies. *Meas. Sci. Technol.* 2003, 14, 1527–1537.
- (19). James TGH Gold Technology in Ancient Egypt. *Gold Bull.* 1972, 5, 38–42.
- (20). Higby GJ Gold in Medicine. *Gold Bull.* 1982, 15, 130–140. [PubMed: 11614517]
- (21). Parish RV Gold in Medicine - Chrysotherapy. *Interdiscip. Sci. Rev.* 1992, 17, 221–228.
- (22). Pricker SP Medical Uses of Gold Compounds: Past, Present and Future. *Gold Bull.* 1996, 29, 53–60.
- (23). Huaizhi Z; Yuantao N China's Ancient Gold Drugs. *Gold Bull.* 2001, 34, 24–29.
- (24). Kean WF; Kean IR Clinical Pharmacology of Gold. *Inflammopharmacology* 2008, 16, 112–125. [PubMed: 18523733]
- (25). Pagel W Paracelsus: An Introduction to Philosophical Medicine in the Era of the Renaissance; Basel & New York, 1958; p 399.
- (26). Multhaus R The Significance of Distillation in Renaissance Medical Chemistry. *Bulletin of Historical Medicine* 1956, 38, 329–346.
- (27). Stillman J The Story of Alchemy and Early Chemistry.; Dover Publication, 1924; p 555.
- (28). Partington J A History of Chemistry; Macmillan, 1961; p 795.

- (29). Starobinski J History of the Treatment of Melancholy from the Earliest Times to 1900; J.R. Geigy, 1972; p 100.
- (30). Zirkle C; Fulton JF; Drabkin IE; Boyer CB; Cohen IB; Strelsky K Eighty-First Critical Bibliography of the History of Science and Its Cultural Influences (to 1 January 1956). *Isis* 1956, 47, 247–360.
- (31). Royal College of Physicians of London and Urdang, G. *Pharmacopeia Londinensis of 1618*; Reproduced facsimile, 1944; p 299.
- (32). Chrestien J De La Methode Latraleptique; Ou Observations. *Edinb. Med. Sur. J.* 1811, 11, 239–243.
- (33). Barclay G The Keeley League. *J. Ill. State Hist. Soc.* 1964, 577, 344–364.
- (34). Koch R Report of Address at 10th International Medical Congress; *Dutch Media Worchenschrift*, Berlin, Germany, 1890. 756–757.
- (35). Forestier J The Treatment of Rheumatoid Arthritis with Gold Salts Injections. *Lancet* 1932, 219, 441–444.
- (36). Dequeker J; Verdickt W; Gevers G; Vanschoubroek K Longterm Experience with Oral Gold in Rheumatoid Arthritis and Psoriatic Arthritis. *Clin. Rheumatol.* 1984, 3, 67–74.
- (37). Gaynor D; Griffith DM The Prevalence of Metal-Based Drugs as Therapeutic or Diagnostic Agents: Beyond Platinum. *Dalton Trans.* 2012, 41, 13239–13257. [PubMed: 22930130]
- (38). Lawrence JS Comparative Toxicity of Gold Preparations in Treatment of Rheumatoid Arthritis. *Ann. Rheum. Dis.* 1976, 35, 171–173. [PubMed: 821403]
- (39). Speerstra F; Reekers P; van de Putte LB; Vandenbroucke JP; Rasker JJ; de Rooij DJ Hla-Dr Antigens and Proteinuria Induced by Aurothioglucose and D-Penicillamine in Patients with Rheumatoid Arthritis. *J. Rheumatol.* 1983, 10, 948–953. [PubMed: 6420562]
- (40). Ammon HV; Fowle SA; Cunningham JA; Komorowski RA; Loeffler RF Effects of Auranofin and Myochrysin on Intestinal Transport and Morphology in the Rat. *Gut* 1987, 28, 829–834. [PubMed: 3115869]
- (41). Tiekink ERT Gold Compounds in Medicine: Potential Anti-Tumour Agents. *Gold Bull.* 2003, 36, 117–124.
- (42). Taukumova LA; Mouravjoy YV; Gribakin SG Mucocutaneous Side Effects and Continuation of Aurotherapy in Patients with Rheumatoid Arthritis. In *Rheumaderm: Current Issues in Rheumatology and Dermatology*, Mallia C, Uitto J, Eds.; Springer US, 1999; pp 367–373.
- (43). Kostova I Gold Coordination Complexes as Anticancer Agents. *Anticancer Agents Med. Chem.* 2006, 6, 19–32. [PubMed: 16475924]
- (44). Ott I; Gust R Non Platinum Metal Complexes as Anti-Cancer Drugs. *Arch. Pharm.* 2007, 340, 117–126.
- (45). Milacic V; Fregona D; Dou QP Gold Complexes as Prospective Metal-Based Anticancer Drugs. *Histol. Histopathol.* 2008, 23, 101–108. [PubMed: 17952862]
- (46). Ott I On the Medicinal Chemistry of Gold Complexes as Anticancer Drugs. *Coord. Chem. Rev.* 2009, 253, 1670–1681.
- (47). Nobili S; Mini E; Landini I; Gabbiani C; Casini A; Messori L Gold Compounds as Anticancer Agents: Chemistry, Cellular Pharmacology, and Preclinical Studies. *Med. Res. Rev* 2010, 30, 550–580. [PubMed: 19634148]
- (48). Liu L-P; Hammond GB Recent Advances in the Isolation and Reactivity of Organogold Complexes. *Chem. Soc. Rev.* 2012, 41, 3129–3139. [PubMed: 22262401]
- (49). Mármol I; Quero J; Rodríguez-Yoldi MJ; Cerrada E Gold as a Possible Alternative to Platinum-Based Chemotherapy for Colon Cancer Treatment. *Cancers (Basel)* 2019, 11, 780–816. [PubMed: 31195711]
- (50). Finkelstein AE; Walz DT; Batista V; Mizraji M; Roisman F; Misher A Auranofin. New Oral Gold Compound for Treatment of Rheumatoid Arthritis. *Ann. Rheum. Dis.* 1976, 35, 251–257. [PubMed: 791161]
- (51). Sutton BM; McGusty E; Walz DT; DiMartino MJ Oral Gold. Antiarthritic Properties of Alkylphosphinegold Coordination Complexes. *J. Med. Chem.* 1972, 15, 1095–1098. [PubMed: 4654656]

- (52). Rothan HA; Stone S; Natekar J; Kumari P; Arora K; Kumar M The Fda-Approved Gold Drug Auranofin Inhibits Novel Coronavirus (Sars-Cov-2) Replication and Attenuates Inflammation in Human Cells. *Virology* 2020, 547, 7–11. [PubMed: 32442105]
- (53). Capparelli EV; Bricker-Ford R; Rogers MJ; McKerrow JH; Reed SL Phase I Clinical Trial Results of Auranofin, a Novel Antiparasitic Agent. *Antimicrob. Agents Chemother.* 2017, 61, No. e01947–01916. [PubMed: 27821451]
- (54). Sannella AR; Casini A; Gabbiani C; Messori L; Bilia AR; Vincieri FF; Majori G; Severini C New Uses for Old Drugs. Auranofin, a Clinically Established Antiarthritic Metallo drug, Exhibits Potent Antimalarial Effects in Vitro: Mechanistic and Pharmacological Implications. *FEBS Lett.* 2008, 582, 844–847. [PubMed: 18294965]
- (55). Madeira JM; Renschler CJ; Mueller B; Hashioka S; Gibson DL; Klegeris A Novel Protective Properties of Auranofin: Inhibition of Human Astrocyte Cytotoxic Secretions and Direct Neuroprotection. *Life Sci.* 2013, 92, 1072–1080. [PubMed: 23624233]
- (56). Messori L; Marcon G Gold Complexes in the Treatment of Rheumatoid Arthritis. *Met. Ions Biol. Syst.* 2004, 41, 279–304. [PubMed: 15206120]
- (57). Furst DE Mechanism of Action, Pharmacology, Clinical Efficacy and Side Effects of Auranofin. An Orally Administered Organic Gold Compound for the Treatment of Rheumatoid Arthritis. *Pharmacotherapy* 1983, 3, 284–298. [PubMed: 6417628]
- (58). Gottlieb NL Pharmacology of Auranofin: Overview and Update. *Scand. J. Rheumatol. Suppl* 1986, 63, 19–28. [PubMed: 3110942]
- (59). Pushpakom S; Iorio F; Eyers PA; Escott KJ; Hopper S; Wells A; Doig A; Williams T; Latimer J; McNamee C; Norris A; Sanseau P; Cavalla D; Pirmohamed M Drug Repurposing: Progress, Challenges and Recommendations. *Nat. Rev. Drug Discovery* 2019, 18, 41–58. [PubMed: 30310233]
- (60). University of Kansas Medical Center The Leukemia Lymphoma Society Kansas Bioscience Authority Therapeutics for Rare Neglected Diseases. Phase I and II Study of Auranofin in Chronic Lymphocytic Leukemia (CLL), 2011. <https://ClinicalTrials.gov/show/NCT01419691> (accessed 03-20-2023).
- (61). Einhorn LH Treatment of Testicular Cancer: A New and Improved Model. *J. Clin. Oncol.* 1990, 8, 1777–1781. [PubMed: 1700077]
- (62). Mayo Clinic; National Cancer Institute. Auranofin and Sirolimus in Treating Participants with Ovarian Cancer, 2018. <https://ClinicalTrials.gov/show/NCT03456700> (accessed 03-20-2023).
- (63). Casañal A; Lohkamp B; Emsley P Current Developments in Coot for Macromolecular Model Building of Electron Cryo-Microscopy and Crystallographic Data. *Protein Sci.* 2020, 29, 1055–1064.
- (64). Maveyraud L; Mourey L Protein X-Ray Crystallography and Drug Discovery. *Molecules* 2020, 25, 1030–1048. [PubMed: 32106588]
- (65). Renaud J-P; Chari A; Ciferri C; Liu W.-t.; Rémy H-W; Stark H; Wiesmann C Cryo-Em in Drug Discovery: Achievements, Limitations and Prospects. *Nat. Rev. Drug Discovery* 2018, 17, 471–492. [PubMed: 29880918]
- (66). Nguyen SS; Prescher JA Developing Bioorthogonal Probes to Span a Spectrum of Reactivities. *Nat. Rev. Chem.* 2020, 4, 476–489. [PubMed: 34291176]
- (67). Arjmand F; Afsan Z; Sharma S; Parveen S; Yousuf I; Sartaj S; Siddique HR; Tabassum S Recent Advances in Metallo drug-Like Molecules Targeting Non-Coding Rnas in Cancer Chemotherapy. *Coord. Chem. Rev.* 2019, 387, 47–59.
- (68). Wenzel M; Casini A Mass Spectrometry as a Powerful Tool to Study Therapeutic Metallo drugs Speciation Mechanisms: Current Frontiers and Perspectives. *Coord. Chem. Rev.* 2017, 352, 432–460.
- (69). Wang H; Zhou Y; Xu X; Li H; Sun H Metalloproteomics in Conjunction with Other Omics for Uncovering the Mechanism of Action of Metallo drugs: Mechanism-Driven New Therapy Development. *Curr. Opin. Chem. Biol.* 2020, 55, 171–179. [PubMed: 32200302]
- (70). Giorgio A; Merlino A Gold Metalation of Proteins: Structural Studies. *Coord. Chem. Rev.* 2020, 407, 213175–213200.

- (71). Merlino A Recent Advances in Protein Metalation: Structural Studies. *Chem. Commun.* 2021, 57, 1295–1307.
- (72). Bindoli A; Rigobello MP; Scutari G; Gabbiani C; Casini A; Messori L Thioredoxin Reductase: A Target for Gold Compounds Acting as Potential Anticancer Drugs. *Coord. Chem. Rev.* 2009, 253, 1692–1707.
- (73). Bhabak KP; Bhuyan BJ; Mugesh G *Bioinorganic and Medicinal Chemistry: Aspects of Gold (I)-Protein Complexes.* *Dalton Trans.* 2011, 40, 2099–2111. [PubMed: 21321730]
- (74). Tepperman K; Finer R; Donovan S; Elder R; Doi J; Ratliff D; Ng K Intestinal Uptake and Metabolism of Auranofin, a New Oral Gold-Based Antiarthritis Drug. *Science* 1984, 225, 430–432. [PubMed: 6429854]
- (75). Weisman MH; Hardison W; Walz DT Studies of the Intestinal Metabolism of Oral Gold. *J. Rheumatol.* 1980, 7, 633–638. [PubMed: 6777493]
- (76). Suwalsky M; Gonzalez R; Villena F; Bolognin S Structural Effects of the Au (I) Drug Auranofin on Cell Membranes and Molecular Models. *J. Chil. Chem. Soc.* 2013, 58, 2001–2004.
- (77). Snyder RM; Mirabelli CK; Crooke ST Cellular Association, Intracellular Distribution, and Efflux of Auranofin Via Sequential Ligand Exchange Reactions. *Biochem. Pharmacol.* 1986, 35, 923–932. [PubMed: 3082334]
- (78). Pickering IJ; Cheng Q; Rengifo EM; Nehzati S; Dolgova NV; Kroll T; Sokaras D; George GN; Arnér ES Direct Observation of Methylmercury and Auranofin Binding to Selenocysteine in Thioredoxin Reductase. *Inorg. Chem.* 2020, 59, 2711–2718. [PubMed: 32049511]
- (79). Saei AA; Gullberg H; Sabatier P; Beusch CM; Johansson K; Lundgren B; Arvidsson PI; Arnér ES; Zubarev RA Comprehensive Chemical Proteomics for Target Deconvolution of the Redox Active Drug Auranofin. *Redox Biol.* 2020, 32, 101491. [PubMed: 32199331]
- (80). Parsonage D; Sheng F; Hirata K; Debnath A; McKerrow JH; Reed SL; Abagyan R; Poole LB; Podust LM X-Ray Structures of Thioredoxin and Thioredoxin Reductase from *Entamoeba Histolytica* and Prevailing Hypothesis of the Mechanism of Auranofin Action. *J. Struct. Biol.* 2016, 194, 180–190. [PubMed: 26876147]
- (81). Ilari A; Baiocco P; Messori L; Fiorillo A; Boffi A; Gramiccia M; Di Muccio T; Colotti G A Gold-Containing Drug against Parasitic Polyamine Metabolism: The X-Ray Structure of Trypanothione Reductase from *Leishmania Infantum* in Complex with Auranofin Reveals a Dual Mechanism of Enzyme Inhibition. *Amino Acids* 2012, 42, 803–811. [PubMed: 21833767]
- (82). Angelucci F; Sayed AA; Williams DL; Boumis G; Brunori M; Dimastrogiovanni D; Miele AE; Pauly F; Bellelli A Inhibition of *Schistosoma Mansoni* Thioredoxin-Glutathione Reductase by Auranofin: Structural and Kinetic Aspects. *J. Biol. Chem.* 2009, 284, 28977–28985. [PubMed: 19710012]
- (83). Angelucci F; Dimastrogiovanni D; Boumis G; Brunori M; Miele AE; Saccoccia F; Bellelli A Mapping the Catalytic Cycle of *Schistosoma Mansoni* Thioredoxin Glutathione Reductase by X-Ray Crystallography. *J. Biol. Chem.* 2010, 285, 32557–32567. [PubMed: 20659890]
- (84). Giles NM; Watts AB; Giles GI; Fry FH; Littlechild JA; Jacob C Metal and Redox Modulation of Cysteine Protein Function. *Chem. Biol.* 2003, 10, 677–693. [PubMed: 12954327]
- (85). Augello G; Azzolina A; Rossi F; Prencipe F; Mangiatordi GF; Saviano M; Ronga L; Cervello M; Tesaro D New Insights into the Behavior of Nhc-Gold Complexes in Cancer Cells. *Pharmaceutics* 2023, 15, 466–478. [PubMed: 36839788]
- (86). Cirri D; Geri A; Massai L; Mannelli M; Gamberi T; Magherini F; Becatti M; Gabbiani C; Pratesi A; Messori L Chemical Modification of Auranofin Yields a New Family of Anticancer Drug Candidates: The Gold (I) Phosphite Analogues. *Molecules* 2023, 28, 1050. [PubMed: 36770719]
- (87). Johnson MW; DiPasquale AG; Bergman RG; Toste FD Synthesis of Stable Gold (III) Pincer Complexes with Anionic Heteroatom Donors. *Organometallics* 2014, 33, 4169–4172. [PubMed: 25180022]
- (88). Arojoye AS; Mertens RT; Ofori S; Parkin SR; Awuah SG Synthesis, Characterization, and Antiproliferative Activity of Novel Chiral [QuinoxP\* AuCl<sub>2</sub>]<sup>+</sup> Complexes. *Molecules* 2020, 25, 5735–5748. [PubMed: 33291802]
- (89). da Silva Maia PI; Deflon VM; Abram U Gold (III) Complexes in Medicinal Chemistry. *Future Med. Chem.* 2014, 6, 1515–1536. [PubMed: 25365235]



- (90). Messori L; Abbate F; Marcon G; Orioli P; Fontani M; Mini E; Mazzei T; Carotti S; O'Connell T; Zanello P Gold (III) Complexes as Potential Antitumor Agents: Solution Chemistry and Cytotoxic Properties of Some Selected Gold (III) Compounds. *J. Med. Chem.* 2000, 43, 3541–3548. [PubMed: 11000008]
- (91). Garcia Santos I; Hagenbach A; Abram U Stable Gold (III) Complexes with Thiosemicarbazone Derivatives. *Dalton Trans.* 2004, 677–682. [PubMed: 15252533]
- (92). Gukathasan S; Parkin S; Awuah SG Cyclometalated Gold (III) Complexes Bearing Dach Ligands. *Inorg. Chem.* 2019, 58, 9326–9340. [PubMed: 31247820]
- (93). Bertrand B; Williams MR; Bochmann M Gold (III) Complexes for Antitumor Applications: An Overview. *Eur. J. Chem.* 2018, 24, 11840–11851.
- (94). Messori L; Orioli P; Tempi C; Marcon G Interactions of Selected Gold (III) Complexes with Calf Thymus DNA. *Biochem. Biophys. Res. Commun.* 2001, 281, 352–360. [PubMed: 11181054]
- (95). Rackham O; Nichols SJ; Leedman PJ; Berners-Price SJ; Filipovska A A Gold (I) Phosphine Complex Selectively Induces Apoptosis in Breast Cancer Cells: Implications for Anticancer Therapeutics Targeted to Mitochondria. *Biochem. Pharmacol.* 2007, 74, 992–1002. [PubMed: 17697672]
- (96). Wedlock LE; Kilburn MR; Cliff JB; Filgueira L; Saunders M; Berners-Price SJ Visualising Gold inside Tumour Cells Following Treatment with an Antitumour Gold (I) Complex. *Metallomics* 2011, 3, 917–925. [PubMed: 21796317]
- (97). Abyar F; Tabrizi L New Cyclometalated Gold (III) Complex Targeting Thioredoxin Reductase: Exploring as Cytotoxic Agents and Mechanistic Insights. *Biometals* 2020, 33, 107–122. [PubMed: 32246384]
- (98). Quero J; Cabello S; Fuertes T; Mármol I; Laplaza R; Polo V; Gimeno MC; Rodriguez-Yoldi MJ; Cerrada E Proteasome Versus Thioredoxin Reductase Competition as Possible Biological Targets in Antitumor Mixed Thiolate-Dithiocarbamate Gold (III) Complexes. *Inorg. Chem.* 2018, 57, 10832–10845. [PubMed: 30117739]
- (99). Zhang J-J; Ng K-M; Lok C-N; Sun RW-Y; Che C-M Deubiquitinases as Potential Anti-Cancer Targets for Gold (III) Complexes. *Chem. Commun.* 2013, 49, 5153–5155.
- (100). Arojojoye AS; Kim JH; Olelewe C; Parkin S; Awuah SG Chiral Gold (III) Complexes: Speciation, in Vitro, and in Vivo Anticancer Profile. *Chem. Commun.* 2022, 58, 10237.
- (101). Zou T; Lum CT; Chui SSY; Che CM Gold (III) Complexes Containing N-Heterocyclic Carbene Ligands: Thiol “Switch-on” Fluorescent Probes and Anti-Cancer Agents. *Angew. Chem., Int. Ed.* 2013, 52, 2930–2933.
- (102). Meier SM; Gerner C; Keppler BK; Cinellu MA; Casini A Mass Spectrometry Uncovers Molecular Reactivities of Coordination and Organometallic Gold (III) Drug Candidates in Competitive Experiments That Correlate with Their Biological Effects. *Inorg. Chem.* 2016, 55, 4248–4259. [PubMed: 26866307]
- (103). Hu D; Liu Y; Lai YT; Tong KC; Fung YM; Lok CN; Che CM Anticancer Gold (III) Porphyrins Target Mitochondrial Chaperone Hsp60. *Angew. Chem., Int. Ed.* 2016, 55, 1387–1391.
- (104). Tong K-C; Hu D; Wan P-K; Lok C-N; Che C-M Anticancer Gold (III) Compounds with Porphyrin or N-Heterocyclic Carbene Ligands. *Front. Chem.* 2020, 8, 587207. [PubMed: 33240849]
- (105). Tong K-C; Lok C-N; Wan P-K; Hu D; Fung YME; Chang X-Y; Huang S; Jiang H; Che C-M An Anticancer Gold (III)-Activated Porphyrin Scaffold That Covalently Modifies Protein Cysteine Thiols. *Proc. Natl. Acad. Sci. U. S. A.* 2020, 117, 1321–1329. [PubMed: 31896586]
- (106). Buac D; Schmitt S; Ventro G; Rani Kona F; Ping Dou Q Dithiocarbamate-Based Coordination Compounds as Potent Proteasome Inhibitors in Human Cancer Cells. *Mini Rev. Med. Chem.* 2012, 12, 1193–1201. [PubMed: 22931591]
- (107). Dalla Via L; Nardon C; Fregona D Targeting the Ubiquitin-Proteasome Pathway with Inorganic Compounds to Fight Cancer: A Challenge for the Future. *Future Med. Chem.* 2012, 4, 525–543. [PubMed: 22416778]
- (108). King AP; Wilson JJ Endoplasmic Reticulum Stress: An Arising Target for Metal-Based Anticancer Agents. *Chem. Soc. Rev.* 2020, 49, 8113–8136. [PubMed: 32597908]

- (109). Olelewe C; Awuah SG Mitochondria as a Target of Third Row Transition Metal-Based Anticancer Complexes. *Curr. Opin. Chem. Biol.* 2023, 72, 102235–102244. [PubMed: 36516614]
- (110). Massai L; Zoppi C; Cirri D; Pratesi A; Messori L Reactions of Medicinal Gold (III) Compounds with Proteins and Peptides Explored by Electrospray Ionization Mass Spectrometry and Complementary Biophysical Methods. *Front. Chem.* 2020, 8, 581648–581662. [PubMed: 33195070]
- (111). Gamberi T; Pratesi A; Messori L; Massai L Proteomics as a Tool to Disclose the Cellular and Molecular Mechanisms of Selected Anticancer Gold Compounds. *Coord. Chem. Rev.* 2021, 438, 213905.
- (112). Messori L; Merlino A Protein Metalation by Metal-Based Drugs: X-Ray Crystallography and Mass Spectrometry Studies. *Chem. Commun.* 2017, 53, 11622–11633.
- (113). Mazzei L; Wenzel MN; Cianci M; Palombo M; Casini A; Ciurli S Inhibition Mechanism of Urease by Au (III) Compounds Unveiled by X-Ray Diffraction Analysis. *ACS Med. Chem. Lett.* 2019, 10, 564–570. [PubMed: 30996797]
- (114). Cirri D; Bazzicalupi C; Ryde U; Bergmann J; Binacchi F; Nocentini A; Pratesi A; Gratteri P; Messori L Computationally Enhanced X-Ray Diffraction Analysis of a Gold (III) Complex Interacting with the Human Telomeric DNA G-Quadruplex. Unravelling Non-Unique Ligand Positioning. *Int. J. Biol. Macromol.* 2022, 211, 506–513. [PubMed: 35561865]
- (115). Elder RC; Eidsness MK Synchrotron X-Ray Studies of Metal-Based Drugs and Metabolites. *Chem. Rev.* 1987, 87, 1027–1046.
- (116). Hummer AA; Rompel A The Use of X-Ray Absorption and Synchrotron Based Micro-X-Ray Fluorescence Spectroscopy to Investigate Anti-Cancer Metal Compounds in Vivo and in Vitro. *Metallomics* 2013, 5, 597–614. [PubMed: 23558305]
- (117). Messori L; Balerna A; Ascone I; Castellano C; Gabbiani C; Casini A; Marchioni C; Jaouen G; Congiu Castellano A X-Ray Absorption Spectroscopy Studies of the Adducts Formed between Cytotoxic Gold Compounds and Two Major Serum Proteins. *J. Bio. Inorg. Chem.* 2011, 16, 491–499. [PubMed: 21181484]
- (118). Merlino A; Marzo T; Messori L Protein Metalation by Anticancer Metalloodrugs: A Joint Esi Ms and Xrd Investigative Strategy. *Eur. J. Chem.* 2017, 23, 6942–6947.
- (119). Adhikarsan Z; Palermo G; Riedel T; Ma Z; Muhammad R; Rothlisberger U; Dyson PJ; Davey CA Allosteric Cross-Talk in Chromatin Can Mediate Drug-Drug Synergy. *Nat. Commun.* 2017, 8, 14860. [PubMed: 28358030]
- (120). Sun H; Zhang Q; Wang R; Wang H; Wong Y-T; Wang M; Hao Q; Yan A; Kao RY-T; Ho P-L Resensitizing Carbapenem- and Colistin-Resistant Bacteria to Antibiotics Using Auranofin. *Nat. Commun.* 2020, 11, 1–13. [PubMed: 31911652]
- (121). Mbugua SN; Njenga LW; Odhiambo RA; Wandiga SO; Onani MO Beyond DNA-Targeting in Cancer Chemotherapy. *Emerging Frontiers-a Review. Curr. Top. Med. Chem.* 2021, 21, 28–47. [PubMed: 32814532]
- (122). Hurley LH DNA and Its Associated Processes as Targets for Cancer Therapy. *Nat. Rev. Cancer* 2002, 2, 188–200. [PubMed: 11990855]
- (123). Mullard A DNA Tags Help the Hunt for Drugs. *Nature* 2016, 530, 367–369. [PubMed: 26887498]
- (124). Nain V; Sahi S; Verma A Cpp-Zfn: A Potential DNA-Targeting Anti-Malarial Drug. *Malar. J.* 2010, 9, 1–6. [PubMed: 20043863]
- (125). Reinhold WC; Thomas A; Pommier Y DNA-Targeted Precision Medicine; Have We Been Caught Sleeping? *Trends in cancer* 2017, 3, 2–6. [PubMed: 28603778]
- (126). Hurley LH; Boyd FL DNA as a Target for Drug Action. *Trends Pharmacol. Sci.* 1988, 9, 402–407. [PubMed: 3078076]
- (127). Rosenberg B; Van Camp L; Krigas T Inhibition of Cell Division in Escherichia Coli by Electrolysis Products from a Platinum Electrode. *Nature* 1965, 205, 698–699. [PubMed: 14287410]
- (128). Rosenberg B; Vancamp L; Trosko JE; Mansour VH Platinum Compounds: A New Class of Potent Antitumour Agents. *Nature* 1969, 222, 385–386. [PubMed: 5782119]

- (129). Roberts J; Thomson A The Mechanism of Action of Antitumor Platinum Compounds. *Prog. Nucleic Acid Res. Mol. Biol.* 1979, 22, 71–133. [PubMed: 392602]
- (130). Dilruba S; Kalayda GV Platinum-Based Drugs: Past, Present and Future. *Cancer Chemother. Pharmacol.* 2016, 77, 1103–1124. [PubMed: 26886018]
- (131). Tchounwou PB; Dasari S; Noubissi FK; Ray P; Kumar S Advances in Our Understanding of the Molecular Mechanisms of Action of Cisplatin in Cancer Therapy. *J. Exp. Pharmacol.* 2021, 13, 303. [PubMed: 33776489]
- (132). Dasari S; Tchounwou PB Cisplatin in Cancer Therapy: Molecular Mechanisms of Action. *Eur. J. Pharmacol.* 2014, 740, 364–378. [PubMed: 25058905]
- (133). Kilic A; Barlak N; Sanli F; Aytatli A; Capik O; Karatas OF Mode of Action of Carboplatin Via Activating P53/Mir-145 Axis in Head and Neck Cancers. *Laryngoscope* 2020, 130, 2818–2824. [PubMed: 31886905]
- (134). Arango D; Wilson A; Shi Q; Corner G; Aranes M; Nicholas C; Lesser M; Mariadason J; Augenlicht L Molecular Mechanisms of Action and Prediction of Response to Oxaliplatin in Colorectal Cancer Cells. *Br. J. Cancer* 2004, 91, 1931–1946. [PubMed: 15545975]
- (135). de Vries G; Rosas-Plaza X; van Vugt MA; Gietema JA; de Jong S Testicular Cancer: Determinants of Cisplatin Sensitivity and Novel Therapeutic Opportunities. *Cancer Treat. Rev.* 2020, 88, 102054. [PubMed: 32593915]
- (136). Tandstad T; Ståhl O; Dahl O; Haugnes H; Håkansson U; Karlsdottir C; Kjellman A; Langberg C; Laurell A; Oldenburg J; et al. Treatment of Stage I Seminoma, with One Course of Adjuvant Carboplatin or Surveillance, Risk-Adapted Recommendations Implementing Patient Autonomy: A Report from the Swedish and Norwegian Testicular Cancer Group (Swenoteca). *Ann. Oncol.* 2016, 27, 1299–1304. [PubMed: 27052649]
- (137). Seidel C; Oechsle K; Lorch A; Dieing A; Hentrich M; Hornig M; Grünwald V; Cathomas R; Meiler J; de Wit M Efficacy and Safety of Gemcitabine, Oxaliplatin, and Paclitaxel in Cisplatin-Refractory Germ Cell Cancer in Routine Care—Registry Data from an Outcomes Research Project of the German Testicular Cancer Study Group. In *Urologic Oncology: Seminars and Original Investigations*, 2016; Elsevier: Vol. 34, pp 168.
- (138). Oun R; Moussa YE; Wheate NJ The Side Effects of Platinum-Based Chemotherapy Drugs: A Review for Chemists. *Dalton Trans.* 2018, 47, 6645–6653. [PubMed: 29632935]
- (139). Um IS; Armstrong-Gordon E; Moussa YE; Gnjidic D; Wheate NJ Platinum Drugs in the Australian Cancer Chemotherapy Healthcare Setting: Is It Worthwhile for Chemists to Continue to Develop Platinums? *Inorg. Chim. Acta* 2019, 492, 177–181.
- (140). Rahman SA; Arifuddin S; Abdullah N Therapeutic Response and Side Effects of Chemotherapy Combination Regimen between Paclitaxel-Cisplatin and Paclitaxel-Carboplatin on Cervical Cancer Stage Iib. *Gynecol Reprod Health* 2019, 3, 1–5.
- (141). Almeida CM; Nascimento GP; Magalhães KG; Iglesias BA; Gatto CC Crystal Structures, DNA-Binding Ability and Influence on Cellular Viability of Gold (I) Complexes of Thiosemicarbazones. *J. Coord. Chem.* 2018, 71, 502–519.
- (142). Cuya SM; Bjornsti M-A; van Waardenburg RC DNA Topoisomerase-Targeting Chemotherapeutics: What's New? *Cancer Chemother. Pharmacol.* 2017, 80, 1–14. [PubMed: 28528358]
- (143). Pommier Y; Leo E; Zhang H; Marchand C DNA Topoisomerases and Their Poisoning by Anticancer and Antibacterial Drugs. *Chem. Biol.* 2010, 17, 421–433. [PubMed: 20534341]
- (144). Mordente A; Meucci E; EttoreMartorana G; Tavian D; Silvestrini A Topoisomerases and Anthracyclines: Recent Advances and Perspectives in Anticancer Therapy and Prevention of Cardiotoxicity. *Curr. Med. Chem.* 2017, 24, 1607–1626. [PubMed: 27978799]
- (145). Marzi L; Agama K; Murai J; Difilippantonio S; James A; Peer CJ; Figg WD; Beck D; Elsayed MS; Cushman M; et al. Novel Fluoroindenoisoquinoline Non-Camptothecin Topoisomerase I Inhibitors/fluoroindenoisoquinoline Top1 Inhibitors. *Mol. Cancer Ther.* 2018, 17, 1694–1704. [PubMed: 29748210]
- (146). Burton JH; Mazcko C; LeBlanc A; Covey JM; Ji J; Kinders RJ; Parchment RE; Khanna C; Paoloni M; Lana S; et al. Nci Comparative Oncology Program Testing of Non-Camptothecin

- Indenoisoquinoline Topoisomerase I Inhibitors in Naturally Occurring Canine Lymphomani-Cop TopII Indenoisoquinolines. *Clin. Cancer Res.* 2018, 24, 5830–5840. [PubMed: 30061364]
- (147). Pommier Y; Cushman M; Doroshow JH Novel Clinical Indenoisoquinoline Topoisomerase I Inhibitors: A Twist around the Camptothecins. *Oncotarget* 2018, 9, 37286. [PubMed: 30647868]
- (148). Marzi L; Szabova L; Gordon M; Weaver Ohler Z; Sharan SK; Beshiri ML; Etemadi M; Murai J; Kelly K; Pommier Y The Indenoisoquinoline Top1 Inhibitors Selectively Target Homologous Recombination-Deficient and Schlafen 11-Positive Cancer Cells and Synergize with Olaparibtop1 Inhibitors Selective for Hrd and Slfn11-Positive Cells. *Clin. Cancer Res.* 2019, 25, 6206–6216. [PubMed: 31409613]
- (149). Matias-Barrios VM; Radaeva M; Song Y; Alperstein Z; Lee AR; Schmitt V; Lee J; Ban F; Xie N; Qi J Discovery of New Catalytic Topoisomerase II Inhibitors for Anticancer Therapeutics. *Front. Oncol.* 2021, 3293.
- (150). Matias-Barrios VM; Radaeva M; Ho C-H; Lee J; Adomat H; Lalous N; Cherkasov A; Dong X Optimization of New Catalytic Topoisomerase II Inhibitors as an Anti-Cancer Therapy. *Cancers (Basel)* 2021, 13, 3675. [PubMed: 34359577]
- (151). Akerman KJ; Fagenson AM; Cyril V; Taylor M; Muller MT; Akerman MP; Munro OQ Gold(III) Macrocycles: Nucleotide-Specific Unconventional Catalytic Inhibitors of Human Topoisomerase I. *J. Am. Chem. Soc.* 2014, 136, 5670–5682. [PubMed: 24694294]
- (152). Che C-M; Sun RW-Y; Yu W-Y; Ko C-B; Zhu N; Sun H Gold(III) Porphyrins as a New Class of Anticancer Drugs: Cytotoxicity, DNA Binding and Induction of Apoptosis in Human Cervix Epitheloid Cancer Cells. *Chem. Commun.* 2003, 1718–1719.
- (153). Sun RWY; Li CKL; Ma DL; Yan JJ; Lok CN; Leung CH; Zhu N; Che CM Stable Anticancer Gold(III)-Porphyrin Complexes: Effects of Porphyrin Structure. *Eur. J. Chem.* 2010, 16, 3097–3113.
- (154). Yan JJ; Chow AL-F; Leung C-H; Sun RW-Y; Ma D-L; Che C-M Cyclometalated Gold (III) Complexes with N-Heterocyclic Carbene Ligands as Topoisomerase I Poisons. *Chem. Commun.* 2010, 46, 3893–3895.
- (155). Li CKL; Sun RWY; Kui SCF; Zhu N; Che CM Anticancer Cyclometalated [AuIII(m(CA^N^C)mL)n+ Compounds: Synthesis and Cytotoxic Properties. *Eur. J. Chem.* 2006, 12, 5253–5266.
- (156). Wilson CR; Fagenson AM; Ruangpradit W; Muller MT; Munro OQ Gold(III) Complexes of Pyridyl- and Isoquinolylamido Ligands: Structural, Spectroscopic, and Biological Studies of a New Class of Dual Topoisomerase I and II Inhibitors. *Inorg. Chem.* 2013, 52, 7889–7906. [PubMed: 23815163]
- (157). Geada IL; Ramezani-Dakhel H; Jamil T; Sulpizi M; Heinz H Insight into Induced Charges at Metal Surfaces and Biointerfaces Using a Polarizable Lennard-Jones Potential. *Nat. Commun.* 2018, 9, 716. [PubMed: 29459638]
- (158). van der Westhuizen D; Slabber CA; Fernandes MA; Joubert DF; Kleinhans G; van der Westhuizen CJ; Stander A; Munro OQ; Bezuidenhout DI A Cytotoxic Bis(1,2,3-Triazol-5-Ylidene)Carbazolide Gold(III) Complex Targets DNA by Partial Intercalation. *Eur. J. Chem.* 2021, 27, 8295–8307.
- (159). Gil-Moles M; Basu U; Büssing R; Hoffmeister H; Türck S; Varchmin A; Ott I Gold Metallodrugs to Target Coronavirus Proteins: Inhibitory Effects on the Spike-Ace2 Interaction and on P1pro Protease Activity by Auranofin and Gold Organometallics. *Eur. J. Chem* 2020, 26, 15140–15144.
- (160). Gabbiani C; Messori L Protein Targets for Anticancer Gold Compounds: Mechanistic Inferences. *Anti-Cancer Agents Med. Chem* 2011, 11, 929–939.
- (161). de Paiva REF Gold(I, III) Complexes Designed for Selective Targeting and Inhibition of Zinc Finger Proteins; Springer, 2018.
- (162). Gamberi T; Magherini F; Fiaschi T; Landini I; Massai L; Valocchia E; Bianchi L; Bini L; Gabbiani C; Nobili S; Mini E; Messori L; Modesti A Proteomic Analysis of the Cytotoxic Effects Induced by the Organogold(III) Complex Aubipyc in Cisplatin-Resistant A2780 Ovarian Cancer Cells: Further Evidence for the Glycolytic Pathway Implication. *Mol. Biosyst.* 2015, 11, 1653–1667. [PubMed: 25906354]

- (163). Gamberi T; Massai L; Magherini F; Landini I; Fiaschi T; Scaletti F; Gabbiani C; Bianchi L; Bini L; Nobili S; Perrone G; Mini E; Messori L; Modesti A Proteomic Analysis of A2780/S Ovarian Cancer Cell Response to the Cytotoxic Organogold(III) Compound Aubipyc. *J. Proteomics* 2014, 103, 103–120. [PubMed: 24705091]
- (164). Zhang X.-w.; Li Q.-h.; Dou J.-j.; et al. Mass Spectrometry-Based Metabolomics in Health and Medical Science: A Systematic Review. *RSC Adv.* 2020, 10, 3092–3104. [PubMed: 35497733]
- (165). Theiner S; Schoeberl A; Schweikert A; Keppler BK; Koellensperger G Mass Spectrometry Techniques for Imaging and Detection of Metallodrugs. *Curr. Opin. Chem. Biol.* 2021, 61, 123–134. [PubMed: 33535112]
- (166). Greco V; Piras C; Pieroni L; Ronci M; Putignani L; Roncada P; Urbani A Applications of Maldi-Tof Mass Spectrometry in Clinical Proteomics. *Expert Rev. Proteom.* 2018, 15, 683–696.
- (167). Riley NM; Bertozzi CR; Pitteri SJ A Pragmatic Guide to Enrichment Strategies for Mass Spectrometry-Based Glycoproteomics. *Mol. Cell. Proteomics* 2021, 20, 100029. [PubMed: 33583771]
- (168). Wright MH; Sieber SA Chemical Proteomics Approaches for Identifying the Cellular Targets of Natural Products. *Nat. Prod. Rep.* 2016, 33, 681–708. [PubMed: 27098809]
- (169). Mora M; Gimeno MC; Visbal R Recent Advances in Gold-Nhc Complexes with Biological Properties. *Chem. Soc. Rev.* 2019, 48, 447–462. [PubMed: 30474097]
- (170). Tong K-C; Hu D; Wan P-K; Lok C-N; Che C-M Anti-Cancer Gold, Platinum and Iridium Compounds with Porphyrin and/or N-Heterocyclic Carbene Ligand (S). In *Adv. Inorg. Chem.*, Vol. 75; Elsevier, 2020; pp 87–119.
- (171). Martínez-Calvo M; Mascareñas JL Organometallic Catalysis in Biological Media and Living Settings. *Coord. Chem. Rev.* 2018, 359, 57–79.
- (172). Steel TR; Hartinger CG Metalloproteomics for Molecular Target Identification of Protein-Binding Anticancer Metallodrugs. *Metallomics* 2020, 12, 1627–1636. [PubMed: 33063808]
- (173). Sanchez TW; Ronzetti MH; Owens AE; Antony M; Voss T; Wallgren E; Talley D; Balakrishnan K; Leyes Porello SE; Rai G; Marugan JJ; Michael SG; Baljinnayam B; Southall N; Simeonov A; Henderson MJ Real-Time Cellular Thermal Shift Assay to Monitor Target Engagement. *ACS Chem. Biol.* 2022, 17, 2471–2482. [PubMed: 36049119]
- (174). Tong K-C; Lok C-N; Wan P-K; Hu D; Fung YME; Chang X-Y; Huang S; Jiang H; Che C-M An Anticancer Gold(III)-Activated Porphyrin Scaffold That Covalently Modifies Protein Cysteine Thiols. *Proc. Natl. Acad. Sci. U. S. A.* 2020, 117, 1321–1329. [PubMed: 31896586]
- (175). Olelewe C; Kim JH; Ofori S; Mertens RT; Gukathasan S; Awuah SG Gold(III)-P-Chirogenic Complex Induces Mitochondrial Dysfunction in Triple-Negative Breast Cancer. *iScience* 2022, 25, 104340. [PubMed: 35602949]
- (176). Fung SK; Zou T; Cao B; Lee P-Y; Fung YME; Hu D; Lok C-N; Che C-M Cyclometalated Gold(III) Complexes Containing N-Heterocyclic Carbene Ligands Engage Multiple Anti-Cancer Molecular Targets. *Angew. Chem., Int. Ed.* 2017, 129, 3950–3954.
- (177). Castaldi MP; Hendricks JA; Zhang AX Design, Synthesis, and Strategic Use of Small Chemical Probes toward Identification of Novel Targets for Drug Development. *Curr. Opin. Chem. Biol.* 2020, 56, 91–97. [PubMed: 32375076]
- (178). Backus KM; Correia BE; Lum KM; Forli S; Horning BD; González-Páez GE; Chatterjee S; Lanning BR; Teijaro JR; Olson AJ; et al. Proteome-Wide Covalent Ligand Discovery in Native Biological Systems. *Nature* 2016, 534, 570–574. [PubMed: 27309814]
- (179). Bak DW; Gao J; Wang C; Weerapana E A Quantitative Chemoproteomic Platform to Monitor Selenocysteine Reactivity within a Complex Proteome. *Cell chem. biol.* 2018, 25, 1157–1167. [PubMed: 29983274]
- (180). Schmidt C; Zollo M; Bonsignore R; Casini A; Hacker SM Competitive Profiling of Ligandable Cysteines in *Staphylococcus Aureus* with an Organogold Compound. *Chem. Commun.* 2022, 58, 5526–5529.
- (181). Bassik MC; Kampmann M; Lebbink RJ; Wang S; Hein MY; Poser I; Weibezahn J; Horlbeck MA; Chen S; Mann M; et al. A Systematic Mammalian Genetic Interaction Map Reveals Pathways Underlying Ricin Susceptibility. *Cell* 2013, 152, 909–922. [PubMed: 23394947]



- (182). Lamb J; Crawford ED; Peck D; Modell JW; Blat IC; Wrobel MJ; Lerner J; Brunet J-P; Subramanian A; Ross KN; et al. The Connectivity Map: Using Gene-Expression Signatures to Connect Small Molecules, Genes, and Disease. *Science* 2006, 313, 1929–1935. [PubMed: 17008526]
- (183). Schenone M; Dan ík V; Wagner BK; Clemons PA Target Identification and Mechanism of Action in Chemical Biology and Drug Discovery. *Nat. Chem. Biol.* 2013, 9, 232–240. [PubMed: 23508189]
- (184). Parsons AB; Lopez A; Givoni IE; Williams DE; Gray CA; Porter J; Chua G; Sopko R; Brost RL; Ho C-H; et al. Exploring the Mode-of-Action of Bioactive Compounds by Chemical-Genetic Profiling in Yeast. *Cell* 2006, 126, 611–625. [PubMed: 16901791]
- (185). Gregori-Puigjané E; Setola V; Hert J; Crews BA; Irwin JJ; Lounkine E; Marnett L; Roth BL; Shoichet BK Identifying Mechanism-of-Action Targets for Drugs and Probes. *Proc. Natl. Acad. Sci. U. S. A.* 2012, 109, 11178–11183. [PubMed: 22711801]
- (186). Kampmann M; Bassik MC; Weissman JS Integrated Platform for Genome-Wide Screening and Construction of High-Density Genetic Interaction Maps in Mammalian Cells. *Proc. Natl. Acad. Sci. U. S. A.* 2013, 110, E2317–E2326. [PubMed: 23739767]
- (187). Ran Y; Liang Z; Gao C Current and Future Editing Reagent Delivery Systems for Plant Genome Editing. *Sci. China Life Sci.* 2017, 60, 490–505. [PubMed: 28527114]
- (188). Cong L; Zhou R; Kuo Y.-c.; Cunniff M; Zhang F Comprehensive Interrogation of Natural Tale DNA-Binding Modules and Transcriptional Repressor Domains. *Nat. Commun.* 2012, 3, 968. [PubMed: 22828628]
- (189). Wu J; Sun L; Chen X; Du F; Shi H; Chen C; Chen ZJ Cyclic Gmp-Amp Is an Endogenous Second Messenger in Innate Immune Signaling by Cytosolic DNA. *Science* 2013, 339, 826–830. [PubMed: 23258412]
- (190). Kim JH; Ofori S; Tagmount A; Vulpe CD; Awuah SG Genome-Wide Crispr Screen Reveal Targets of Chiral Gold (I) Anticancer Compound in Mammalian Cells. *ACS omega* 2022, 7, 39197–39205. [PubMed: 36340096]
- (191). Bratsch SG Standard Electrode Potentials and Temperature Coefficients in Water at 298.15 K. *J. Phys. Chem. Ref. Data* 1989, 18, 1–21.
- (192). Yam VW-W; Choi SW-K; Lai T-F; Lee W-K Syntheses, Crystal Structures and Photophysics of Organogold(III) Diimine Complexes. *Dalton Trans* 1993, 1001–1002.
- (193). Yam VW-W; Wong KM-C; Hung L-L; Zhu N Luminescent Gold(III) Alkynyl Complexes: Synthesis, Structural Characterization, and Luminescence Properties. *Angew. Chem., Int. Ed.* 2005, 44, 3107–3110.
- (194). Tang M-C; Chan M-Y; Yam VW-W Molecular Design of Luminescent Gold(III) Emitters as Thermally Evaporable and Solution-Processable Organic Light-Emitting Device (OLED) Materials. *Chem. Rev.* 2021, 121, 7249–7279. [PubMed: 34142806]
- (195). Mihaly JJ; Stewart DJ; Grusenmeyer TA; Phillips AT; Haley JE; Zeller M; Gray TG Photophysical Properties of Organogold(I) Complexes Bearing a Benzothiazole-2,7-Fluorenyl Moiety: Selection of Ancillary Ligand Influences White Light Emission. *Dalton Trans.* 2019, 48, 15917–15927. [PubMed: 31501841]
- (196). Bartolomé C; Carrasco-Rando M; Coco S; Cordovilla C; Martín-Alvarez JM; Espinet P Luminescent Gold(I) Carbenes from 2-Pyridylisocyanide Complexes: Structural Consequences of Intramolecular Versus Intermolecular Hydrogen-Bonding Interactions. *Inorg. Chem.* 2008, 47, 1616–1624. [PubMed: 18237121]
- (197). Li T.-y.; Muthiah Ravinson DS; Haiges R; Djurovich PI; Thompson ME Enhancement of the Luminescent Efficiency in Carbene-Au(I)-Aryl Complexes by the Restriction of Renner-Teller Distortion and Bond Rotation. *J. Am. Chem. Soc.* 2020, 142, 6158–6172. [PubMed: 32118418]
- (198). Pujadas M; Rodríguez L Luminescent Phosphine Gold(I) Alkynyl Complexes. Highlights from 2010 to 2018. *Coord. Chem. Rev.* 2020, 408, 213179.
- (199). Li M; Li F; Liu S; Zhao Q Luminescent Coordination Compounds for Cell Imaging. In *Fluorescent Materials for Cell Imaging*, Wu F-G, Ed.; Springer Singapore, 2020; pp 217–247.
- (200). López-de-Luzuriaga JM; Monge M; Olmos ME Luminescent Aryl-Group Eleven Metal Complexes. *Dalton Trans.* 2017, 46, 2046–2067. [PubMed: 28094379]



- (201). Redrado M; Benedi A; Marzo I; García-Otín AL; Fernández-Moreira V; Concepción Gimeno M Multifunctional Heterometallic IrIII-AuI Probes as Promising Anticancer and Antiangiogenic Agents. *Eur. J. Chem.* 2021, 27, 9885–9897.
- (202). Vaidya SP; Gadre S; Kamiseti RT; Patra M Challenges and Opportunities in the Development of Metal-Based Anticancer Theranostic Agents. *Biosci. Rep.* 2022, 42. DOI: 10.1042/BSR20212160
- (203). Huang Z; Wilson JJ Therapeutic and Diagnostic Applications of Multimetallic Rhenium(I) Tricarbonyl Complexes. *Eur. J. Inorg. Chem.* 2021, 2021, 1312–1324.
- (204). Barnard PJ; Wedlock LE; Baker MV; Berners-Price SJ; Joyce DA; Skelton BW; Steer JH Luminescence Studies of the Intracellular Distribution of a Dinuclear Gold(I) N-Heterocyclic Carbene Complex. *Angew. Chem., Int. Ed.* 2006, 45, 5966–5970.
- (205). Kathewad N; Kumar N; Dasgupta R; Ghosh M; Pal S; Khan S The Syntheses and Photophysical Properties of Pnp-Based Au (I) Complexes with Strong Intramolecular Au... Au Interactions. *Dalton Trans.* 2019, 48, 7274–7280. [PubMed: 30762852]
- (206). Guevara-Vela JM; Hess K; Rocha-Rinza T; Pendás ÁM; Flores-Álamo M; Moreno-Alcántar G Stronger-Together: The Cooperativity of Auophilic Interactions. *Chem. Commun.* 2022, 58, 1398–1401.
- (207). Ott I; Qian X; Xu Y; Vlecken DHW; Marques IJ; Kubutat D; Will J; Sheldrick WS; Jesse P; Prokop A; Bagowski CP A Gold(I) Phosphine Complex Containing a Naphthalimide Ligand Functions as a Trxr Inhibiting Antiproliferative Agent and Angiogenesis Inhibitor. *J. Med. Chem.* 2009, 52, 763–770. [PubMed: 19123857]
- (208). Bagowski CP; You Y; Scheffler H; Vlecken DH; Schmitz DJ; Ott I Naphthalimide Gold(I) Phosphine Complexes as Anticancer Metallodrugs. *Dalton Trans.* 2009, 10799–10805. [PubMed: 20023909]
- (209). Langdon-Jones EE; Lloyd D; Hayes AJ; Wainwright SD; Mottram HJ; Coles SJ; Horton PN; Pope SJ Alkynyl-Naphthalimide Fluorophores: Gold Coordination Chemistry and Cellular Imaging Applications. *Inorg. Chem.* 2015, 54, 6606–6615. [PubMed: 26086352]
- (210). Vergara E; Cerrada E; Casini A; Zava O; Laguna M; Dyson PJ Antiproliferative Activity of Gold(I) Alkyne Complexes Containing Water-Soluble Phosphane Ligands. *Organometallics* 2010, 29, 2596–2603.
- (211). Che C-M; Chao H-Y; Miskowski VM; Li Y; Cheung K-K Luminescent M-Ethynediyl and M-Butadiynediyl Binuclear Gold(I) Complexes: Observation of  $3(\Pi\pi^*)$  Emissions from Bridging Cn2- Units. *J. Am. Chem. Soc.* 2001, 123, 4985–4991. [PubMed: 11457326]
- (212). Yam VW-W; Kam-Wing Lo K; Man-Chung Wong K Luminescent Polynuclear Metal Acetylides. *J. Organomet. Chem.* 1999, 578, 3–30.
- (213). Lu W; Zhu N; Che C-M Polymorphic Forms of a Gold(I) Arylacetylide Complex with Contrasting Phosphorescent Characteristics. *J. Am. Chem. Soc.* 2003, 125, 16081–16088. [PubMed: 14678000]
- (214). Ferrer M; Rodriguez L; Rossell O; Pina F; Lima JC; Bardia MF; Solans X Linear Ditopic Acetylide Gold or Mercury Complexes: Synthesis and Photophysical Studies: X-Ray Crystal Structure of Pph4[Au(C Cc5h4n)2]. *J. Organomet. Chem.* 2003, 678, 82–89.
- (215). Hunks WJ; MacDonald M-A; Jennings MC; Puddephatt RJ Luminescent Binuclear Gold(I) Ring Complexes. *Organometallics* 2000, 19, 5063–5070.
- (216). Irwin MJ; Vittal JJ; Puddephatt RJ Luminescent Gold(I) Acetylides: From Model Compounds to Polymers. *Organometallics* 1997, 16, 3541–3547.
- (217). Chao H-Y; Lu W; Li Y; Chan MCW; Che C-M; Cheung K-K; Zhu N Organic Triplet Emissions of Arylacetylide Moieties Harnessed through Coordination to [Au(Pcy3)]+. Effect of Molecular Structure Upon Photoluminescent Properties. *J. Am. Chem. Soc.* 2002, 124, 14696–14706. [PubMed: 12465981]
- (218). Vicente J; Gil-Rubio J; Barquero N; Jones PG; Bautista D Synthesis of Luminescent Alkynyl Gold Metalaligands Containing 2,2'-Bipyridine-5-Yl and 2,2':6',2''-Terpyridine-4-Yl Donor Groups. *Organometallics* 2008, 27, 646–659.
- (219). Tikhomirov AS; Shtil AA; Shchekotikhin AE Advances in the Discovery of Anthraquinone-Based Anticancer Agents. *Recent Pat. Anticancer Drug Discovery* 2018, 13, 159–183.

- (220). Cheemalamarri C; Batchu UR; Thallamapuram NP; Katragadda SB; Reddy Shetty P A Review on Hydroxy Anthraquinones from Bacteria: Crosstalk's of Structures and Biological Activities. *Nat. Prod. Res.* 2022, 1–20.
- (221). Balasingham RG; Williams CF; Mottram HJ; Coogan MP; Pope SJA Gold(I) Complexes Derived from Alkynyoxy-Substituted Anthraquinones: Syntheses, Luminescence, Preliminary Cytotoxicity, and Cell Imaging Studies. *Organometallics* 2012, 31, 5835–5843.
- (222). Vaddamanu M; Sathyanarayana A; Masaya Y; Sugiyama S; Kazuhisa O; Velappan K; Nandeshwar M; Hisano K; Tsutsumi O; Prabusankar G Acridine N-Heterocyclic Carbene Gold (I) Compounds: Tuning from Yellow to Blue Luminescence. *Chem. Asian J.* 2021, 16, 521–529. [PubMed: 33442961]
- (223). Perez SA; de Haro C; Vicente C; Donaire A; Zamora A; Zajac J; Kosthunova H; Brabec V; Bautista D; Ruiz J New Acridine Thiourea Gold (I) Anticancer Agents: Targeting the Nucleus and Inhibiting Vasculogenic Mimicry. *ACS Chem. Biol.* 2017, 12, 1524–1537. [PubMed: 28388047]
- (224). Arcau J; Andermark V; Aguiló E; Gandioso A; Moro A; Cetina M; Lima JC; Rissanen K; Ott I; Rodríguez L Luminescent Alkynyl-Gold (I) Coumarin Derivatives and Their Biological Activity. *Dalton Trans.* 2014, 43, 4426–4436. [PubMed: 24302256]
- (225). Cerrada E; Fernández-Moreira V; Gimeno MC Gold and Platinum Alkynyl Complexes for Biomedical Applications. *Adv. Organomet. Chem.* 2019, 71, 227–258.
- (226). Rousselle B; Massot A; Privat M; Dondaine L; Trommschlagel A; Bouyer F; Bayardon J; Ghiringhelli F; Bettaieb A; Goze C; et al. Conception and Evaluation of Fluorescent Phosphine-Gold Complexes: From Synthesis to in Vivo Investigations. *ChemMedChem.* 2022, 17, No. e202100773.
- (227). Trommschlagel A; Chotard F; Bertrand B; Amor S; Dondaine L; Picquet M; Richard P; Bettaieb A; Le Gendre P; Paul C; Goze C; Bodio E Gold(I)-Bodipy-Imidazole Bimetallic Complexes as New Potential Anti-Inflammatory and Anticancer Trackable Agents. *Dalton Trans.* 2017, 46, 8051–8056. [PubMed: 28594007]
- (228). Lescure R; Privat M; Pliquett J; Massot A; Baffroy O; Busser B; Bellaye P-S; Collin B; Denat F; Bettaieb A; Sancey L; Paul C; Goze C; Bodio E Near-Infrared Emitting Fluorescent Homobimetallic Gold(I) Complexes Displaying Promising In vitro and In vivo Therapeutic Properties. *Eur. J. Med. Chem.* 2021, 220, 113483. [PubMed: 33915372]
- (229). Luengo A; Fernández-Moreira V; Marzo I; Gimeno MC Trackable Metallodrugs Combining Luminescent Re(I) and Bioactive Au(I) Fragments. *Inorg. Chem.* 2017, 56, 15159–15170. [PubMed: 29172469]
- (230). Fernández-Moreira V; Marzo I; Gimeno MC Luminescent Re(I) and Re(I)/Au(I) Complexes as Cooperative Partners in Cell Imaging and Cancer Therapy. *Chem. Sci.* 2014, 5, 4434–4446.
- (231). Luengo A; Redrado M; Marzo I; Fernández-Moreira V; Gimeno MC Luminescent Re(I)/Au(I) Species as Selective Anticancer Agents for HeLa Cells. *Inorg. Chem.* 2020, 59, 8960–8970. [PubMed: 32420746]
- (232). Luengo A; Fernández-Moreira V; Marzo I; Gimeno MC Bioactive Heterobimetallic Re(I)/Au(I) Complexes Containing Bidentate N-Heterocyclic Carbenes. *Organometallics* 2018, 37, 3993–4001.
- (233). Boselli L; Carraz M; Mazères S; Paloque L; González G; Benoit-Vical F; Valentin A; Hemmert C; Gornitzka H Synthesis, Structures, and Biological Studies of Heterobimetallic Au(I)-Ru(II) Complexes Involving N-Heterocyclic Carbene-Based Multidentate Ligands. *Organometallics* 2015, 34, 1046–1055.
- (234). Luengo A; Marzo I; Reback M; Daubit IM; Fernández-Moreira V; Metzler-Nolte N; Gimeno MC Luminescent Bimetallic Ir(III)/Au(I) Peptide Bioconjugates as Potential Theranostic Agents. *Eur. J. Chem* 2020, 26, 12158–12167.
- (235). Kumar A; Sun S-S; Lees AJ Photophysics and Photochemistry of Organometallic Rhenium Diimine Complexes. In *Photophysics of Organometallics*; Lees AJ, Ed.; Springer Berlin Heidelberg, 2010; pp 37–71.

- (236). Luengo A; Marzo I; Fernández-Moreira V; Gimeno MC Synthesis and Antiproliferative Study of Phosphorescent Multimetallic Re(I)/Au(I) Complexes Containing Fused Imidazo[4,5-F]-1,10-Phenanthroline Core. *Appl. Organomet. Chem.* 2022, No. e6661.
- (237). Wenzel M; de Almeida A; Bigaeva E; Kavanagh P; Picquet M; Le Gendre P; Bodio E; Casini A New Luminescent Polynuclear Metal Complexes with Anticancer Properties: Toward Structure-Activity Relationships. *Inorg. Chem.* 2016, 55, 2544–2557. [PubMed: 26867101]
- (238). Wilde AP; King KA; Watts RJ Resolution and Analysis of the Components in Dual Emission of Mixed-Chelate/Ortho-Metalate Complexes of Iridium(III). *J. Phys. Chem.* 1991, 95, 629–634.
- (239). Li T-Y; Wu J; Wu Z-G; Zheng Y-X; Zuo J-L; Pan Y Rational Design of Phosphorescent Iridium(III) Complexes for Emission Color Tunability and Their Applications in Oleds. *Coord. Chem. Rev.* 2018, 374, 55–92.
- (240). Lo KK-W; Zhang KY; Li SP-Y Design of Cyclometalated Iridium(III) Polypyridine Complexes as Luminescent Biological Labels and Probes. *Pure Appl. Chem.* 2011, 83, 823–840.
- (241). Caporale C; Massi M Cyclometalated Iridium(III) Complexes for Life Science. *Coord. Chem. Rev.* 2018, 363, 71–91.
- (242). Tsai JL-L; Chan AO-Y; Che C-M A Luminescent Cyclometalated Gold(III)-Avidin Conjugate with a Long-Lived Emissive Excited State That Binds to Proteins and DNA and Possesses Anti-Proliferation Capacity. *Chem. Commun.* 2015, 51, 8547–8550.
- (243). Wang F; Lan M; To W-P; Li K; Lok C-N; Wang P; Che C-M A Macromolecular Cyclometalated Gold(III) Amphiphile Displays Long-Lived Emissive Excited State in Water: Self-Assembly and in Vitro Photo-Toxicity. *Chem. Commun.* 2016, 52, 13273–13276.
- (244). Norton JR; Sowa J Introduction: Metal Hydrides. *Chem. Rev.* 2016, 116, 8315–8317. [PubMed: 27506870]
- (245). Schmidbaur H; Raubenheimer HG; Dobrzańska L The Gold-Hydrogen Bond, Au-H, and the Hydrogen Bond to Gold, Au... H-X. *Chem. Soc. Rev.* 2014, 43, 345–380. [PubMed: 23999756]
- (246). Wang X; Andrews L Gold Hydrides AuH and (H<sub>2</sub>)AuH and the AuH<sub>3</sub> Transition State Stabilized in (H<sub>2</sub>)AuH<sub>3</sub>: Infrared Spectra and Dft Calculations. *J. Am. Chem. Soc.* 2001, 123, 12899–12900. [PubMed: 11749548]
- (247). Wang X; Andrews L Gold Is Noble but Gold Hydride Anions Are Stable. *Angew. Chem., Int. Ed.* 2003, 42, 5201–5206.
- (248). Andrews L; Wang X Infrared Spectra and Structures of the Stable CuH<sub>2</sub><sup>-</sup>, AgH<sub>2</sub><sup>-</sup>, AuH<sub>2</sub><sup>-</sup>, and AuH<sub>4</sub><sup>-</sup> Anions and the AuH<sub>2</sub>Molecule. *J. Am. Chem. Soc.* 2003, 125, 11751–11760. [PubMed: 13129380]
- (249). Andrews L Matrix Infrared Spectra and Density Functional Calculations of Transition Metal Hydrides and Dihydrogen Complexes. *Chem. Soc. Rev.* 2004, 33, 123–132. [PubMed: 14767507]
- (250). Tsui EY; Müller P; Sadighi JP Reactions of a Stable Monomeric Gold(I) Hydride Complex. *Angew. Chem., Int. Ed.* 2008, 47, 8937–8940.
- (251). Escalle A; Mora G; Gagosz F; Mézailles N; Le Goff XF; Jean Y; Le Floch P Cationic Dimetallic Gold Hydride Complex Stabilized by a Xantphos-Phosphole Ligand: Synthesis, X-Ray Crystal Structure, and Density Functional Theory Study. *Inorg. Chem.* 2009, 48, 8415–8422. [PubMed: 19650647]
- (252). Rosca D-A; Smith DA; Hughes DL; Bochmann M A Thermally Stable Gold(III) Hydride: Synthesis, Reactivity, and Reductive Condensation as a Route to Gold(II) Complexes. *Angew. Chem., Int. Ed.* 2012, 51, 10643–10646.
- (253). Pintus A; Rocchigiani L; Fernandez-Cestau J; Budzelaar PHM; Bochmann M Stereo- and Regioselective Alkyne Hydrometallation with Gold(III) Hydrides. *Angew. Chem., Int. Ed.* 2016, 55, 12321–12324.
- (254). Luo H; Cao B; Chan ASC; Sun RW-Y; Zou T Cyclometalated Gold(III)-Hydride Complexes Exhibit Visible Light-Induced Thiol Reactivity and Act as Potent Photo-Activated Anti-Cancer Agents. *Angew. Chem., Int. Ed.* 2020, 132, 11139–11145.
- (255). Sheppard C; Goodell JP; Hahn P Colloidal Gold Containing the Radioactive Isotope Au<sup>198</sup> in the Selective Internal Radiation Therapy of Diseases of the Lymphoid System. *J. Lab. Clin. Med.* 1947, 32, 1437–1441. [PubMed: 20272605]

- (256). Säterborg N-E The Distribution of  $^{198}\text{Au}$  Injected Intravenously as a Colloid and in Solution. *Acta Radiol. Ther. Phys. Biol.* 1973, 12, 509–528. [PubMed: 4207000]
- (257). Bottenus BN; Kan P; Jenkins T; Ballard B; Rold TL; Barnes C; Cutler C; Hoffman TJ; Green MA; Jurisson SS Gold(III) Bis-Thiosemicarbazonato Complexes: Synthesis, Characterization, Radiochemistry and X-Ray Crystal Structure Analysis. *Nucl. Med. Biol.* 2010, 37, 41–49. [PubMed: 20122667]
- (258). Akerman MP; Munro OQ; Mongane M; van Staden JA; Rae WID; Bester CJ; Marjanovic-Painter B; Szucs Z; Zeevaart JR Biodistribution (as Determined by the Radiolabelled Equivalent) of a Gold(III) Bis(Pyrrrolide-Imine) Schiff Base Complex: A Potential Chemotherapeutic. *J. Labelled Compd. Radiopharm.* 2013, 56, 530–535.
- (259). Guarra F; Terenzi A; Pirker C; Passannante R; Baier D; Zangrando E; Gómez-Vallejo V; Biver T; Gabbiani C; Berger W; Llop J; Salassa L  $^{124}\text{I}$  Radiolabeling of a Au(III)-NHC Complex for in Vivo Biodistribution Studies. *Angew. Chem., Int. Ed.* 2020, 59, 17130–17136.
- (260). Koch R An Address on Bacteriological Research. *Br. Med. J.* 1890, 2, 380.
- (261). Koch R A Further Communication on a Remedy for Tuberculosis. *Br. Med. J.* 1890, 2, 1193.
- (262). Feldt A The Chemotherapy of Relapsing Fever with Gold and Sulphonamide Compounds. *Klin. Wochenschr.* 1941, 20.
- (263). Feldt A Zur Chemotherapie Der Tuberkulose Mit Gold. *DMW-Deutsche Medizinische Wochenschrift* 1913, 39, 549–551.
- (264). Fordos M-J; Gélis A Action Du Perchlorure D'or Sur L'hyposulfite De Soude; Bachelier, 1845.
- (265). McCluskey KL; Eichelberger L New Methods for the Preparation of Sodium Aurothiosulfate. *J. Am. Chem. Soc.* 1926, 48, 136–139.
- (266). Kayne GG The Use of Sanocrysin in the Treatment of Pulmonary Tuberculosis: (Section of Medicine). *Proc. R. Soc. Med.* 1935, 28, 1463–1468. [PubMed: 19990422]
- (267). SECHER K Traitement De La Tuberculose Par La Sanocrysin. Munksgaard L, a., Ed.; Copenhagen, 1932.
- (268). Secher K; Host E; Beitr Z; Klin DT 1934, 107.
- (269). Bang O Sanocrysin Und Experimentelle Tuberkulose. *Ztschr. Tuberk.* 1926, 44, 298.
- (270). Benedek TG The History of Gold Therapy for Tuberculosis. *J. Hist. Med. Allied Sci.* 2004, 59, 50–89. [PubMed: 15011812]
- (271). Permin G Über Sanocrysinbehandlung Von Schwerer Tuberkulose Mit Kleinen Anfangsdosen. *Acta Tuberc. Scand.* 1925, 1, 306325.
- (272). Council TMR The Gold Treatment of Tuberculosis. *Br. Med. J.* 1925, 1, 735. [PubMed: 20772016]
- (273). Forestier J Rheumatoid Arthritis and Its Treatment by Gold Salts. *Lancet* 1934, 224, 646–648.
- (274). Atakhodzhaeva Z; IaA S Comparative Effectiveness of Chrysanol and Auranofin in Rheumatoid Arthritis. *Ter. Arkh.* 1987, 59, 30–33.
- (275). Miranda VM Medicinal Inorganic Chemistry: An Updated Review on the Status of Metallodrugs and Prominent Metallodrug Candidates. *Rev. Inorg. Chem.* 2022, 42, 29–52.
- (276). Aronson JK Meyler's Side Effects of Drugs: The International Encyclopedia of Adverse Drug Reactions and Interactions; Elsevier, 2015.
- (277). Cummins S; Wigley J Discussion on the Therapeutic Value of Gold Compounds. *Proc. R. Soc. Med.* 1930, 17–33.
- (278). Barber HW Sarcoid: Effect of Krysolgan Treatment: Gradual Absorption of Sarcoid Nodules, with Development of Prurigo (Twice Previously Shown). *Proc. R. Soc. Med.* 1928, 21, 671–672. [PubMed: 19986323]
- (279). Haldin-Davis H Four Cases of Lupus Erythematosus Treated with Gold Preparations. *Proc. R. Soc. Med.* 1928, 22, 89–92.
- (280). WILE UJ; COURVILLE CJ Pityriasis-Rosea-Like Dermatitis Following Gold Therapy: Report of Two Cases. *Arch. Derm. Syphilol.* 1940, 42, 1105–1112.
- (281). Jessop J; Vernon-Roberts B; Harris J Effects of Gold Salts and Prednisolone on Inflammatory Cells. I. Phagocytic Activity of Macrophages and Polymorphs in Inflammatory Exudates Studied

- by a "Skin-Window" Technique in Rheumatoid and Control Patients. *Ann. Rheum. Dis.* 1973, 32, 294. [PubMed: 4580005]
- (282). Fan C; Zheng W; Fu X; Li X; Wong Y; Chen T Enhancement of Auranofin-Induced Lung Cancer Cell Apoptosis by Selenocystine, a Natural Inhibitor of Trx1 In Vitro and in Vivo. *Cell Death Dis.* 2014, 5, No. e1191.
- (283). Li H; Hu J; Wu S; Wang L; Cao X; Zhang X; Dai B; Cao M; Shao R; Zhang R; et al. Auranofin-Mediated Inhibition of Pi3k/Akt/Mtor Axis and Anticancer Activity in Non-Small Cell Lung Cancer Cells. *Oncotarget* 2016, 7, 3548. [PubMed: 26657290]
- (284). Marzano C; Gandin V; Folda A; Scutari G; Bindoli A; Rigobello MP Inhibition of Thioredoxin Reductase by Auranofin Induces Apoptosis in Cisplatin-Resistant Human Ovarian Cancer Cells. *Free Radic. Biol. Med.* 2007, 42, 872–881. [PubMed: 17320769]
- (285). Hou G-X; Liu P-P; Zhang S; Yang M; Liao J; Yang J; Hu Y; Jiang W-Q; Wen S; Huang P Elimination of Stem-Like Cancer Cell Side-Population by Auranofin through Modulation of Ros and Glycolysis. *Cell Death Dis.* 2018, 9, 1–15. [PubMed: 29298988]
- (286). Madeira J; Gibson D; Kean W; Klegeris A The Biological Activity of Auranofin: Implications for Novel Treatment of Diseases. *Inflammopharmacology* 2012, 20, 297–306. [PubMed: 22965242]
- (287). Thangamani S; Mohammad H; Abushahba MF; Sobreira TJ; Hedrick VE; Paul LN; Seleem MN Antibacterial Activity and Mechanism of Action of Auranofin against Multi-Drug Resistant Bacterial Pathogens. *Sci. Rep.* 2016, 6, 1–13. [PubMed: 28442746]
- (288). Elkashif A; Seleem MN Investigation of Auranofin and Gold-Containing Analogues Antibacterial Activity against Multidrug-Resistant *Neisseria Gonorrhoeae*. *Sci. Rep.* 2020, 10, 1–9. [PubMed: 31913322]
- (289). Onodera T; Momose I; Kawada M Potential Anticancer Activity of Auranofin. *Chem. Pharm. Bull. (Tokyo)* 2019, 67, 186–191. [PubMed: 30827998]
- (290). Cirri D; Massai L; Giacomelli C; Trincavelli ML; Guerri A; Gabbiani C; Messori L; Pratesi A Synthesis, Chemical Characterization, and Biological Evaluation of a Novel Auranofin Derivative as an Anticancer Agent. *Dalton Trans.* 2022, 51, 13527–13539. [PubMed: 36000524]
- (291). Diaz RS; Shytaj IL; Giron LB; Obermaier B; della Libera E Jr; Galinskas J; Dias D; Hunter J; Janini M; Gosuen G; et al. Potential Impact of the Antirheumatic Agent Auranofin on Proviral Hiv-1 DNA in Individuals under Intensified Antiretroviral Therapy: Results from a Randomised Clinical Trial. *Int. J. Antimicrob. Agents* 2019, 54, 592–600. [PubMed: 31394172]
- (292). de Almeida Baptista MV; da Silva LT; Samer S; Oshiro TM; Shytaj IL; Giron LB; Pena NM; Cruz N; Gosuen GC; Ferreira PRA; et al. Immunogenicity of Personalized Dendritic-Cell Therapy in Hiv-1 Infected Individuals under Suppressive Antiretroviral Treatment: Interim Analysis from a Phase II Clinical Trial. *AIDS Res. Ther.* 2022, 19, 1–15. [PubMed: 34996470]
- (293). Vaccine Gene Therapy Institute, Florida University of Miami. Oral Auranofin for Reduction of Latent Viral Reservoir in Patients with Hiv Infection, 2023. <https://ClinicalTrials.gov/show/NCT02176135> (accessed 03-20-2023).
- (294). National Institute of Allergy Infectious Diseases. Auranofin Pk Following Oral Dose Administration, 2014. <https://ClinicalTrials.gov/show/NCT02089048> (accessed 03-20-2023).
- (295). Clinic Mayo. Auranofin in Treating Patients with Recurrent Epithelial Ovarian, Primary Peritoneal, or Fallopian Tube Cancer, 2012. <https://ClinicalTrials.gov/show/NCT01747798> (accessed 03-20-2023).
- (296). Mayo Clinic; National Cancer Institute. Auranofin in Decreasing Pain in Patients with Paclitaxel-Induced Pain Syndrome, 2014. <https://ClinicalTrials.gov/show/NCT02063698> (accessed 03-20-2023).
- (297). National Institute of Allergy Infectious Diseases Auranofin for Giardia Protozoa, 2016. <https://ClinicalTrials.gov/show/NCT02736968> (accessed 03-20-2023).
- (298). Mayo Clinic; National Cancer Institute. Auranofin and Sirolimus in Treating Patients with Advanced Solid Tumors or Recurrent Non-Small Cell Lung Cancer, 2013. <https://ClinicalTrials.gov/show/NCT02126527> (accessed 03-20-2023).



- (299). Mayo Clinic; National Cancer Institute. Sirolimus and Auranofin in Treating Patients with Advanced or Recurrent Non-Small Cell Lung Cancer or Small Cell Lung Cancer, 2012. <https://ClinicalTrials.gov/show/NCT01737502> (accessed 03-20-2023).
- (300). Federal University of São Paulo Fundação de Amparo à Pesquisa do Estado de São Paulo Conselho Nacional de Desenvolvimento Científico e Tecnológico ViiV Healthcare Multi Interventional Study Exploring Hiv-1 Residual Replication: A Step Towards Hiv-1 Eradication and Sterilizing Cure, 2015. <https://ClinicalTrials.gov/show/NCT02961829> (accessed 03-20-2023).
- (301). The Aurum Institute NPC Tb Host Directed Therapy, 2016. <https://ClinicalTrials.gov/show/NCT02968927> (accessed 03-20-2023).
- (302). University of Ulm Reliable Cancer Therapies Anticancer Fund, Belgium A Proof-of-Concept Clinical Trial Assessing the Safety of the Coordinated Undermining of Survival Paths by 9 Repurposed Drugs Combined with Metronomic Temozolomide (Cusp9v3 Treatment Protocol) for Recurrent Glioblastoma, 2016. <https://ClinicalTrials.gov/show/NCT02770378> (accessed 03-20-2023).
- (303). Pfizer. Comparative Analysis of Outcomes among Patients Initiating Xeljanz in Combination with Oral Mtx Who Withdraw Mtx Versus Continue Mtx. (accessed 03-20-2023).
- (304). Roche Hoffmann-La. An Observational Study of Mabthera/Rituxan (Rituximab) and Alternative Tnf-Inhibitors in Patients with Rheumatoid Arthritis and an Inadequate Response to a Single Previous Tnf-Inhibitor, 2009. <https://ClinicalTrials.gov/show/NCT01557348> (accessed 03-20-2023).
- (305). Ghannoum MA; Rice LB Antifungal Agents: Mode of Action, Mechanisms of Resistance, and Correlation of These Mechanisms with Bacterial Resistance. *Clin. Microbiol. Rev.* 1999, 12, 501–517. [PubMed: 10515900]
- (306). Dennis EK; Kim JH; Parkin S; Awuah SG; Garneau-Tsodikova S Distorted Gold(I)-Phosphine Complexes as Antifungal Agents. *J. Med. Chem.* 2020, 63, 2455–2469. [PubMed: 31841324]
- (307). Yang L; Powell DR; Houser RP Structural Variation in Copper (I) Complexes with Pyridylmethylamide Ligands: Structural Analysis with a New Four-Coordinate Geometry Index, T 4. *Dalton Trans.* 2007, 955–964. [PubMed: 17308676]
- (308). Stevanovi NL; Kljun J; Aleksic I; Bogojevic SS; Milivojevic D; Veselinovic A; Turel I; Djuran MI; Nikodinovic-Runic J; Gliši B Clinically Used Antifungal Azoles as Ligands for Gold(III) Complexes: The Influence of the Au(III) Ion on the Antimicrobial Activity of the Complex. *Dalton Trans.* 2022, 51, 5322–5334. [PubMed: 35293926]
- (309). Bassetti M; Peghin M; Vena A; Giacobbe DR Treatment of Infections Due to Mdr Gram-Negative Bacteria. *Front. Med.* 2019, 6, 74.
- (310). Ratia C; Soengas RG; Soto SM Gold-Derived Molecules as New Antimicrobial Agents. *Front. Microbiol.* 2022, 13, 772.
- (311). Delcour AH Outer Membrane Permeability and Antibiotic Resistance. *Biochimica et Biophysica Acta (BBA)-Proteins and Proteomics* 2009, 1794, 808–816. [PubMed: 19100346]
- (312). Silver LL Challenges of Antibacterial Discovery. *Clin. Microbiol. Rev.* 2011, 24, 71–109. [PubMed: 21233508]
- (313). Cassetta MI; Marzo T; Fallani S; Novelli A; Messori L Drug Repositioning: Auranofin as a Prospective Antimicrobial Agent for the Treatment of Severe Staphylococcal Infections. *Biometals* 2014, 27, 787–791. [PubMed: 24820140]
- (314). Torres NS; Abercrombie JJ; Srinivasan A; Lopez-Ribot JL; Ramasubramanian AK; Leung KP Screening a Commercial Library of Pharmacologically Active Small Molecules against *Staphylococcus Aureus* Biofilms. *Antimicrob. Agents Chemother.* 2016, 60, 5663–5672. [PubMed: 27401577]
- (315). Torres NS; Montelongo-Jauregui D; Abercrombie JJ; Srinivasan A; Lopez-Ribot JL; Ramasubramanian AK; Leung KP Antimicrobial and Antibiofilm Activity of Synergistic Combinations of a Commercially Available Small Compound Library with Colistin against *Pseudomonas Aeruginosa*. *Front. Microbiol.* 2018, 9, 2541. [PubMed: 30410476]
- (316). Wu B; Yang X; Yan M Synthesis and Structure-Activity Relationship Study of Antimicrobial Auranofin against Escape Pathogens. *J. Med. Chem.* 2019, 62, 7751–7768. [PubMed: 31386365]



- (317). Epstein TD; Wu B; Moulton KD; Yan M; Dube DH Sugar-Modified Analogs of Auranofin Are Potent Inhibitors of the Gastric Pathogen *Helicobacter Pylori*. *ACS Infect. Dis.* 2019, 5, 1682–1687. [PubMed: 31487153]
- (318). Maydaniuk D; Wu B; Truong D; Liyanage SH; Hogan AM; Yap ZL; Yan M; Cardona ST New Auranofin Analogs with Antibacterial Properties against *Burkholderia* Clinical Isolates. *Antibiotics* 2021, 10, 1443. [PubMed: 34943654]
- (319). Owings JP; McNair NN; Mui YF; Gustafsson TN; Holmgren A; Contel M; Goldberg JB; Mead JR Auranofin and N-Heterocyclic Carbene Gold-Analogs Are Potent Inhibitors of the Bacteria *Helicobacter Pylori*. *FEMS Microbiol. Lett.* 2016, 363, fnw148. [PubMed: 27279627]
- (320). Schmidt C; Karge B; Misgeld R; Prokop A; Franke R; Brönstrup M; Ott I Gold (I) NHC Complexes: Antiproliferative Activity, Cellular Uptake, Inhibition of Mammalian and Bacterial Thioredoxin Reductases, and Gram-Positive Directed Antibacterial Effects. *Eur. J. Chem.* 2017, 23, 1869–1880.
- (321). Roymahapatra G; M Mandal S; F Porto W; Samanta T; Giri S; Dinda J; L Franco O; K Chattaraj P Pyrazine Functionalized Ag (I) and Au (I)-NHC Complexes Are Potential Antibacterial Agents. *Curr. Med. Chem.* 2012, 19, 4184–4193. [PubMed: 22680631]
- (322). Vellé A; Maguire R; Kavanagh K; Sanz Miguel PJ; Montagner D Steroid-AuI-Nhc Complexes: Synthesis and Antibacterial Activity. *ChemMedChem.* 2017, 12, 841–844. [PubMed: 28463422]
- (323). Büssing R; Karge B; Lippmann P; Jones PG; Brönstrup M; Ott I Gold (I) and Gold (III) N-Heterocyclic Carbene Complexes as Antibacterial Agents and Inhibitors of Bacterial Thioredoxin Reductase. *ChemMedChem.* 2021, 16, 3402–3409. [PubMed: 34268875]
- (324). Chen X; Sun S; Huang S; Yang H; Ye Q; Lv L; Liang Y; Shan J; Xu J; Liu W; et al. Gold (I) Selenium N-Heterocyclic Carbene Complexes as Potent Antibacterial Agents against Multidrug-Resistant Gram-Negative Bacteria Via Inhibiting Thioredoxin Reductase. *Redox Biol.* 2023, 60, 102621. [PubMed: 36758467]
- (325). Stenger-Smith J; Chakraborty I; Mascharak PK Cationic Au (I) Complexes with Aryl-Benzothiazoles and Their Antibacterial Activity. *J. Inorg. Biochem.* 2018, 185, 80–85. [PubMed: 29800748]
- (326). Hikiş P; Szczupak L; Koceva-Chyła A; Guspier A; Oehninger L; Ott I; Therrien B; Solecka J; Kowalski K Anticancer and Antibacterial Activity Studies of Gold (I)-Alkynyl Chromones. *Molecules* 2015, 20, 19699–19718. [PubMed: 26528965]
- (327). Pintus A; Aragoni MC; Cinellu MA; Maiore L; Isaia F; Lippolis V; Orru G; Tuveri E; Zucca A; Arca M [Au (Pyb-H)(Mnt)]: A Novel Gold (III) 1, 2-Dithiolene Cyclometalated Complex with Antimicrobial Activity (Pyb-H= C-Deprotonated 2-Benzylpyridine; Mnt= 1, 2-Dicyanoethene-1, 2-Dithiolate). *J. Inorg. Biochem.* 2017, 170, 188–194. [PubMed: 28260677]
- (328). Fontinha D; Sousa SA; Morais TS; Prudêncio M; Leitão JH; Le Gal Y; Lorcy D; Silva RA; Velho MF; Belo D; et al. Gold (III) Bis (Dithiolene) Complexes: From Molecular Conductors to Prospective Anticancer, Antimicrobial and Anti-plasmodial Agents. *Metallomics* 2020, 12, 974–987. [PubMed: 32391537]
- (329). Chakraborty P; Oosterhuis D; Bonsignore R; Casini A; Olinga P; Scheffers DJ An Organogold Compound as Potential Antimicrobial Agent against Drug-Resistant Bacteria: Initial Mechanistic Insights. *ChemMedChem.* 2021, 16, 3060–3070. [PubMed: 34181818]
- (330). Ilari A; Baiocco P; Messori L; Fiorillo A; Boffi A; Gramiccia M; Di Muccio T; Colotti G A Gold-Containing Drug against Parasitic Polyamine Metabolism: The X-Ray Structure of Trypanothione Reductase from *Leishmania Infantum* in Complex with Auranofin Reveals a Dual Mechanism of Enzyme Inhibition. *Amino Acids* 2012, 42, 803–811. [PubMed: 21833767]
- (331). Sharlow ER; Leimgruber S; Murray S; Lira A; Sciotti RJ; Hickman M; Hudson T; Leed S; Caridha D; Barrios AM; Close D; Grögl M; Lazo JS Auranofin Is an Apoptosis-Simulating Agent with in Vitro and in Vivo Anti-Leishmanial Activity. *ACS Chem. Biol.* 2014, 9, 663–672. [PubMed: 24328400]
- (332). Rosa LB; Aires RL; Oliveira LS; Fontes JV; Miguel DC; Abbehausen CA “Golden Age” for the Discovery of New Antileishmanial Agents: Current Status of Leishmanicidal Gold Complexes and Prospective Targets Beyond the Trypanothione System. *ChemMedChem.* 2021, 16, 1682–1696.

- (333). Mota VZ; de Carvalho GS; da Silva AD; Costa LA; de Almeida Machado P; Coimbra ES; Ferreira CV; Shishido SM; Cuin A Gold Complexes with Benzimidazole Derivatives: Synthesis, Characterization and Biological Studies. *Biometals* 2014, 27, 183–194. [PubMed: 24442571]
- (334). Minori K; Rosa LB; Bonsignore R; Casini A; Miguel DC Comparing the Antileishmanial Activity of Gold(I) and Gold(III) Compounds in *L. Amazonensis* and *L. Braziliensis* in Vitro. *ChemMedChem*. 2020, 15, 2146–2150. [PubMed: 32830445]
- (335). Oujji M; Delmas SB; Álvarez ÁF; Augereau J-M; Valentin A; Hemmert C; Gornitzka H; Benoit-Vical F Design, Synthesis and Efficacy of Hybrid Triclosan-Gold Based Molecules on Artemisinin-Resistant *Plasmodium Falciparum* and *Leishmania Infantum* Parasites. *ChemistrySelect* 2020, 5, 619–625.
- (336). Zhang C; Bourgeade Delmas S; Fernández Álvarez A; Valentin A; Hemmert C; Gornitzka H Synthesis, Characterization, and Antileishmanial Activity of Neutral N-Heterocyclic Carbenes Gold(I) Complexes. *Eur. J. Med. Chem.* 2018, 143, 1635–1643. [PubMed: 29133045]
- (337). Chaves JDS; Tunes LG; de J. Franco CH; Francisco TM; Corrêa CC; Murta SMF; Monte-Neto RL; Silva H; Fontes APS; de Almeida MV Novel Gold(I) Complexes with 5-Phenyl-1,3,4-Oxadiazole-2-Thione and Phosphine as Potential Anti-cancer and Antileishmanial Agents. *Eur. J. Med. Chem.* 2017, 127, 727–739. [PubMed: 27823888]
- (338). Espinosa AV; Costa D. d. S.; Tunes LG; Monte-Neto R. L. d.; Grazul RM; de Almeida MV; Silva H Anticancer and Antileishmanial in Vitro Activity of Gold(I) Complexes with 1,3,4-Oxadiazole-2(3h)-Thione Ligands Derived from  $\alpha$ -D-Gluconolactone. *Chem. Biol. Drug Des.* 2021, 97, 41–50. [PubMed: 32657521]
- (339). Tunes LG; Morato RE; Garcia A; Schmitz V; Steindel M; Corrêa-Junior JD; Dos Santos HF; Frézard F; de Almeida MV; Silva H; Moretti NS; de Barros ALB; do Monte-Neto RL Preclinical Gold Complexes as Oral Drug Candidates to Treat Leishmaniasis Are Potent Trypanothione Reductase Inhibitors. *ACS Infect. Dis.* 2020, 6, 1121–1139. [PubMed: 32283915]
- (340). Wallace DC Mitochondria and Cancer. *Nat. Rev. Cancer* 2012, 12, 685–698. [PubMed: 23001348]
- (341). Missiroli S; Perrone M; Genovese I; Pinton P; Giorgi C Cancer Metabolism and Mitochondria: Finding Novel Mechanisms to Fight Tumours. *EBioMedicine* 2020, 59, 102943. [PubMed: 32818805]
- (342). Vyas S; Zaganjor E; Haigis MC Mitochondria and Cancer. *Cell* 2016, 166, 555–566. [PubMed: 27471965]
- (343). Zong W-X; Rabinowitz JD; White E Mitochondria and Cancer. *Mol. Cell* 2016, 61, 667–676. [PubMed: 26942671]
- (344). Newmeyer DD; Ferguson-Miller S Mitochondria: Releasing Power for Life and Unleashing the Machineries of Death. *Cell* 2003, 112, 481–490. [PubMed: 12600312]
- (345). Grasso D; Zampieri LX; Capelôa T; Van de Velde JA; Sonveaux P Mitochondria in Cancer. *Cell stress* 2020, 4, 114. [PubMed: 32548570]
- (346). Bock FJ; Tait SW Mitochondria as Multifaceted Regulators of Cell Death. *Nat. Rev. Mol. Cell Biol.* 2020, 21, 85–100. [PubMed: 31636403]
- (347). Chandel NS Evolution of Mitochondria as Signaling Organelles. *Cell Metab.* 2015, 22, 204–206. [PubMed: 26073494]
- (348). Chakrabarty RP; Chandel NS Mitochondria as Signaling Organelles Control Mammalian Stem Cell Fate. *Cell Stem Cell* 2021, 28, 394–408. [PubMed: 33667360]
- (349). Galluzzi L; Kepp O; Kroemer G Mitochondria: Master Regulators of Danger Signalling. *Nat. Rev. Mol. Cell Biol.* 2012, 13, 780–788. [PubMed: 23175281]
- (350). Tait SW; Green DR Mitochondria and Cell Death: Outer Membrane Permeabilization and Beyond. *Nat. Rev. Mol. Cell Biol.* 2010, 11, 621–632. [PubMed: 20683470]
- (351). Tait SW; Green DR Mitochondria and Cell Signalling. *J. Cell Sci.* 2012, 125, 807–815. [PubMed: 22448037]
- (352). Berners-Price SJ; Mirabelli CK; Johnson RK; Mattern MR; McCabe FL; Faucette LF; Sung C-M; Mong S-M; Sadler PJ; Crooke ST In Vivo Antitumor Activity and in Vitro Cytotoxic Properties of Bis [1, 2-Bis (Diphenylphosphino) Ethane] Gold (I) Chloride. *Cancer Res.* 1986, 46, 5486–5493. [PubMed: 3756897]

- (353). Barnard PJ; Berners-Price SJ Targeting the Mitochondrial Cell Death Pathway with Gold Compounds. *Coord. Chem. Rev.* 2007, 251, 1889–1902.
- (354). Xiao Q; Liu Y; Jiang G; Liu Y; Huang Y; Liu W; Zhang Z Heteroleptic Gold (I)-BisNHC Complex with Excellent Activity in Vitro, Ex Vivo and in Vivo against Endometrial Cancer. *Eur. J. Med. Chem.* 2022, 236, 114302. [PubMed: 35395440]
- (355). Mertens RT; Jennings WC; Ofori S; Kim JH; Parkin S; Kwakye GF; Awuah SG Synthetic Control of Mitochondrial Dynamics: Developing Three-Coordinate Au(I) Probes for Perturbation of Mitochondria Structure and Function. *JACS Au* 2021, 1, 439–449. [PubMed: 34467306]
- (356). Mertens RT; Greif CE; Coogle JT; Berger G; Parkin S; Watson MD; Awuah SG Stable Au (I) Catalysts for Oxidant-Free Ch Functionalization with Iodoarenes. *Journal of catalysis* 2022, 408, 109–114. [PubMed: 35368720]
- (357). Zhang X; Frezza M; Milacic V; Ronconi L; Fan Y; Bi C; Fregona D; Dou QP Inhibition of Tumor Proteasome Activity by Gold-Dithiocarbamate Complexes Via Both Redox-Dependent and-Independent Processes. *J. Cell. Biochem.* 2010, 109, 162–172. [PubMed: 19911377]
- (358). Milacic V; Chen D; Ronconi L; Landis-Piwowar KR; Fregona D; Dou QP A Novel Anticancer Gold(III) Dithiocarbamate Compound Inhibits the Activity of a Purified 20s Proteasome and 26s Proteasome in Human Breast Cancer Cell Cultures and Xenografts. *Cancer Res.* 2006, 66, 10478–10486. [PubMed: 17079469]
- (359). Tomasello MF; Nardon C; Lanza V; Di Natale G; Pettenuzzo N; Salmaso S; Milardi D; Caliceti P; Pappalardo G; Fregona D New Comprehensive Studies of a Gold(III) Dithiocarbamate Complex with Proven Anticancer Properties: Aqueous Dissolution with Cyclodextrins, Pharmacokinetics and Upstream Inhibition of the Ubiquitin-Proteasome Pathway. *Eur. J. Med. Chem.* 2017, 138, 115–127. [PubMed: 28651154]
- (360). Adokoh CK Therapeutic Potential of Dithiocarbamate Supported Gold Compounds. *RSC Adv.* 2020, 10, 2975–2988. [PubMed: 35496096]
- (361). Mertens RT; Parkin S; Awuah SG Cancer Cell-Selective Modulation of Mitochondrial Respiration and Metabolism by Potent Organogold(III) Dithiocarbamates. *Chem. Sci.* 2020, 11, 10465–10482. [PubMed: 34094305]
- (362). Kim JH; Ofori S; Parkin S; Vekaria H; Sullivan PG; Awuah SG Anticancer Gold(III)-Bisphosphine Complex Alters the Mitochondrial Electron Transport Chain to Induce in Vivo Tumor Inhibition. *Chem. Sci.* 2021, 12, 7467–7479. [PubMed: 34163837]
- (363). Kim JH; Reeder E; Parkin S; Awuah SG Gold(I/III)-Phosphine Complexes as Potent Antiproliferative Agents. *Sci. Rep.* 2019, 9, 1–18. [PubMed: 30626917]
- (364). Hyun Kim J; Ofori S; Mertens RT; Parkin S; Awuah SG Water-Soluble Gold(III)-Metformin Complex Alters Mitochondrial Bioenergetics in Breast Cancer Cells. *ChemMedChem.* 2021, 16, 3222–3230. [PubMed: 34159760]
- (365). Babak MV; Chong KR; Rapta P; Zannikou M; Tang HM; Reichert L; Chang MR; Kushnarev V; Heffeter P; Meier-Menches SM; Lim ZC; Yap JY; Casini A; Balyasnikova IV; Ang WH Interfering with Metabolic Profile of Triple-Negative Breast Cancers Using Rationally Designed Metformin Prodrugs. *Angew. Chem., Int. Ed.* 2021, 60, 13405–13413.
- (366). Machado JF; Correia JDG; Morais TS Emerging Molecular Receptors for the Specific-Target Delivery of Ruthenium and Gold Complexes into Cancer Cells. *Molecules* 2021, 26.3153 [PubMed: 35011258]
- (367). Smiłowicz D; Słotweg JC; Metzler-Nolte N Bioconjugation of Cyclometalated Gold(III) Lipoic Acid Fragments to Linear and Cyclic Breast Cancer Targeting Peptides. *Mol. Pharmaceutics* 2019, 16, 4572–4581.
- (368). Bertrand B; O'Connell MA; Waller ZAE; Bochmann M A Gold(III) Pincer Ligand Scaffold for the Synthesis of Binuclear and Bioconjugated Complexes: Synthesis and Anticancer Potential. *Chemistry (Easton)* 2018, 24, 3613–3622.
- (369). Ortega E; Zamora A; Basu U; Lippmann P; Rodríguez V; Janiak C; Ott I; Ruiz J An Erlotinib Gold(I) Conjugate for Combating Triple-Negative Breast Cancer. *J. Inorg. Biochem.* 2020, 203, 110910. [PubMed: 31683128]

- (370). Curado N; Dewaele-Le Roi G; Poty S; Lewis JS; Contel M Trastuzumab Gold-Conjugates: Synthetic Approach and in Vitro Evaluation of Anticancer Activities in Breast Cancer Cell Lines. *Chem. Commun.* 2019, 55, 1394–1397.
- (371). Sen S; Won M; Levine MS; Noh Y; Sedgwick AC; Kim JS; Sessler JL; Arambula JF Metal-Based Anticancer Agents as Immunogenic Cell Death Inducers: The Past, Present, and Future. *Chem. Soc. Rev.* 2022, 51, 1212–1233. [PubMed: 35099487]
- (372). Sen S; Karoscik K; Maier E; Arambula JF Immunogenic Cell Death-Inducing Metal Complexes: From the Benchtop to the Clinic. *Curr. Opin. Chem. Biol.* 2023, 73, 102277. [PubMed: 36867977]
- (373). Eisler R Chrysotherapy: A Synoptic Review. *Inflamm. Res.* 2003, 52, 487–501. [PubMed: 14991077]
- (374). van der Most RG; Robinson BW; Lake RA Combining Immunotherapy with Chemotherapy to Treat Cancer. *Discovery Med.* 2005, 5, 265–270.
- (375). Gandhi L; Rodríguez-Abreu D; Gadgeel S; Esteban E; Felip E; De Angelis F; Domine M; Clingan P; Hochmair MJ; Powell SF; Cheng SY; Bischoff HG; Peled N; Grossi F; Jennens RR; Reck M; Hui R; Garon EB; Boyer M; Rubio-Viqueira B; Novello S; Kurata T; Gray JE; Vida J; Wei Z; Yang J; Raftopoulos H; Pietanza MC; Garassino MC Pembrolizumab Plus Chemotherapy in Metastatic Non-Small-Cell Lung Cancer. *N. Engl. J. Med.* 2018, 378, 2078–2092. [PubMed: 29658856]
- (376). Cao G; Wang J; Zheng X; Wei H; Tian Z; Sun R Tumor Therapeutics Work as Stress Inducers to Enhance Tumor Sensitivity to Natural Killer (Nk) Cell Cytolysis by up-Regulating Nkp30 Ligand B7-H6. *J. Biol. Chem.* 2015, 290, 29964–29973. [PubMed: 26472927]
- (377). Mármol I; Virumbrales-Muñoz M; Quero J; Sánchez-de-Diego C; Fernández L; Ochoa I; Cerrada E; Yoldi MJR Alkynyl Gold(I) Complex Triggers Necroptosis Via Ros Generation in Colorectal Carcinoma Cells. *J. Inorg. Biochem.* 2017, 176, 123–133. [PubMed: 28892675]
- (378). Jeon KI; Byun MS; Jue DM Gold Compound Auranofin Inhibits Ikkappa Kinase (Ikk) by Modifying Cys-179 of Ikkbeta Subunit. *Exp. Mol. Med.* 2003, 35, 61–66. [PubMed: 12754408]
- (379). Kim I; Crippen GM; Amidon GL Structure and Specificity of a Human Valacyclovir Activating Enzyme: A Homology Model of Bphl. *Mol. Pharmaceutics* 2004, 1, 434–446.
- (380). Baeck M; Goossens A Systemic Contact Dermatitis to Corticosteroids. *Allergy* 2012, 67, 1580–1585. [PubMed: 23033862]
- (381). Elie BT; Pecheny Y; Uddin F; Contel M A Heterometallic Ruthenium-Gold Complex Displays Antiproliferative, Antimigratory, and Antiangiogenic Properties and Inhibits Metastasis and Angiogenesis-Associated Proteases in Renal Cancer. *J. Biol. Inorg. Chem.* 2018, 23, 399–411. [PubMed: 29508136]
- (382). Rachmawati D; Alsalem IW; Bontkes HJ; Verstege MI; Gibbs S; von Blomberg BM; Scheper RJ; van Hoogstraten IM Innate Stimulatory Capacity of High Molecular Weight Transition Metals Au (Gold) and Hg (Mercury). *Toxicol. In Vitro* 2015, 29, 363–369. [PubMed: 25458486]
- (383). Martin SF; Esser PR; Weber FC; Jakob T; Freudenberg MA; Schmidt M; Goebeler M Mechanisms of Chemical-Induced Innate Immunity in Allergic Contact Dermatitis. *Allergy* 2011, 66, 1152–1163. [PubMed: 21599706]
- (384). Zitvogel L; Kepp O; Kroemer G Immune Parameters Affecting the Efficacy of Chemotherapeutic Regimens. *Nat. Rev. Clin. Oncol.* 2011, 8, 151–160. [PubMed: 21364688]
- (385). Tang H; Xu X; Chen Y; Xin H; Wan T; Li B; Pan H; Li D; Ping Y Reprogramming the Tumor Microenvironment through Second-near-Infrared-Window Photothermal Genome Editing of Pd-L1 Mediated by Supramolecular Gold Nanorods for Enhanced Cancer Immunotherapy. *Adv. Mater.* 2021, 33, No. e2006003.
- (386). Liang R; Liu L; He H; Chen Z; Han Z; Luo Z; Wu Z; Zheng M; Ma Y; Cai L Oxygen-Boosted Immunogenic Photodynamic Therapy with Gold Nanocages@Manganese Dioxide to Inhibit Tumor Growth and Metastases. *Biomaterials* 2018, 177, 149–160. [PubMed: 29890364]
- (387). Sen S; Hufnagel S; Maier EY; Aguilar I; Selvakumar J; DeVore JE; Lynch VM; Arumugam K; Cui Z; Sessler JL; Arambula JF Rationally Designed Redox-Active Au(I) N-Heterocyclic Carbene: An Immunogenic Cell Death Inducer. *J. Am. Chem. Soc.* 2020, 142, 20536–20541. [PubMed: 33237764]

- (388). Reya T; Morrison SJ; Clarke MF; Weissman IL Stem Cells, Cancer, and Cancer Stem Cells. *Nature* 2001, 414, 105–111. [PubMed: 11689955]
- (389). Gasch C; Ffrench B; O’Leary JJ; Gallagher MF Catching Moving Targets: Cancer Stem Cell Hierarchies, Therapy-Resistance & Considerations for Clinical Intervention. *Mol. Cancer* 2017, 16, 1–15. [PubMed: 28093071]
- (390). Zheng Q; Zhang M; Zhou F; Zhang L; Meng X The Breast Cancer Stem Cells Traits and Drug Resistance. *Front. Pharmacol.* 2021, 11, 599965. [PubMed: 33584277]
- (391). Zou T; Lum CT; Lok C-N; To W-P; Low K-H; Che C-M A Binuclear Gold (I) Complex with Mixed Bridging Diphosphine and Bis (N-Heterocyclic Carbene) Ligands Shows Favorable Thiol Reactivity and Inhibits Tumor Growth and Angiogenesis in Vivo. *Angew. Chem., Int. Ed.* 2014, 126, 5920–5924.
- (392). Roesch S; Fermi V; Rominger F; Herold-Mende C; Romero-Nieto C Correction: Gold (I) Complexes Based on Six-Membered Phosphorus Heterocycles as Bio-Active Molecules against Brain Cancer. *Chem. Commun.* 2020, 56, 15088–15088.
- (393). Johnson A; Olelewe C; Kim JH; Northcote-Smith J; Mertens RT; Passeri G; Singh K; Awuah SG; Suntharalingam K The Anti-Breast Cancer Stem Cell Properties of Gold (I)-Non-Steroidal Anti-Inflammatory Drug Complexes. *Chem. Sci.* 2023.14557
- (394). Lum CT; Wong AS-T; Lin MC; Che C-M; Sun RW-Y A Gold(III) Porphyrin Complex as an Anti-Cancer Candidate to Inhibit Growth of Cancer-Stem Cells. *Chem. Commun.* 2013, 49, 4364–4366.
- (395). Cascella M; Rajnik M; Aleem A; Dulebohn SC; Di Napoli R Features, Evaluation, and Treatment of Coronavirus (Covid-19); StatPearls Publishing LLC., 2022.
- (396). Fonteh PN; Keter FK; Meyer D Hiv Therapeutic Possibilities of Gold Compounds. *Biometals* 2010, 23, 185–196. [PubMed: 20127392]
- (397). Bowman M-C; Ballard TE; Ackerson CJ; Feldheim DL; Margolis DM; Melander C Inhibition of Hiv Fusion with Multivalent Gold Nanoparticles. *J. Am. Chem. Soc.* 2008, 130, 6896–6897. [PubMed: 18473457]
- (398). Fonseca C; Aureliano M Biological Activity of Gold Compounds against Viruses and Parasitosis: A Systematic Review. *BioChem.* 2022, 2, 145–159.
- (399). Sonzogni-Desautels K; Ndao M Will Auranofin Become a Golden New Treatment against Covid-19? *Front. Immunol.* 2021, 12, 683694. [PubMed: 34630379]
- (400). O’Donovan SM; Imami A; Eby H; Henkel ND; Creeden JF; Asah S; Zhang X; Wu X; Alnafisah R; Taylor RT; Reigle J; Thorman A; Shamsaei B; Meller J; McCullumsmith RE Identification of Candidate Repurposable Drugs to Combat Covid-19 Using a Signature-Based Approach. *Sci. Rep.* 2021, 11, 4495. [PubMed: 33627767]
- (401). Ena J; Pasquau F Once-a-Day Highly Active Antiretroviral Therapy: A Systematic Review. *Clin. Infect. Dis.* 2003, 36, 1186–1190. [PubMed: 12715315]
- (402). Tam LW; Chui CK; Brumme CJ; Bangsberg DR; Montaner JS; Hogg RS; Harrigan PR The Relationship between Resistance and Adherence in Drug-Naive Individuals Initiating Haart Is Specific to Individual Drug Classes. *J. Acquir. Immune Defic. Syndr.* 2008, 49, 266–271. [PubMed: 18845950]
- (403). Burda ST; Viswanath R; Zhao J; Kinge T; Anyangwe C; Tinyami ET; Haldar B; Powell RL; Jarido V; Hewlett IK; Nyambi PN Hiv-1 Reverse Transcriptase Drug-Resistance Mutations in Chronically Infected Individuals Receiving or Naive to Haart in Cameroon. *J. Med. Virol.* 2010, 82, 187–196. [PubMed: 20029816]
- (404). Chirullo B; Sgarbanti R; Limongi D; Shytaj IL; Alvarez D; Das B; Boe A; DaFonseca S; Chomont N; Liotta L; Petricoin EI; Norelli S; Pelosi E; Garaci E; Savarino A; Palamara AT A Candidate Anti-Hiv Reservoir Compound, Auranofin, Exerts a Selective ‘Anti-Memory’ Effect by Exploiting the Baseline Oxidative Status of Lymphocytes. *Cell Death Dis.* 2013, 4, No. e944.
- (405). Mphahlele M; Papathanasopoulos M; Cinellu MA; Coyanis M; Mosebi S; Traut T; Modise R; Coates J; Hewer R Modification of Hiv-1 Reverse Transcriptase and Integrase Activity by Gold(III) Complexes in Direct Biochemical Assays. *Bioorg. Med. Chem.* 2012, 20, 401–407. [PubMed: 22104436]



- (406). Milacic V; Dou QP The Tumor Proteasome as a Novel Target for Gold(III) Complexes: Implications for Breast Cancer Therapy. *Coord. Chem. Rev.* 2009, 253, 1649–1660. [PubMed: 20047011]
- (407). Kirschner S; Wei Y-K; Francis D; Bergman JG Anticancer and Potential Antiviral Activity of Complex Inorganic Compounds. *J. Med. Chem.* 1966, 9, 369–372. [PubMed: 5960909]
- (408). Aires RL; Santos IA; Fontes JV; Bergamini FRG; Jardim ACG; Abbehausen C Triphenylphosphine Gold(I) Derivatives Promote Antiviral Effects against the Chikungunya Virus. *Metallomics* 2022, 14. DOI: 10.1093/mtomcs/mfac056
- (409). Anthony EJ; Bolitho EM; Bridgewater HE; Carter OWL; Donnelly JM; Imberti C; Lant EC; Lermite F; Needham RJ; Palau M; Sadler PJ; Shi H; Wang F-X; Zhang W-Y; Zhang Z Metallodrugs Are Unique: Opportunities and Challenges of Discovery and Development. *Chem. Sci.* 2020, 11, 12888–12917. [PubMed: 34123239]
- (410). Traber KE; Okamoto H; Kurono C; Baba M; Saliou C; Soji T; Packer L; Okamoto T Anti-Rheumatic Compound Aurothioglucose Inhibits Tumor Necrosis Factor-Alpha-Induced Hiv-1 Replication in Latently Infected Om10.1 and Ach2 Cells. *Int. Immunol.* 1999, 11, 143–150. [PubMed: 10069412]
- (411). Evans GF; Zuckerman SH Pharmacologic Modulation of Tnf Production by Endotoxin Stimulated Macrophages: In Vitro and in Vivo Effects of Auranofin and Other Chrysotherapeutic Compounds. *Agents Actions* 1989, 26, 329–334. [PubMed: 2500010]
- (412). Youn HS; Lee JY; Saitoh SI; Miyake K; Hwang DH Auranofin, as an Anti-Rheumatic Gold Compound, Suppresses Lps-Induced Homodimerization of Tlr4. *Biochem. Biophys. Res. Commun.* 2006, 350, 866–871. [PubMed: 17034761]
- (413). Jeon K-I; Jeong J-Y; Jue D-M Thiol-Reactive Metal Compounds Inhibit Nf-Kb Activation by Blocking Ixb Kinase. *J. Immunol.* 2000, 164, 5981–5989. [PubMed: 10820281]
- (414). Trávní ek Z; Starha P; Van o J; Silha T; Hošek J; Suchý P Jr.; Pražanová G Anti-Inflammatory Active Gold(I) Complexes Involving 6-Substituted-Purine Derivatives. *J. Med. Chem.* 2012, 55, 4568–4579. [PubMed: 22541000]
- (415). Van o J; Gálíková J; Hošek J; Dvo ák Z; Paráková L; Trávní ek Z Gold (I) Complexes of 9-Deazahypoxanthine as Selective Antitumor and Anti-Inflammatory Agents. *PLoS One* 2014, 9, No. e109901.
- (416). Wempe L; Mohamed R; Warinner J; Goretsky T; Avdiushko M; Kim J; Abomhya A; Lee G; Awuah S; Barrett T; Kapur N Auphos, a “First-in Class” Oral Agent for Correcting Metabolic Dysfunction in Ibd. *Gastroenterology* 2022, 162, S2.
- (417). Mohamed R; Warinner J; Wempe L; Avdiushko M; Goretsky T; Kim J; Abomhya A; Lee G; Awuah S; Barrett T; Kapur N Auphos, a Novel Therapeutic That Improves Mitochondrial Function and Ameliorates Chronic Colitis. *Gastroenterology* 2022, 162, S2–S3.
- (418). Shashikanth N; Liu Y; Xing T; Turner J Novel Contributions of Claudin-4 to Epithelial Barrier Regulation and Colitis. *Inflamm. Bowel Dis.* 2022, 28, S51–S52.
- (419). Cheng Z; Li M; Dey R; Chen Y Nanomaterials for Cancer Therapy: Current Progress and Perspectives. *J. Hematol. Oncol.* 2021, 14, 1–27. [PubMed: 33402199]
- (420). Sanna V; Pala N; Sechi M Targeted Therapy Using Nanotechnology: Focus on Cancer. *Int. J. Nanomedicine* 2014, 9, 467. [PubMed: 24531078]
- (421). Silva CO; Pinho JO; Lopes JM; Almeida AJ; Gaspar MM; Reis C Current Trends in Cancer Nanotheranostics: Metallic, Polymeric, and Lipid-Based Systems. *Pharmaceutics* 2019, 11, 22. [PubMed: 30625999]
- (422). Patra JK; Das G; Fraceto LF; Campos EVR; Rodriguez-Torres M. d. P.; Acosta-Torres LS; Diaz-Torres LA; Grillo R; Swamy MK; Sharma S; et al. Nano Based Drug Delivery Systems: Recent Developments and Future Prospects. *J. Nanobiotechnology* 2018, 16, 1–33. [PubMed: 29321058]
- (423). Farinha P; Pinho JO; Matias M; Gaspar MM Nanomedicines in the Treatment of Colon Cancer: A Focus on Metallodrugs. *Drug Delivery Transl. Res.* 2022, 12, 49–66.
- (424). Phillips MA; Gran ML; Peppas NA Targeted Nanodelivery of Drugs and Diagnostics. *Nano today* 2010, 5, 143–159. [PubMed: 20543895]



- (425). Maeda H; Wu J; Sawa T; Matsumura Y; Hori K Tumor Vascular Permeability and the Epr Effect in Macromolecular Therapeutics: A Review. *J. Controlled Release* 2000, 65, 271–284.
- (426). Banerjee A; Pathak S; Subramaniam VD; Dharanivasan G; Murugesan R; Verma RS Strategies for Targeted Drug Delivery in Treatment of Colon Cancer: Current Trends and Future Perspectives. *Drug Discovery* 2017, 22, 1224–1232.
- (427). Attia MF; Anton N; Wallyn J; Omran Z; Vandamme TF An Overview of Active and Passive Targeting Strategies to Improve the Nanocarriers Efficiency to Tumour Sites. *J. Pharm. Pharmacol.* 2019, 71, 1185–1198. [PubMed: 31049986]
- (428). Moreno-Alcántar G; Picchetti P; Casini A Gold Complexes in Anticancer Therapy: From New Design Principles to Particle-Based Delivery Systems. *Angew. Chem., Int. Ed.* 2023. DOI: 10.1002/anie.202218000
- (429). Dantas KCF; Rosário J. d. S.; Silva-Caldeira PP Polymeric Nanosystems Applied for Metal-Based Drugs and Photosensitizers Delivery: The State of the Art and Recent Advancements. *Pharmaceutics* 2022, 14, 1506. [PubMed: 35890401]
- (430). Callari M; Aldrich-Wright JR; de Souza PL; Stenzel MH Polymers with Platinum Drugs and Other Macromolecular Metal Complexes for Cancer Treatment. *Prog. Polym. Sci.* 2014, 39, 1614–1643.
- (431). Lin Y-X; Gao Y-J; Wang Y; Qiao Z-Y; Fan G; Qiao S-L; Zhang R-X; Wang L; Wang H Ph-Sensitive Polymeric Nanoparticles with Gold (I) Compound Payloads Synergistically Induce Cancer Cell Death through Modulation of Autophagy. *Mol. Pharmaceutics* 2015, 12, 2869–2878.
- (432). Ahmad S; Isab AA; Ali S; Al-Arfaj AR Perspectives in Bioinorganic Chemistry of Some Metal Based Therapeutic Agents. *Polyhedron* 2006, 25, 1633–1645.
- (433). Mirabelli CK; Johnson RK; Sung CM; Faucette L; Muirhead K; Crooke ST Evaluation of the in Vivo Antitumor Activity and in Vitro Cytotoxic Properties of Auranofin, a Coordinated Gold Compound, in Murine Tumor Models. *Cancer Res.* 1985, 45, 32–39. [PubMed: 3917372]
- (434). Pearson S; Lu H; Stenzel MH Glycopolymer Self-Assemblies with Gold (I) Complexed to the Core as a Delivery System for Auranofin. *Macromolecules* 2015, 48, 1065–1076.
- (435). Nardon C; Boscutti G; Dalla Via L; Ringhieri P; Di Noto V; Morelli G; Accardo A; Fregona D Cck8 Peptide-Labeled Pluronic® F127 Micelles as a Targeted Vehicle of Gold-Based Anticancer Chemotherapeutics. *MedChemComm* 2015, 6, 155–163.
- (436). Chung CY-S; Fung S-K; Tong K-C; Wan P-K; Lok C-N; Huang Y; Chen T; Che C-M A Multi-Functional Pegylated Gold(III) Compound: Potent Anti-Cancer Properties and Self-Assembly into Nanostructures for Drug Co-Delivery. *Chem. Sci.* 2017, 8, 1942–1953. [PubMed: 28451309]
- (437). Lee P; Lok C-N; Che C-M; Kao WJ A Multifunctional Hydrogel Delivers Gold Compound and Inhibits Human Lung Cancer Xenograft. *Pharm. Res.* 2019, 36, 1–10.
- (438). Lee P-Y; Lok C-N; Che C-M; Kao WJ Multifunctional Microparticles Incorporating Gold Compound Inhibit Human Lung Cancer Xenograft. *Pharm. Res.* 2020, 37, 1–10.
- (439). Ringhieri P; Iannitti R; Nardon C; Palumbo R; Fregona D; Morelli G; Accardo A Target Selective Micelles for Bombesin Receptors Incorporating Au(III)-Dithiocarbamate Complexes. *Int. J. Pharm.* 2014, 473, 194–202. [PubMed: 25014371]
- (440). MaHam A; Tang Z; Wu H; Wang J; Lin Y Protein-Based Nanomedicine Platforms for Drug Delivery. *Small* 2009, 5, 1706–1721. [PubMed: 19572330]
- (441). Ma-Ham A; Wu H; Wang J; Kang X; Zhang Y; Lin Y Apoferritin-Based Nanomedicine Platform for Drug Delivery: Equilibrium Binding Study of Daunomycin with DNA. *J. Mater. Chem.* 2011, 21, 8700–8708.
- (442). Tosi G; Belletti D; Pederzoli F; Ruozi B Apoferritin Nanocage as Drug Reservoir: Is It a Reliable Drug Delivery System? *Exp. Opin. Drug Delivery* 2016, 13, 1341–1343.
- (443). Ferraro G; Monti DM; Amoresano A; Pontillo N; Petruk G; Pane F; Cinellu MA; Merlino A Gold-Based Drug Encapsulation within a Ferritin Nanocage: X-Ray Structure and Biological Evaluation as a Potential Anticancer Agent of the Auoxo3-Loaded Protein. *Chem. Commun.* 2016, 52, 9518–9521.
- (444). Messori L; Scaletti F; Massai L; Cinellu MA; Russo Krauss I; Di Martino G; Vergara A; Paduano L; Merlino A Interactions of Gold-Based Drugs with Proteins: Crystal Structure of

- the Adduct Formed between Ribonuclease a and a Cytotoxic Gold(III) Compound. *Metallomics* 2014, 6, 233–236. [PubMed: 24287583]
- (445). Russo Krauss I; Messori L; Cinellu MA; Marasco D; Sirignano R; Merlino A Interactions of Gold-Based Drugs with Proteins: The Structure and Stability of the Adduct Formed in the Reaction between Lysozyme and the Cytotoxic Gold(III) Compound Auoxo3. *Dalton Trans.* 2014, 43, 17483–17488. [PubMed: 25340580]
- (446). Zhang J; Zhang Z; Jiang M; Li S; Yuan H; Sun H; Yang F; Liang H Developing a Novel Gold(III) Agent to Treat Glioma Based on the Unique Properties of Apoferritin Nanoparticles: Inducing Lethal Autophagy and Apoptosis. *J. Med. Chem.* 2020, 63, 13695–13708. [PubMed: 33185442]
- (447). Bouchoucha M; Cote M-F; Gaudreault R; Fortin M-A; Kleitz F Size-Controlled Functionalized Mesoporous Silica Nanoparticles for Tunable Drug Release and Enhanced Anti-Tumoral Activity. *Chem. Mater.* 2016, 28, 4243–4258.
- (448). Farjadian F; Roointan A; Mohammadi-Samani S; Hosseini M Mesoporous Silica Nanoparticles: Synthesis, Pharmaceutical Applications, Biodistribution, and Biosafety Assessment. *Chem. Eng. J.* 2019, 359, 684–705.
- (449). Gao Y; Gao D; Shen J; Wang Q A Review of Mesoporous Silica Nanoparticle Delivery Systems in Chemo-Based Combination Cancer Therapies. *Front. Chem.* 2020, 8, 598722. [PubMed: 33330389]
- (450). Croissant JG; Fatieiev Y; Almalik A; Khashab NM Mesoporous Silica and Organosilica Nanoparticles: Physical Chemistry, Biosafety, Delivery Strategies, and Biomedical Applications. *Adv. Healthc. Mater* 2018, 7, 1700831.
- (451). Li T; Shi S; Goel S; Shen X; Xie X; Chen Z; Zhang H; Li S; Qin X; Yang H; et al. Recent Advancements in Mesoporous Silica Nanoparticles Towards Therapeutic Applications for Cancer. *Acta Biomater.* 2019, 89, 1–13. [PubMed: 30797106]
- (452). He L; Chen T; You Y; Hu H; Zheng W; Kwong WL; Zou T; Che CM A Cancer-Targeted Nanosystem for Delivery of Gold(III) Complexes: Enhanced Selectivity and Apoptosis-Inducing Efficacy of a Gold(III) Porphyrin Complex. *Angew. Chem., Int. Ed.* 2014, 126, 12740–12744.
- (453). Zhang S Fabrication of Novel Biomaterials through Molecular Self-Assembly. *Nat. Biotechnol.* 2003, 21, 1171–1178. [PubMed: 14520402]
- (454). Cui H; Webber MJ; Stupp SI Self-Assembly of Peptide Amphiphiles: From Molecules to Nanostructures to Biomaterials. *J. Pept. Sci.* 2010, 94, 1–18.
- (455). Lopez-Silva TL; Schneider JP From Structure to Application: Progress and Opportunities in Peptide Materials Development. *Curr. Opin. Chem. Biol.* 2021, 64, 131–144. [PubMed: 34329941]
- (456). Cancemi P; Buttacavoli M; Roz E; Feo S Expression of Alpha-Enolase (Eno1), Myc Promoter-Binding Protein-1 (Mbp-1) and Matrix Metalloproteinases (Mmp-2 and Mmp-9) Reflect the Nature and Aggressiveness of Breast Tumors. *Int. J. Mol. Sci.* 2019, 20, 3952. [PubMed: 31416219]
- (457). Sumi T; Nakatani T; Yoshida H; Hyun Y; Yasui T; Matsumoto Y; Nakagawa E; Sugimura K; Kawashima H; Ishiko O Expression of Matrix Metalloproteinases 7 and 2 in Human Renal Cell Carcinoma. *Oncol. Rep.* 2003, 10, 567–570. [PubMed: 12684625]
- (458). Marciano Y; Del Solar V; Nayeem N; Dave D; Son J; Contel M; Ulijn RV Encapsulation of Gold-Based Anticancer Agents in Protease-Degradable Peptide Nanofilaments Enhances Their Potency. *J. Am. Chem. Soc.* 2022.1451234
- (459). Wang Z; Medforth CJ; Shelnut JA Self-Metallization of Photocatalytic Porphyrin Nanotubes. *J. Am. Chem. Soc.* 2004, 126, 16720–16721. [PubMed: 15612699]
- (460). Zhong Y; Wang J; Zhang R; Wei W; Wang H; Lü X; Bai F; Wu H; Haddad R; Fan H Morphology-Controlled Self-Assembly and Synthesis of Photocatalytic Nanocrystals. *Nano Lett.* 2014, 14, 7175–7179. [PubMed: 25365754]
- (461). Wang J; Wang Z; Zhong Y; Zou Y; Wang C; Wu H; Lee A; Yang W; Wang X; Liu Y; et al. Central Metal-Derived Co-Assembly of Biomimetic GdtpP/Zntpp Porphyrin Nanocomposites for Enhanced Dual-Modal Imaging-Guided Photodynamic Therapy. *Biomaterials* 2020, 229, 119576. [PubMed: 31704467]

- (462). Wang X; Wang J; Wang J; Zhong Y; Han L; Yan J; Duan P; Shi B; Bai F Noncovalent Self-Assembled Smart Gold(III) Porphyrin Nanodrug for Synergistic Chemo-Photothermal Therapy. *Nano Lett.* 2021, 21, 3418–3425. [PubMed: 33827216]
- (463). Gukathasan S; Awuah SG Synthetic Strategies for the Preparation of Gold-Based Anticancer Agents. *Encyclopedia of Inorganic and Bioinorganic Chemistry* 2022, 1–32.

Author Manuscript

Author Manuscript

Author Manuscript

Author Manuscript

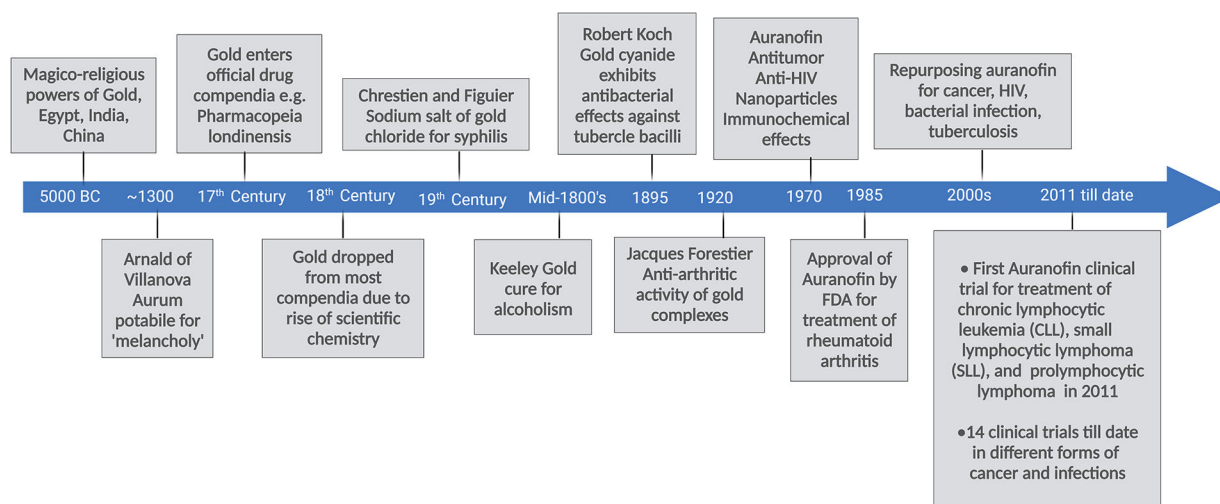


**Figure 1.**  
Timeline of gold in medicine highlighting key steps toward the development of gold in the clinical setting.

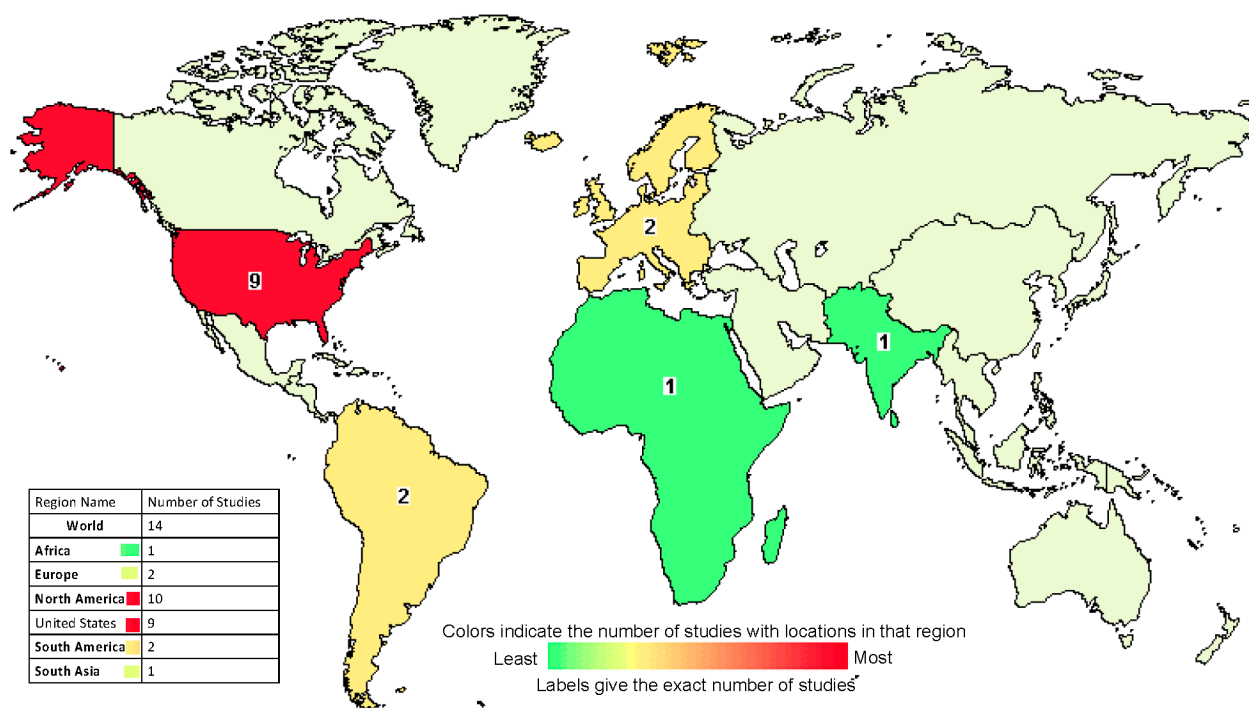


**Figure 2.**  
Global map of auranofin clinical trial sites.

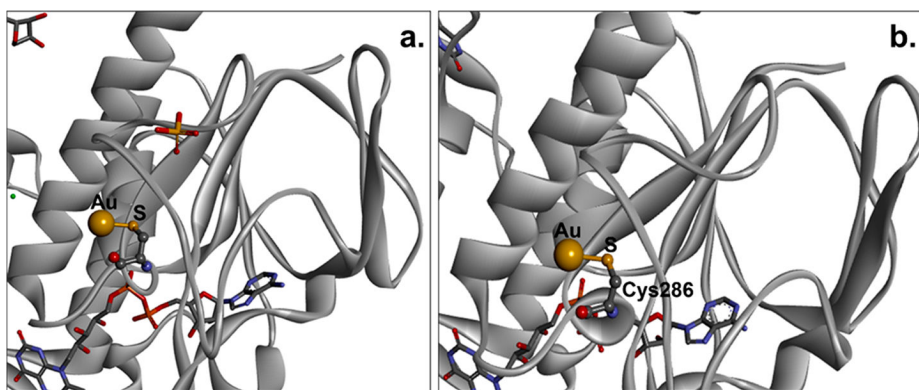


**Figure 3.** Crystal structure of Au(I)-protein adduct: (a) Au(I)-EhTrxR adduct (PDB code: 4A65, gold source: AuCN), (b) Au(I)-EhTrxR adduct (PDB code: 4CBQ, gold source: auranofin).<sup>80</sup>



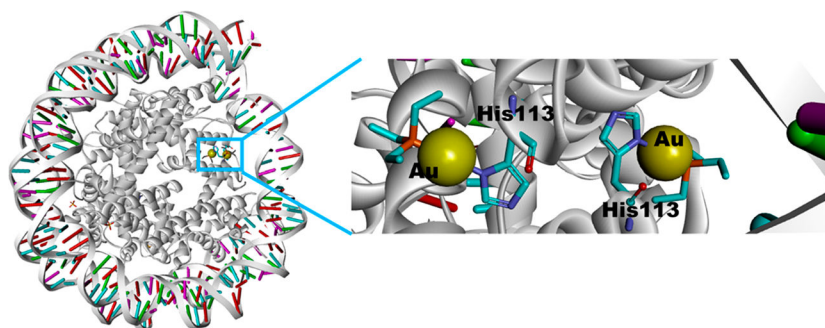


**Figure 4.** X-ray crystal structure of RAPTA-T/auranofin-nucleosome core particle (NCP). Structure reveals auranofin and RAPTA-T adduct sites. NCP is depicted on the left and zoomed adduct site displayed on the right. Gold atom (gold) bearing triethylphosphine (PET<sub>3</sub>) bound to His113 (PDB: 5DNN, gold source: auranofin).

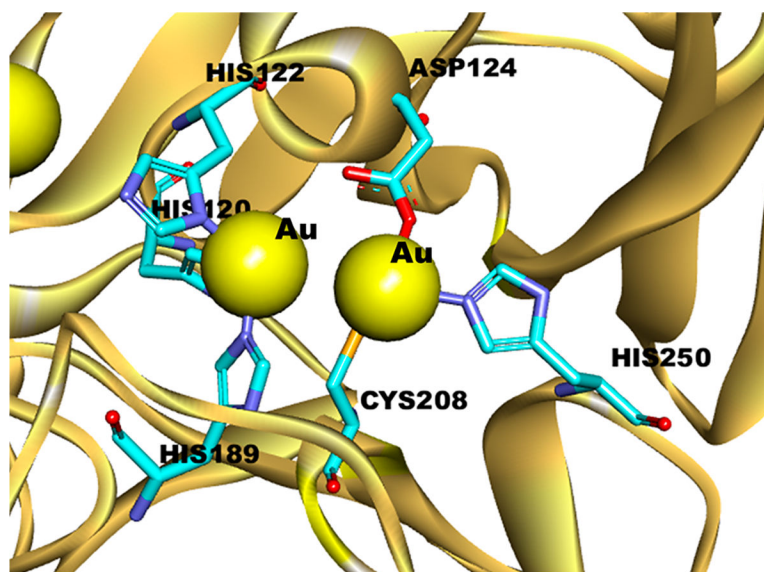


**Figure 5.** Crystal structure of the active site of Au-NDM-1 (PDB ID: 6LHE, gold source: auranofin) displaying Au ions as yellow spheres and omitting water molecules that contribute to a tetrahedral geometry. Annotated amino acid side chains within the protein active site are depicted in cyan with distinctly colored heteroatoms (N, blue; O, red; S, yellow).

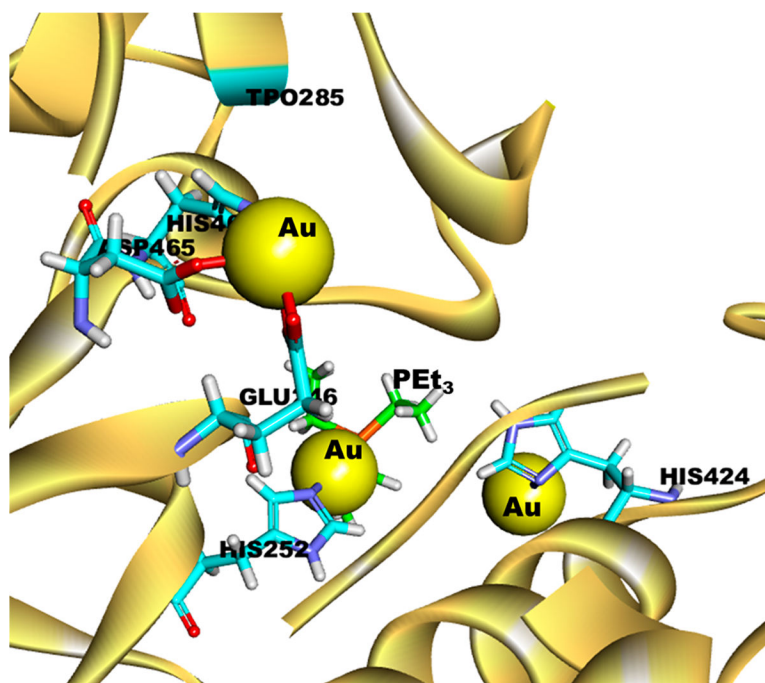


**Figure 6.** Crystal structure of the active site of Au-MCR-1 (PDB ID: 6LI6, gold source:  $\text{PEt}_3\text{AuCl}$ ) displaying Au ions as yellow spheres. Annotated amino acid side chains within the protein active site is depicted in cyan with distinctly colored heteroatoms (N, blue; O, red; S, yellow). Triethylphosphine ligand is shown as green (C atoms) and orange (P atom).

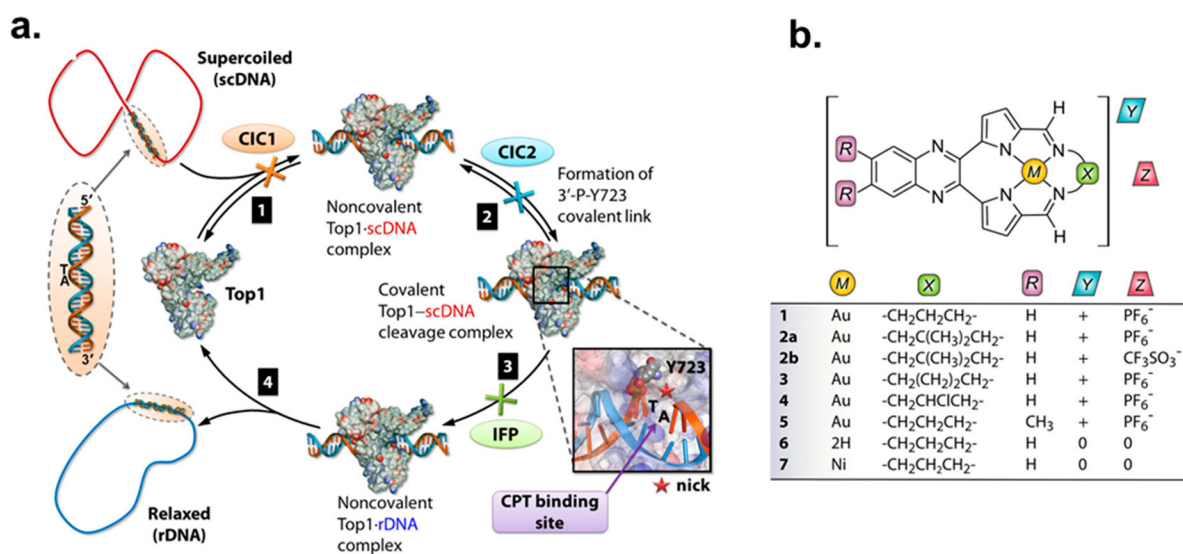


**Figure 7.**  
 (A) Schematic representation showing the important events in the catalytic cycle of the human Topoisomerase IB (TOP1) enzyme. Detailed step by step description of the catalytic process is given in ref 151. (B) General chemical structure and derivatives of Au(III) macrocycles. Reproduced from ref 151. Copyright 2014 American Chemical Society.

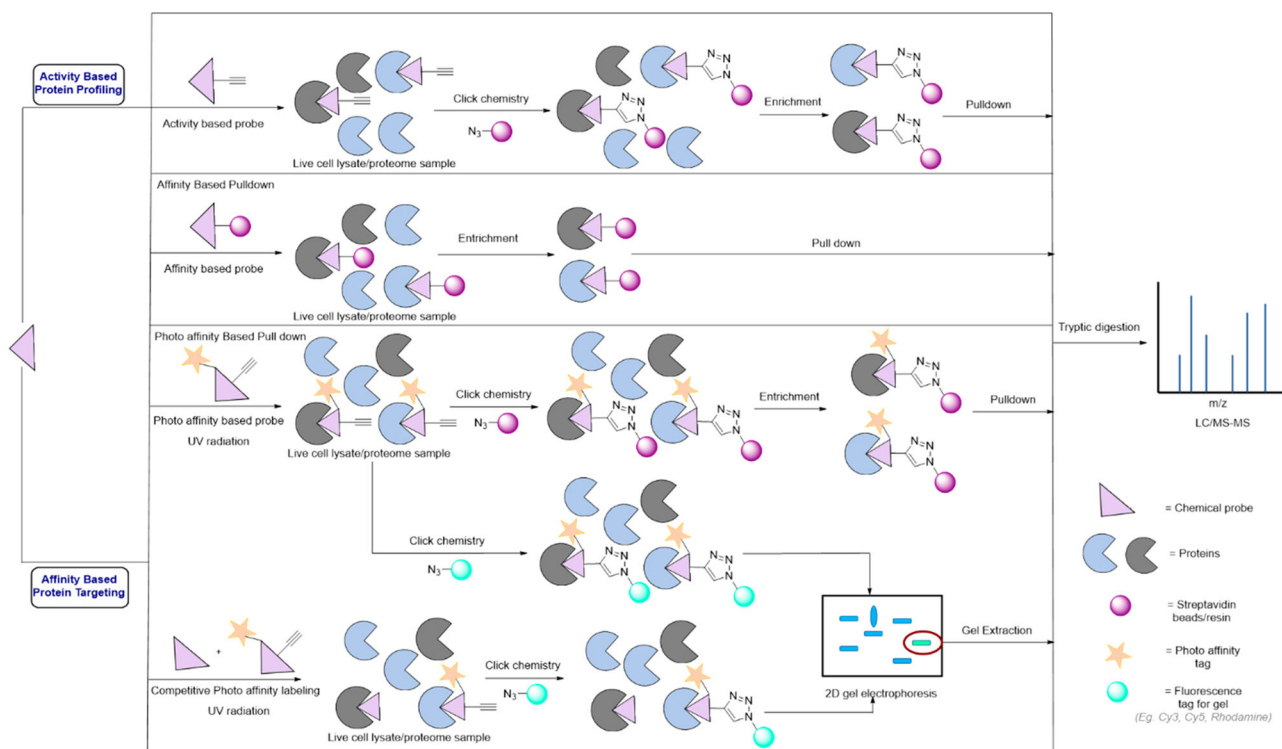


**Figure 8.** General schemes for affinity-based target identification and activity-based protein profiling.

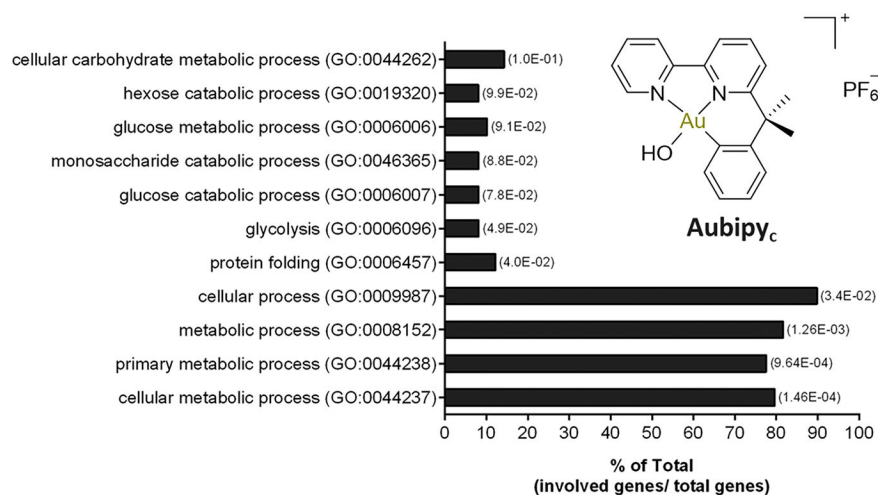


**Figure 9.** Classical proteomics strategy to study drug action by gel electrophoresis, mass spectrometry, bioinformatics, and validation of the organometallic Au(III), Aubipy<sub>c</sub>. Reproduced from ref 162. Copyright 2015 Royal Society of Chemistry.



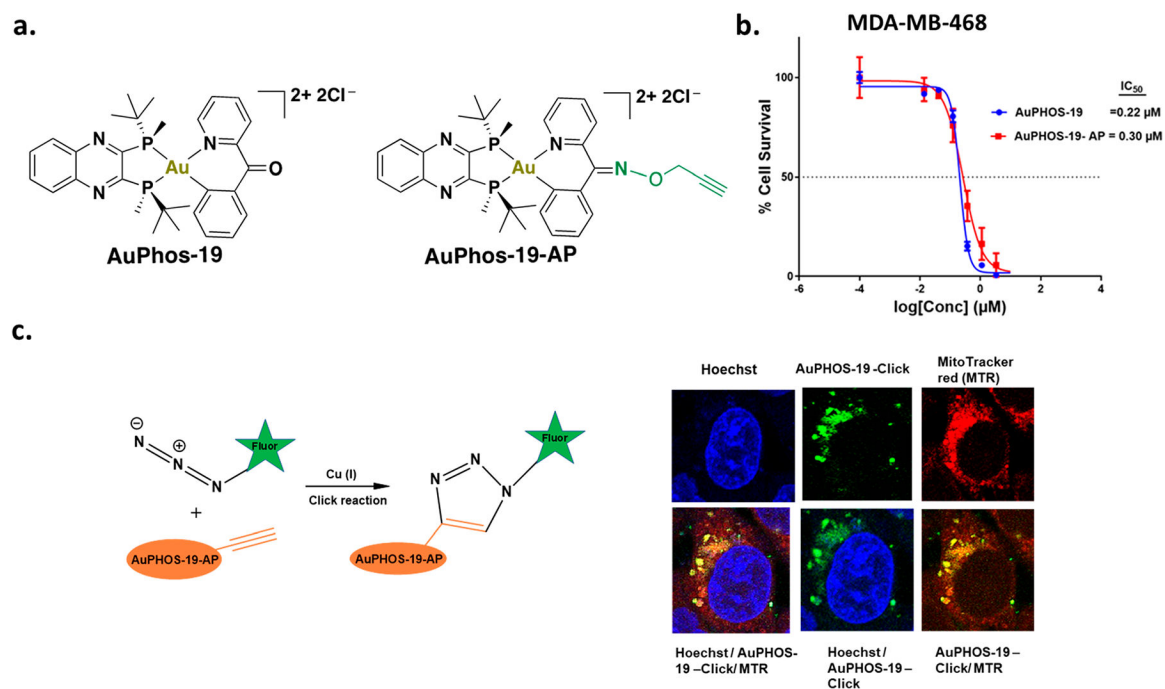


**Figure 10.**

(a) *P*-chirogenic Au(III) molecule (AuPhos-19) and the alkyne functionalized probe (AuPhos-19-AP). (b) Assessment of cell viability in MDA-468 cells treated with parent molecule (AuPhos-19) versus AuPhos-19-AP. (c) Representation and result of biorthogonal Cu(I)-catalyzed azide–alkyne cycloaddition (CuAAC) reaction using an azide-tagged FITC fluorophore. Reproduced with permission from ref 175. Copyright 2022 Elsevier.

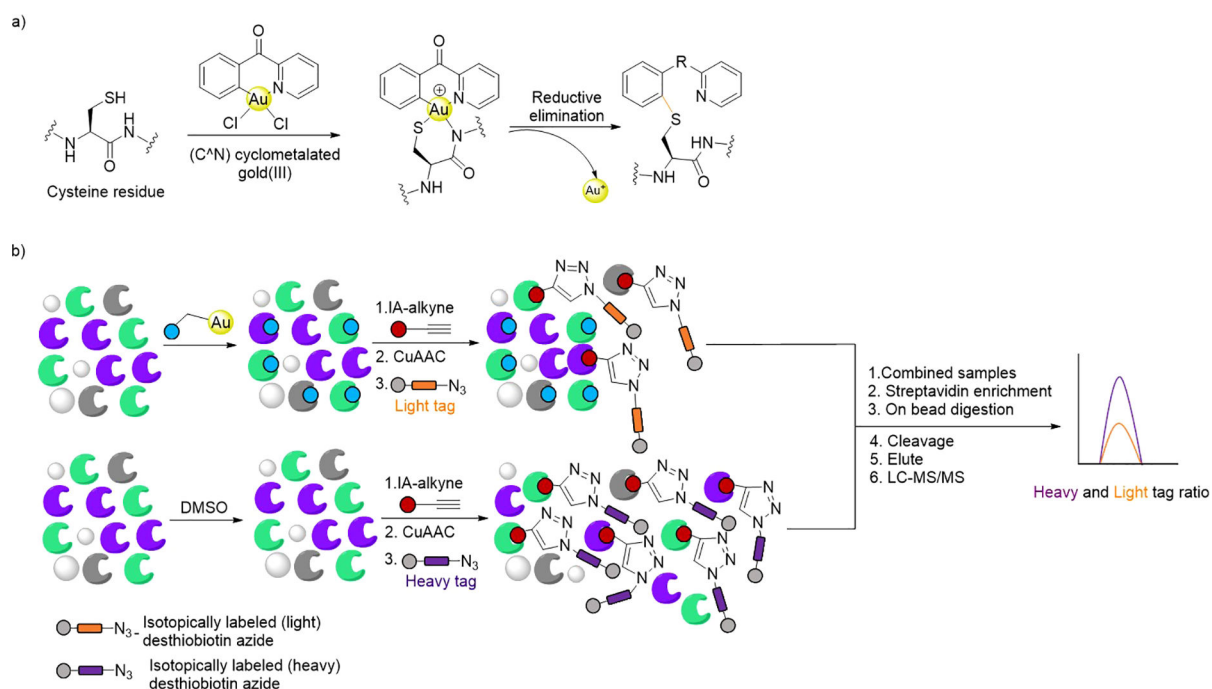


**Figure 11.**

(a) Mechanism of cystine arylation via Au(III) complex reductive elimination. (b) Workflow of isotopically labeled desthiobiotin activity based protein profiling (isoDTB-ABPP). Figure reproduced from ref 180. Copyright 2022 Royal Society of Chemistry.

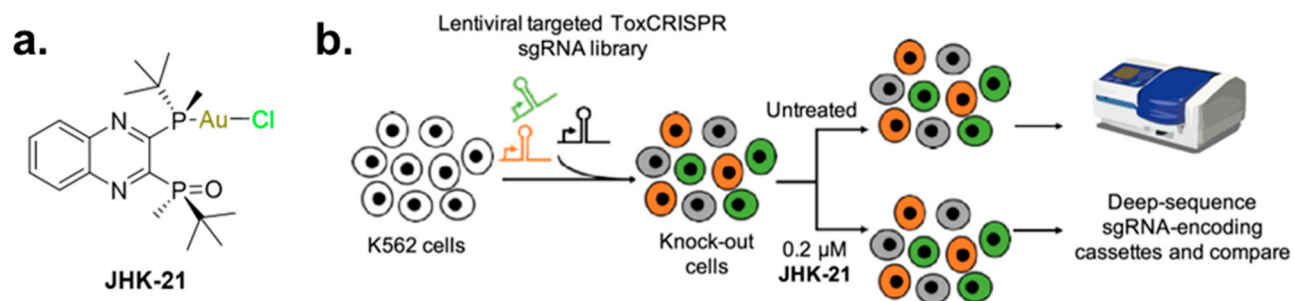


**Figure 12.**

(a) Structure of **JHK-21**. (b) Diagram illustrating the combined CRISPR-Cas9 screening method to identify **JHK-21** cellular target and mode of action. Reproduced from ref 190. Copyright 2022 American Chemical Society.

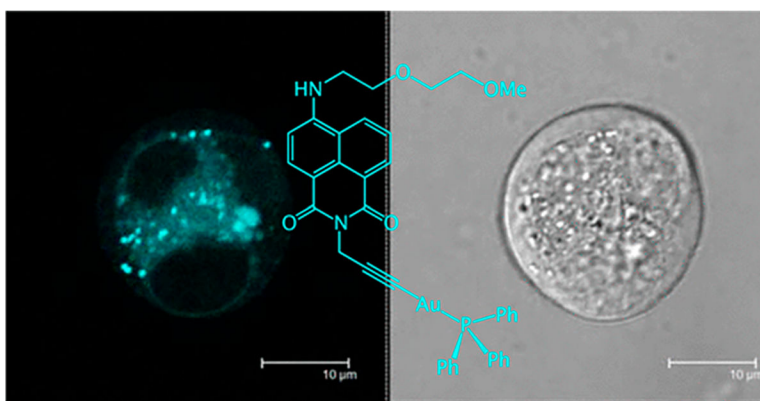
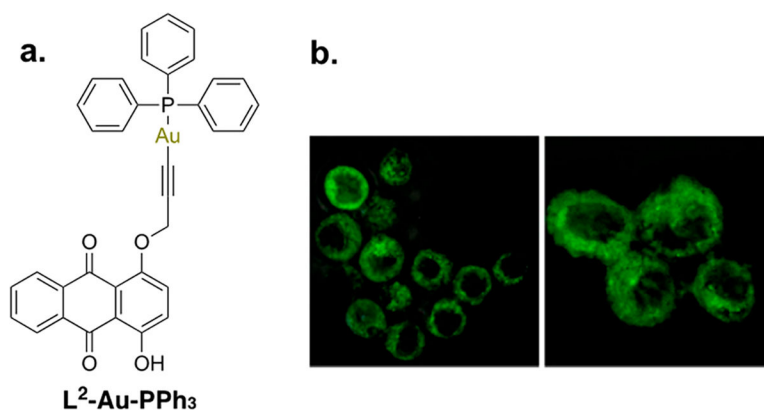
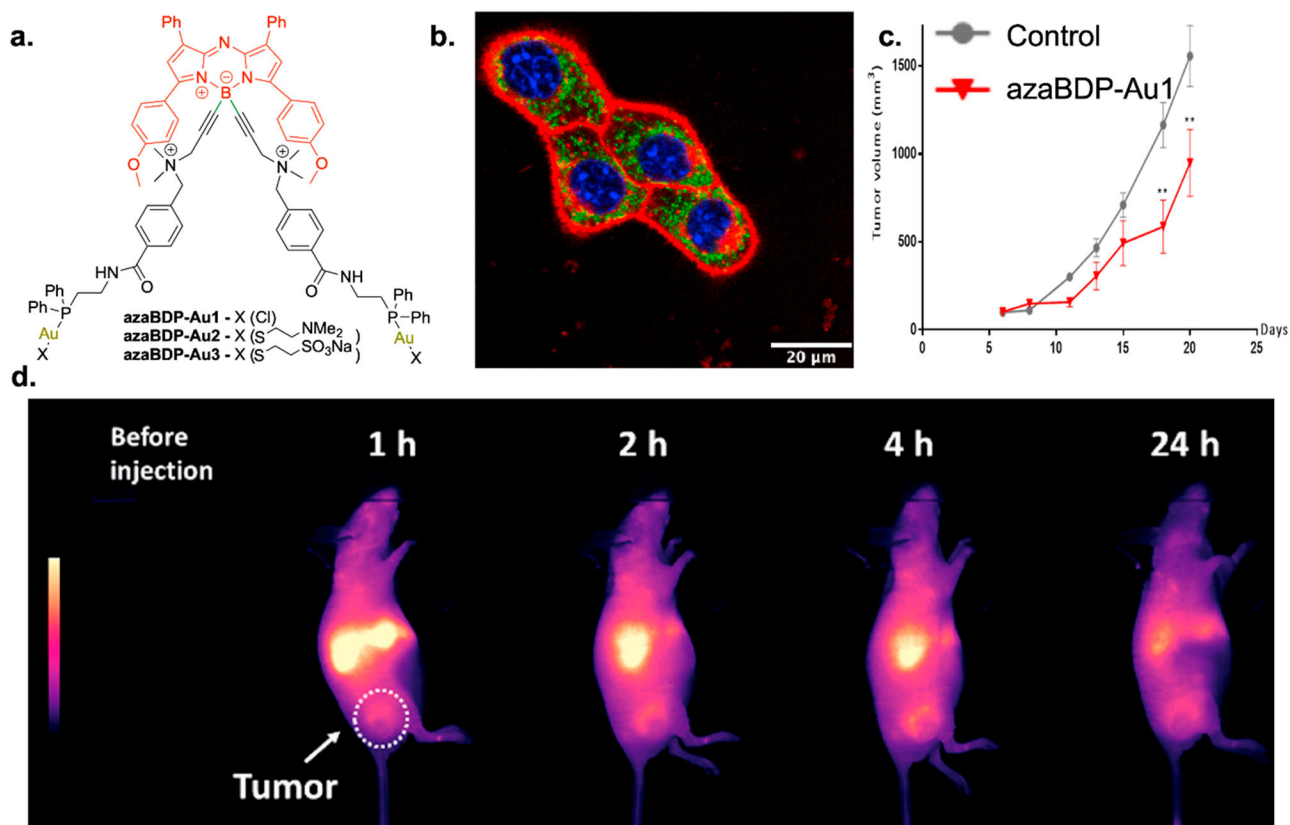


**Figure 13.** Au(I) fluorescent alkynyl-naphthalimide complexes for cell imaging. Reproduced from ref 209. Copyright 2015 American Chemical Society.



**L<sup>2</sup>-Au-PPh<sub>3</sub>**

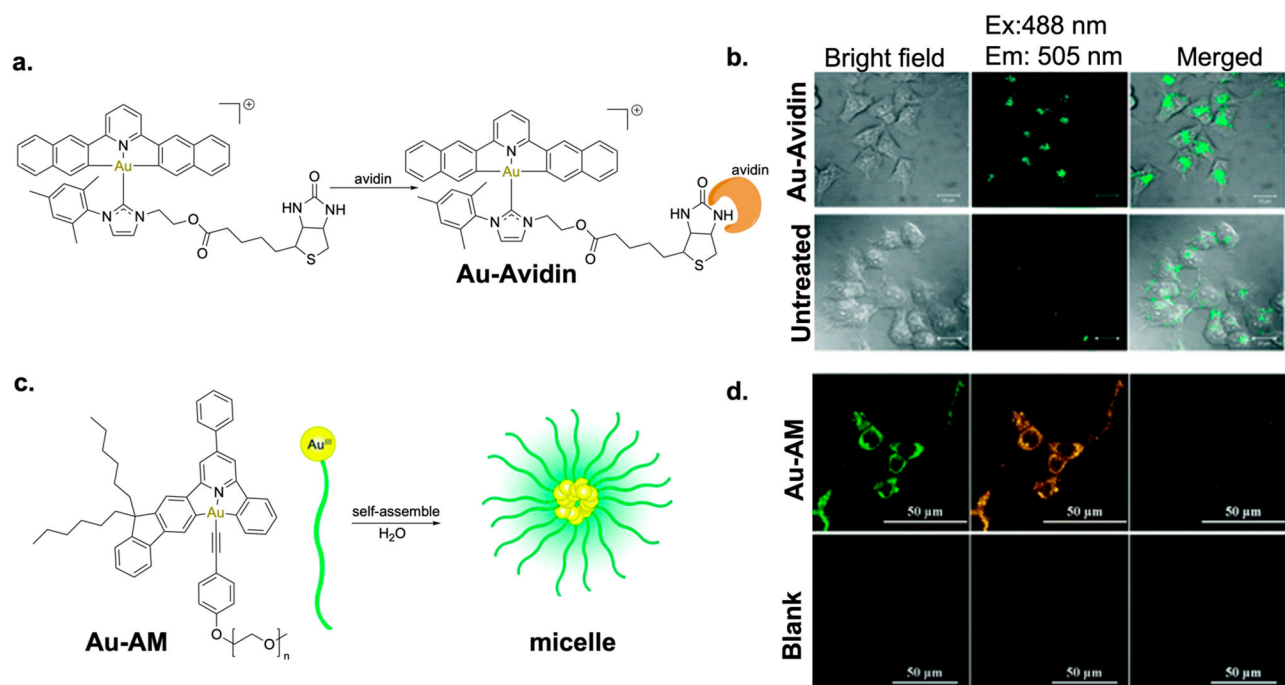
**Figure 14.** Images of MCF-7 cells incubated with [L<sup>2</sup>-Au-PPh<sub>3</sub>] (100  $\mu\text{g}/\text{mL}$ , 4  $^{\circ}\text{C}$ , 30 min). Excited at 405 nm, acquired 530–580 nm. Reproduced from ref 221. Copyright 2012 American Chemical Society.



**Figure 15.**

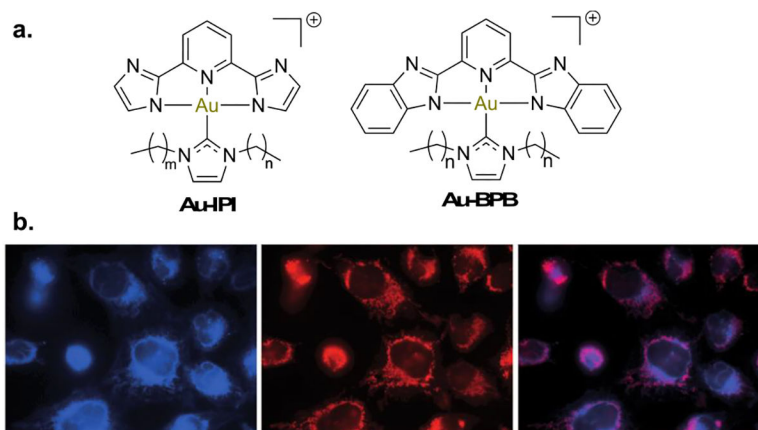
(a) Recently reported NIR aza-BODIPY dinuclear Au(I) complexes, (b) **azaBDP-Au-1** localization in 4T1 cells visualized by confocal microscopy. 4T1 cells were incubated with **azaBDP-Au-Cl** (red) for 45 min at 5 μM, nuclei counterstain with blue, fluorescent dye (Hoesct 33342, and mitochondria labeling was done with mito-tracker green, (c) azaBDP-Au1 distribution in tumor bearing mice. (d) An intravenous injection was administered, and images were collected at the indicated times. Accumulation of the compound in the tumor area was observed as shown with arrow. Reproduced with permission from ref 228. Copyright 2021 Elsevier.



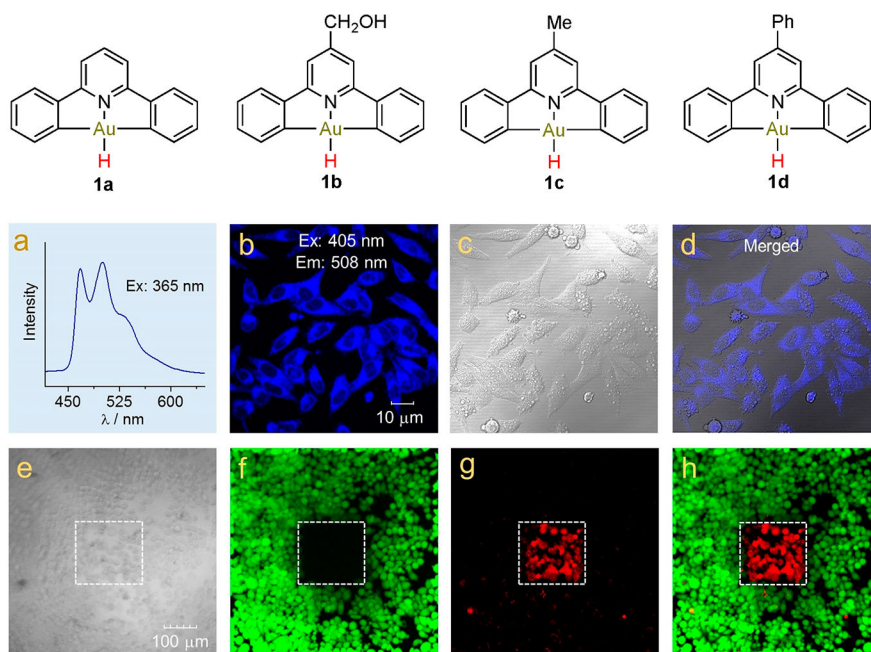


**Figure 16.**

(a) Synthetic scheme of **Au-Avidin**, (b) confocal imaging of HeLa cells treated with conjugate **Au-Avidin** for 4 h followed by a fluorescently tagged biotin. Reproduced from ref 242. Copyright 2015 Royal Society of Chemistry. (c) Synthesis of **Au-AM** self-assembled micelles. (D) Confocal microscopy images of A549 cells treated with **Au-AM** (33  $\mu\text{g}/\text{mL}$ ) (upper panel) for 4 h and without **Au-AM** (lower panel) under bright field or fluorescence field excitation at 405 nm. Reproduced from ref 243. Copyright 2016 Royal Society of Chemistry.

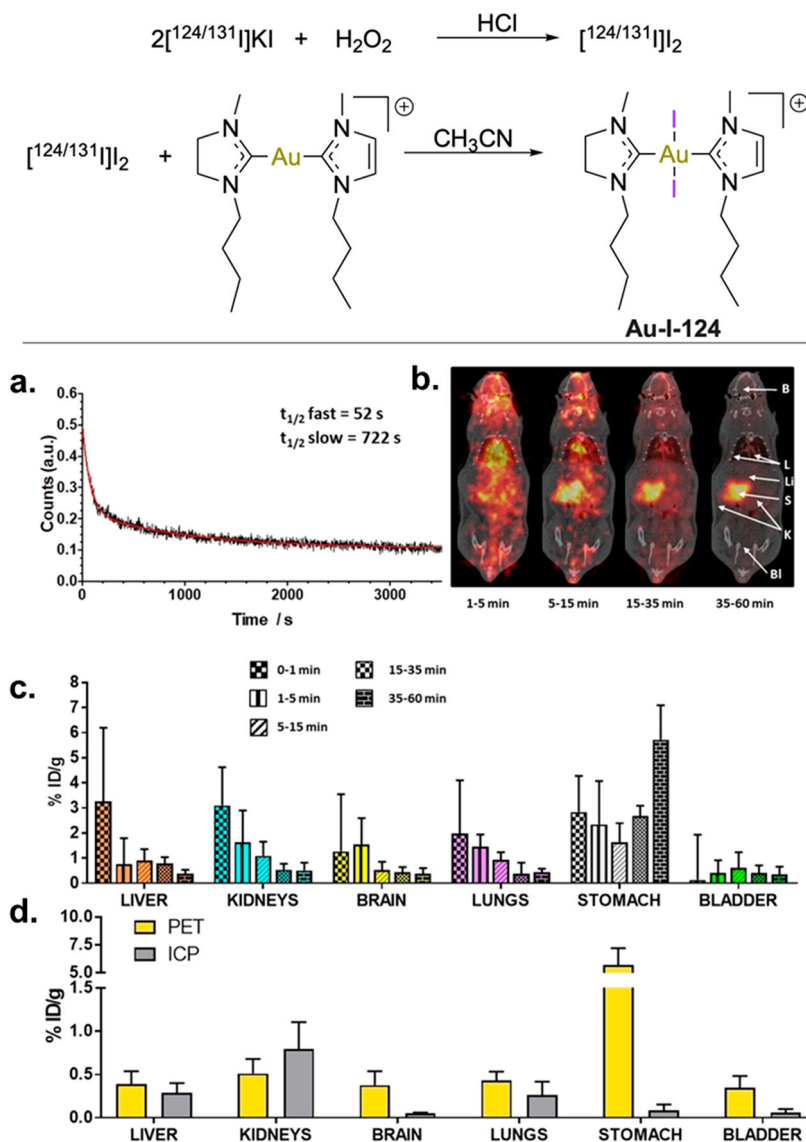


**Figure 17.** (a) Chemical structure of Au(III)-complexes **Au-IPI** and **Au-BPB**. (b) Fluorescence images of **Au-BPB** derivative (left, 365 nm excitation), mitochondria-specific Mito-tracker Red stain (middle, 546 nm excitation), and the merged image (right). Reproduced from ref 101. Copyright 2013 John Wiley and Sons.

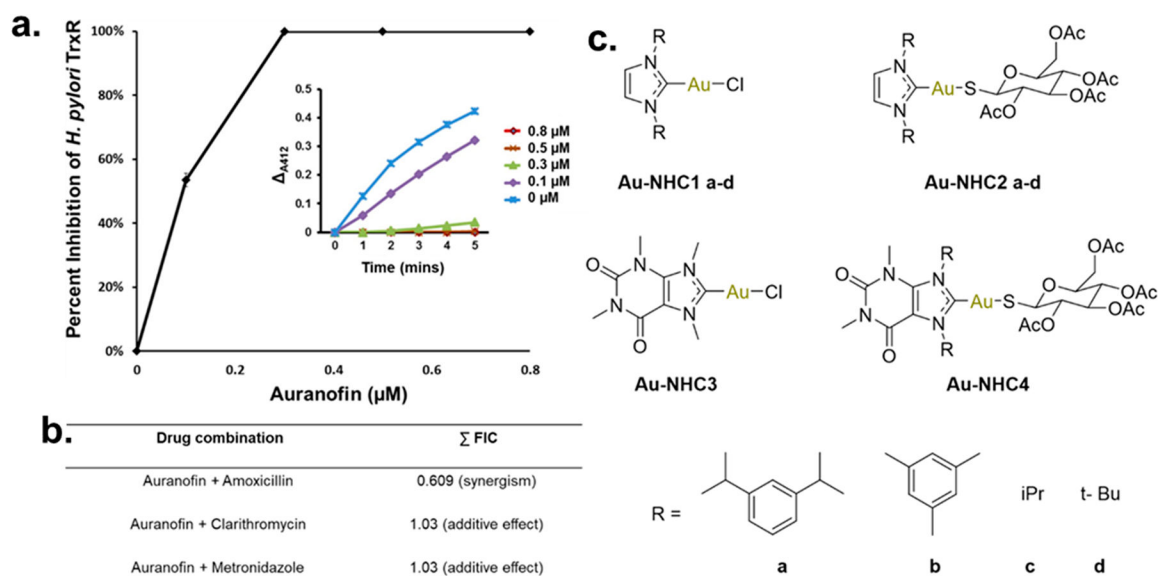


**Figure 18.**

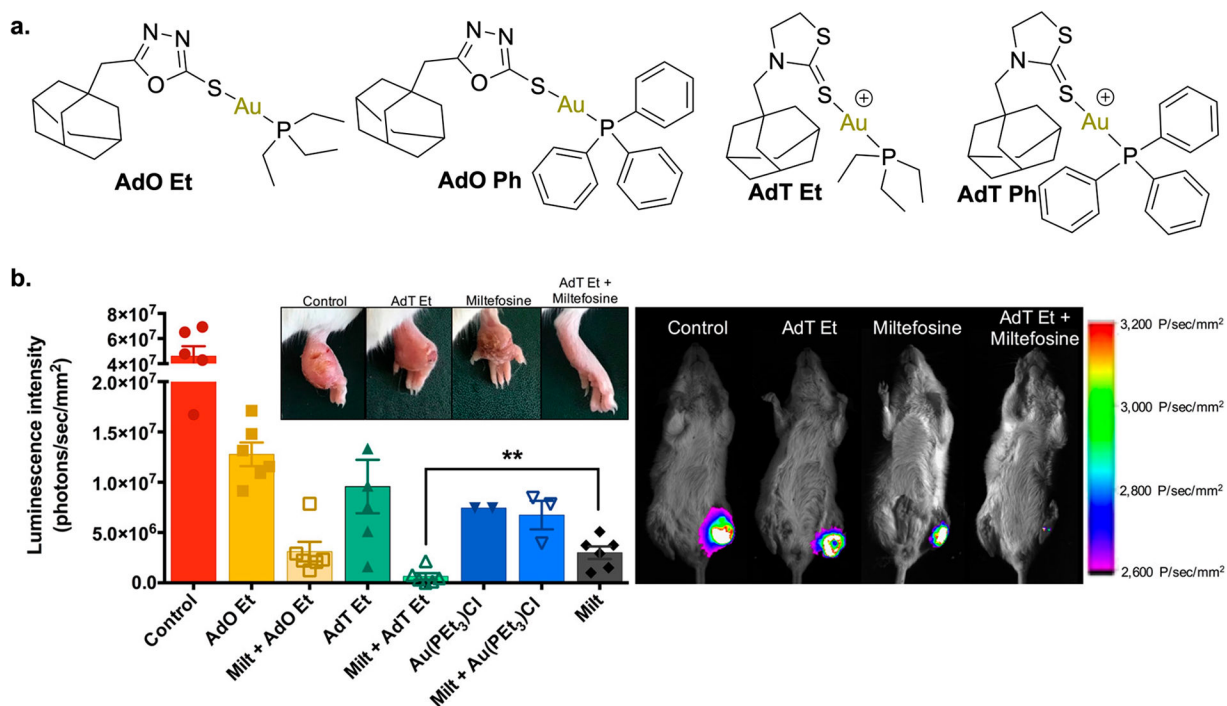
Top. Chemical structure of  $[(\hat{C}\hat{N}\hat{C})\text{AuH}]$  complexes **1a–d**, Bottom. (a) Emission spectrum of **1b** in dichloromethane. (b) Fluorescence microscopy image of HepG2 cells treated with 10  $\mu\text{M}$  of **1b** for 1 h. (c) Bright field showing characteristics of apoptotic morphology change after irradiation. (d) Merged image. (e–h) Fluorescent images of HepG2 cells treated with 10  $\mu\text{M}$  of **1b** for 1 h followed by 405 nm laser irradiation at selected region (dashed box) for 2 min (e) bright field; (f) green channel; (g) red channel; (h) merged fluorescent image. Reproduced with permission from ref 254. Copyright 2020 John Wiley and Sons.

**Figure 19.**

(a) Radioactivity curve of arterial blood determined by online blood sampling following the administration of **Au-I-124** intravenously. (b) PET images gotten at different intervals following administration of **Au-I-124** intravenously. (c) Representation of the radioactivity concentration in distinct organs at different time intervals assessed from the PET images following the administration of **Au-I-124**. (d) Representation of the radioactivity concentration (assessed from the PET images) and Au concentration (determined by ICP-MS) in distinct organs. Panels a–d are reproduced from ref 259. Copyright 2020 John Wiley and Sons.

**Figure 20.**

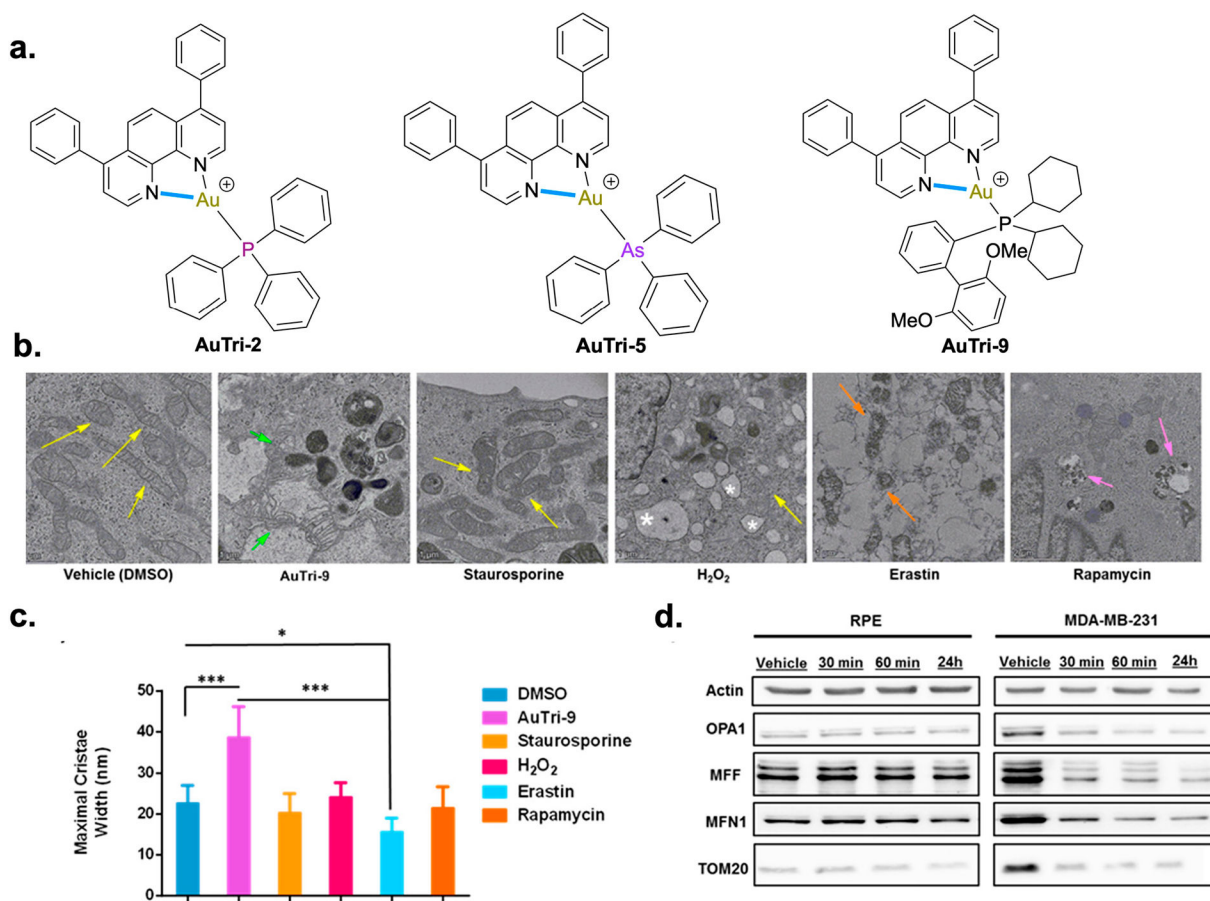
(a) Inhibitory effect of auranofin on the activity of *H. pylori* TrxR. Reproduced from ref 319. Copyright 2016 Oxford University Press. (b) Combination studies of Auranofin with known *H. pylori* antibiotics. (c) Structures of NHC-Auranofin studied against *H. pylori*.



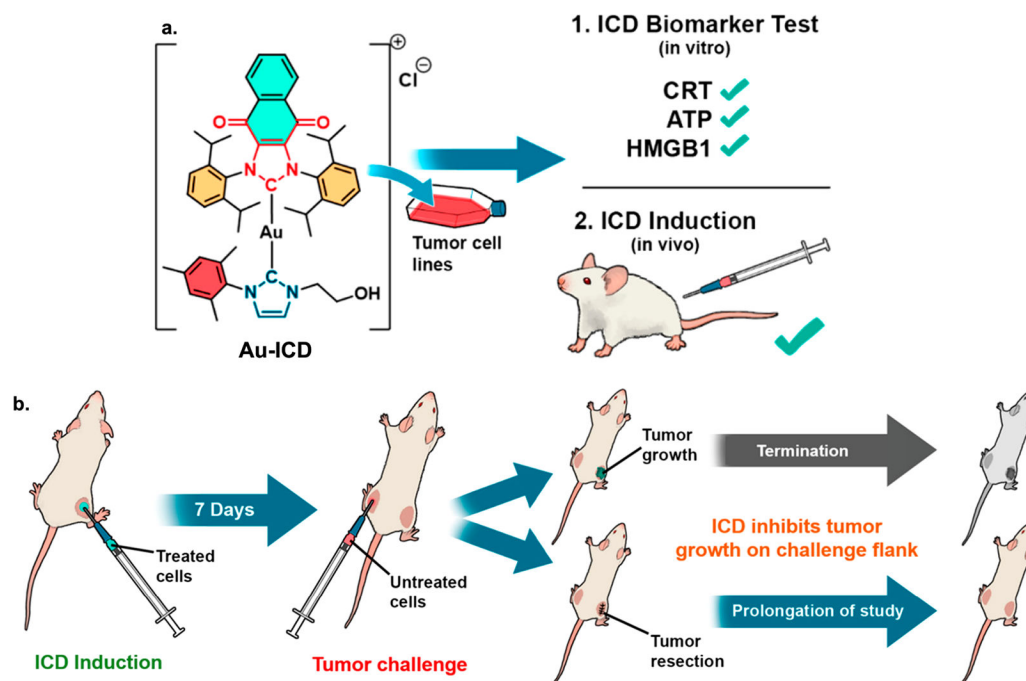
**Figure 21.**

(A) Chemical structures of adamantane Au(I)-oxazole/thiazolidinone derivatives. (B) *In vivo* efficacy of Au complexes in combination with Miltefosine. Reproduced from ref 339. Copyright 2020 American Chemical Society.

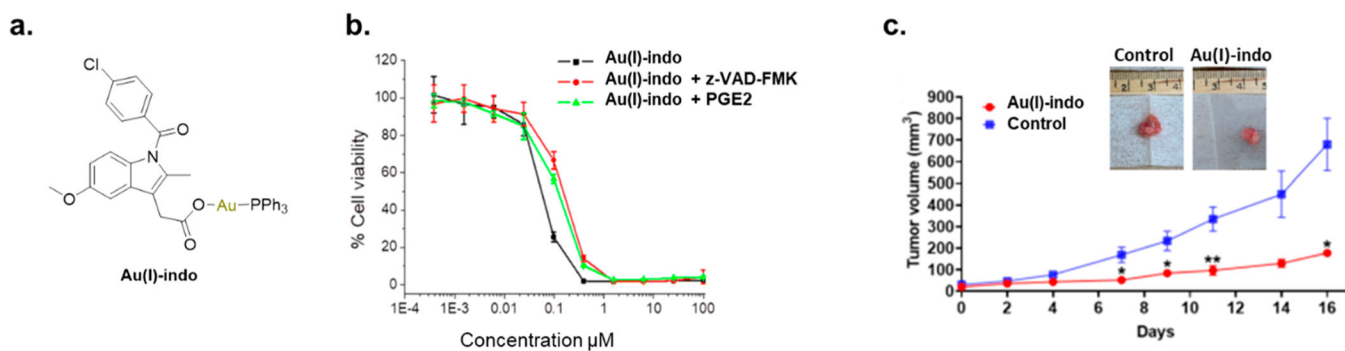


**Figure 22.**

(a) Chemical structures of three-coordinate Au(I), AuTri complexes. (b) Transmission electron microscopy of known cell death inducers, vehicle control, and **AuTri-9** in MDA-MB-231. (c) Maximal cristae width. Data are representative of 10 cells chosen at random  $n = 10$ , where mitochondria were also chosen at random. (d) Immunoblots of OPA1, MFF, MFN1, and TOM20. Reproduced from ref 355. Copyright 2021 American Chemical Society.

**Figure 23.**

(a) Au(I) complex **Au-ICD** induces immunogenic cell death (ICD) in a CT26 colon cancer cell. (b) Depiction of *in vivo* experiments carried out with **Au-ICD**. Reproduced from ref 387. Copyright 2020 American Chemical Society.

**Figure 24.**

(a) Chemical structure of gold(I) complex bearing indomethacin moiety, identified as **Au(I)-indo**. (b) Assessment of the cell viability of HMLER-shEcad cells treated with **Au(I)-indo** only and in combination with z-VAD-FMK and PGE2 at 5  $\mu\text{M}$  and 20  $\mu\text{M}$  respectively. (c) *In vivo* efficacy of **Au(I)-indo** in 4T1 tumor bearing mice. Reproduced with permission from ref 393. Copyright 2023 Royal Society of Chemistry.

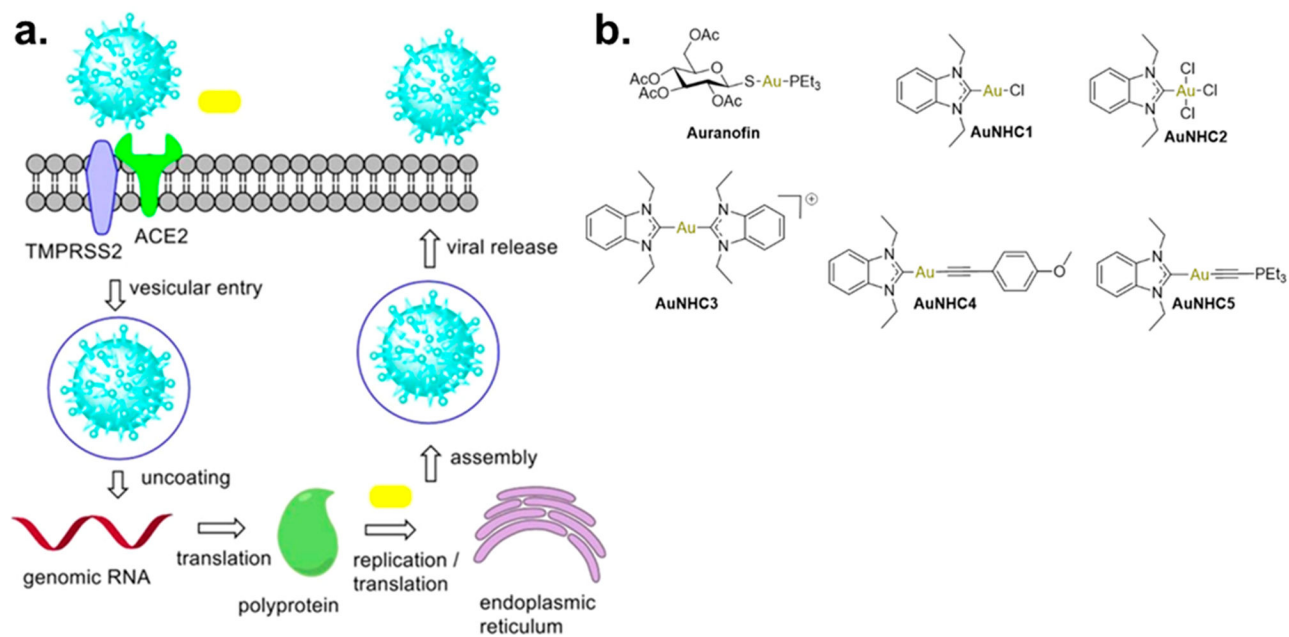


**Figure 25.**

(a) Simple illustration of the life cycle of the SARS-CoV-2, golden bars represent gold drugs that target viral entry process and replication. Reproduced from ref 159. Copyright 2020 John Wiley and Sons. (b) Gold(I) and gold(III) benzimidazole complexes used in evaluating antiviral properties against SARS-CoV-2.

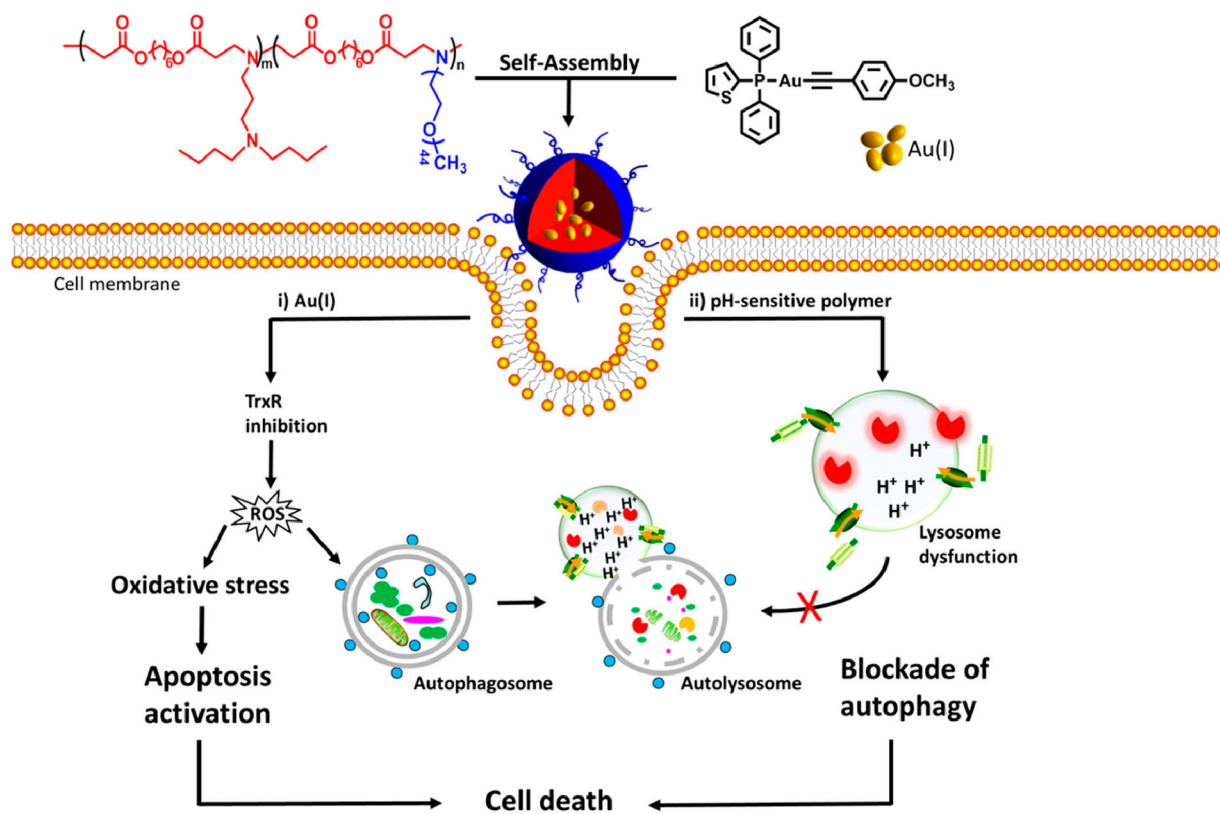


**Figure 26.** Diagram showing dissociation of pH sensitive gold(I)-loaded poly( $\beta$ -amino ester)s micelle-like nanoparticles in the lysosomes and mechanism of synergistic induction of cell death. Reproduced from ref 431. Copyright 2015 American Chemical Society.

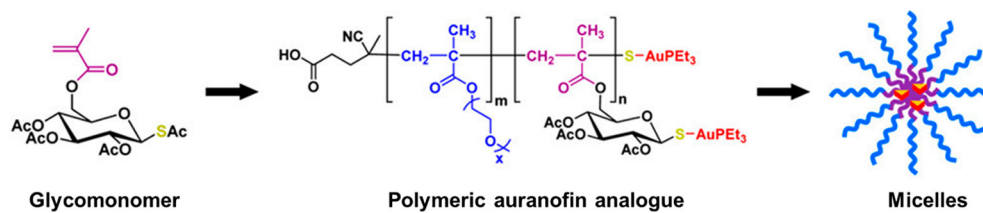


**Figure 27.**  
Formation of spherical micelles from polymeric auranofin. Reproduced from ref 434.  
Copyright 2015 American Chemical Society.



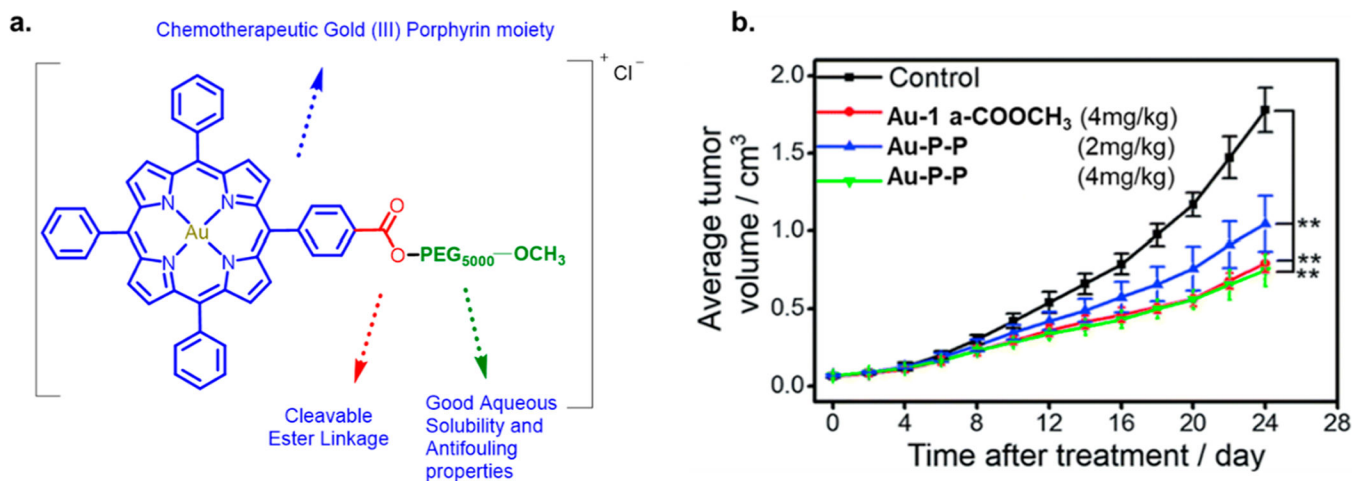


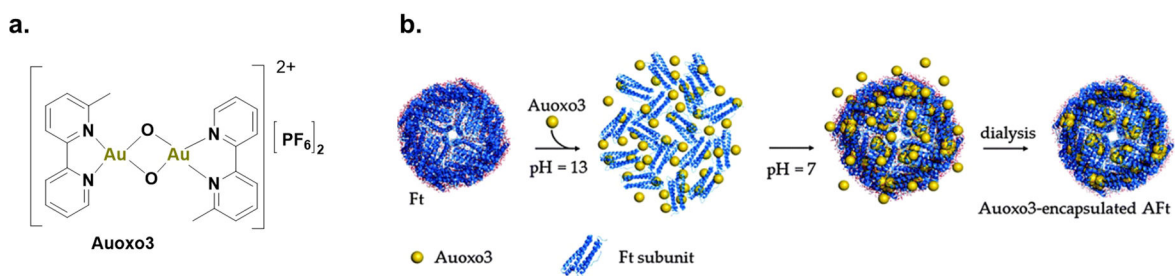
**Figure 28.**

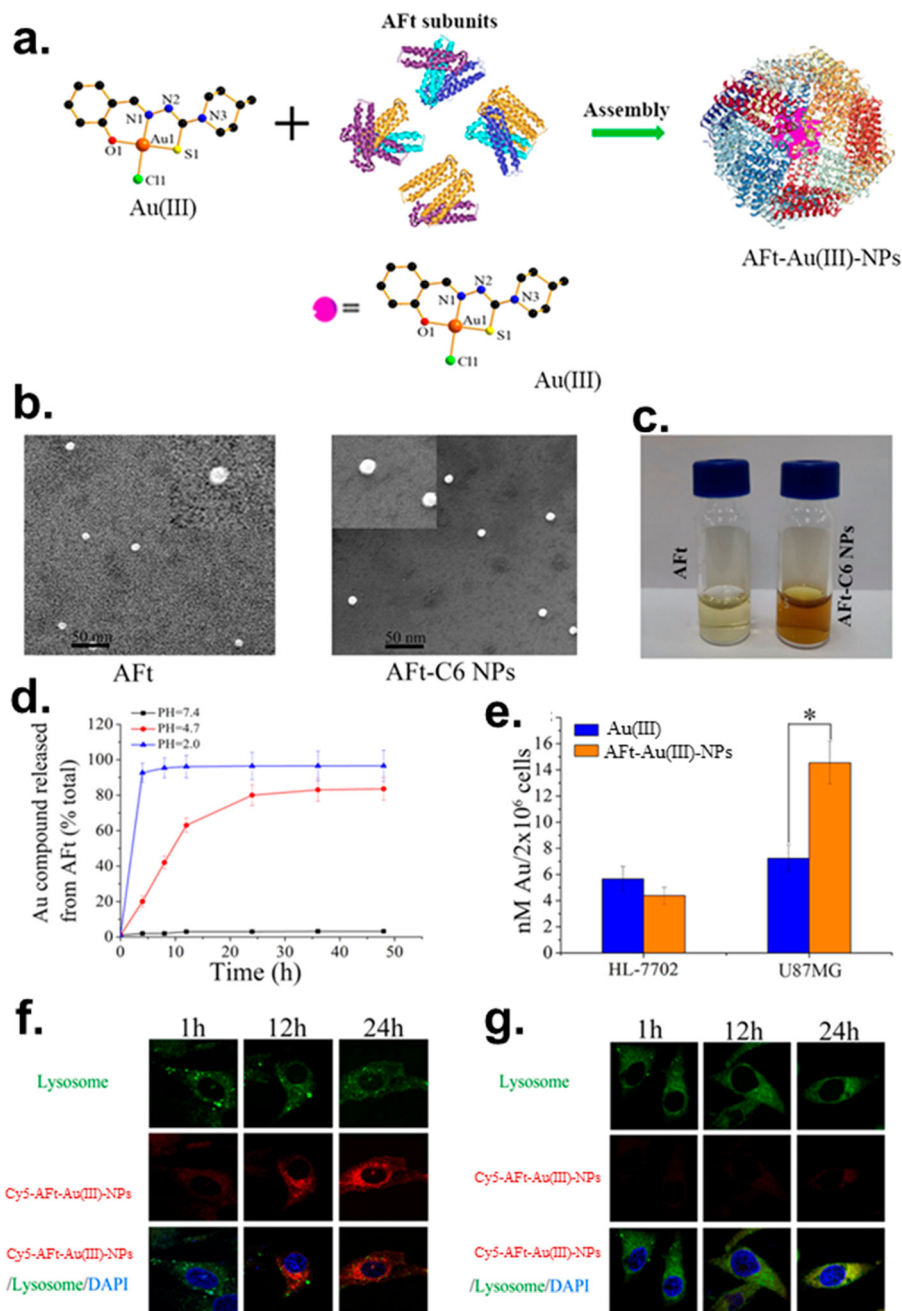
(A) Structure of Au(III) porphyrin-PEG conjugate  $[\text{Au}(\text{TPP}-\text{COO}-\text{PEG}_{5000}-\text{OCH}_3)]\text{Cl}$

(Au-P-P). (B) Changes in tumor volume in HCT116 xenografts tumor bearing mice

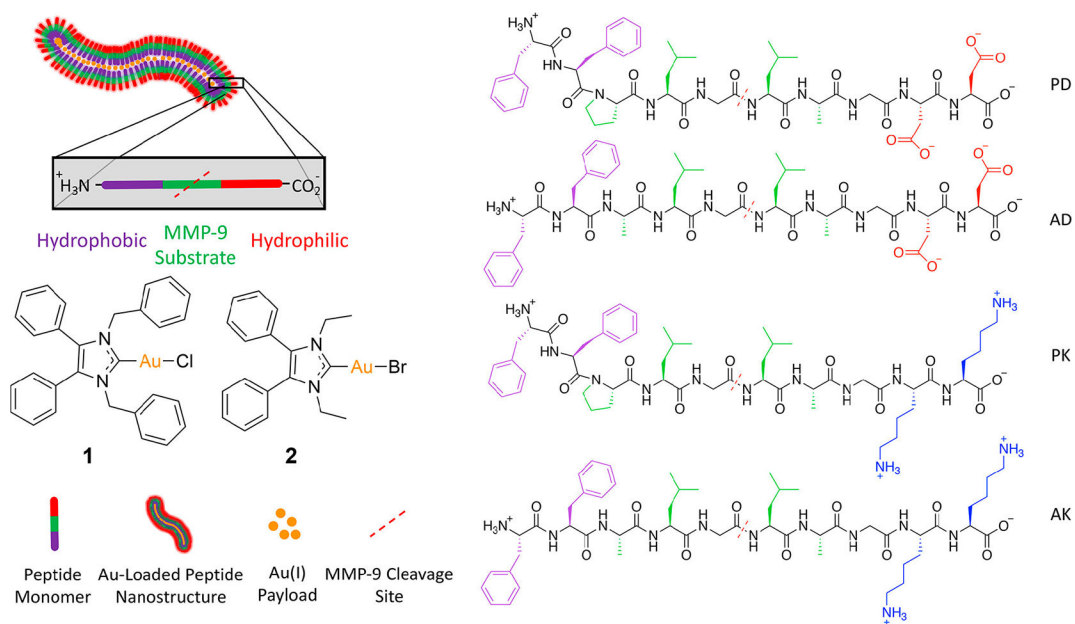
after treatment with the indicated complexes. Reproduced with permission from ref 436.

Copyright 2017 Royal Society of Chemistry.

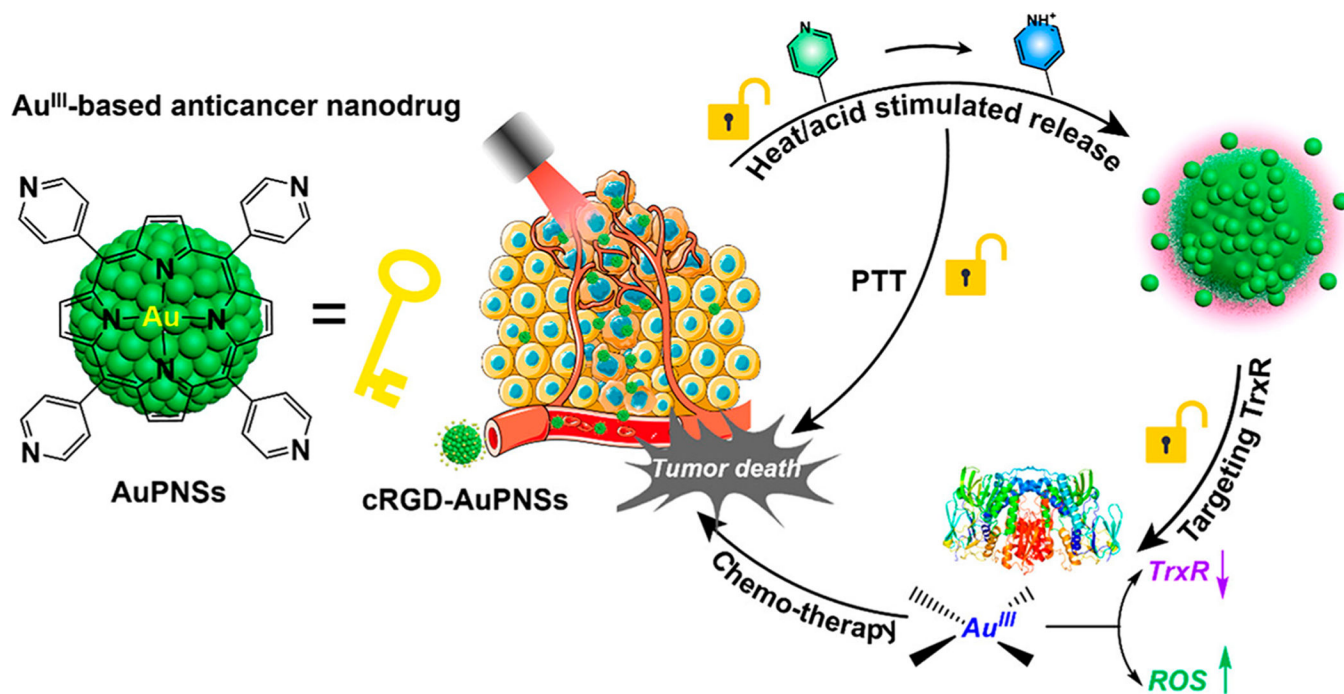


**Figure 30.**

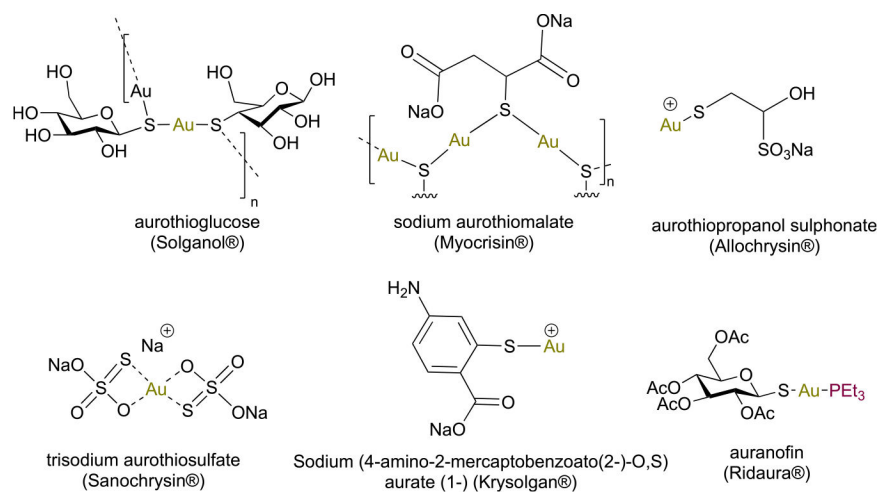
Development of the AFT-NP based Au(III) delivery system. (a) Loading of Au(III) into apoferritin. (b) Acquired SEM images of Aft nanocage and Aft-Au(III) NPs. (c) Aft and Aft-Au(III) NPs in glass vials. (d) Graph showing Au(III) release *in vitro* from the Aft-Au(III) NPs. (e) The ability of Aft-Au(III) NPs cells to target U87MG cells *in vitro* is assessed via ICP-MS analysis. (f) The intracellular uptake of Cy5.5-labeled Aft-Au(III) NPs by U87MG tumor cells is examined by confocal microscopy. (g) The intracellular uptake of Cy5.5-labeled Aft-Au(III) NPs by HL-7702 tumor cells is examined by confocal microscopy. Reproduced from ref 446. Copyright 2020 American Chemical Society.



**Figure 31.** Illustration of drug-loaded peptides and structures of drugs and peptides used in this study. Reproduced from ref 458. Copyright 2022 American Chemical Society.

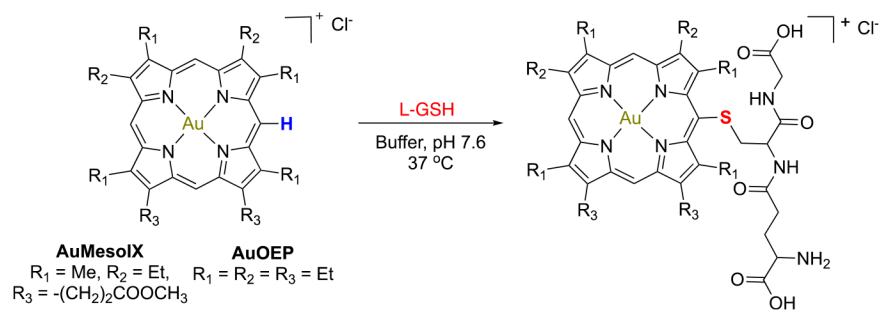


**Figure 32.** Schematic illustration of the noncovalent self-assembled Au(III) porphyrin and the heat/acid dual responsiveness of cRGD-AuPNSs for synergistic chemo-photothermal therapy of a tumor. Reproduced from ref 462. Copyright 2022 American Chemical Society.

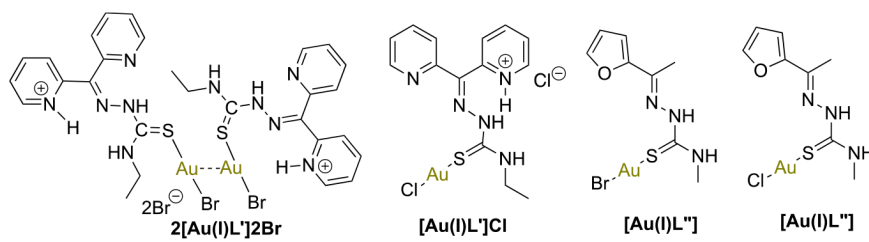


**Chart 1.**  
Clinically Used Gold Complexes

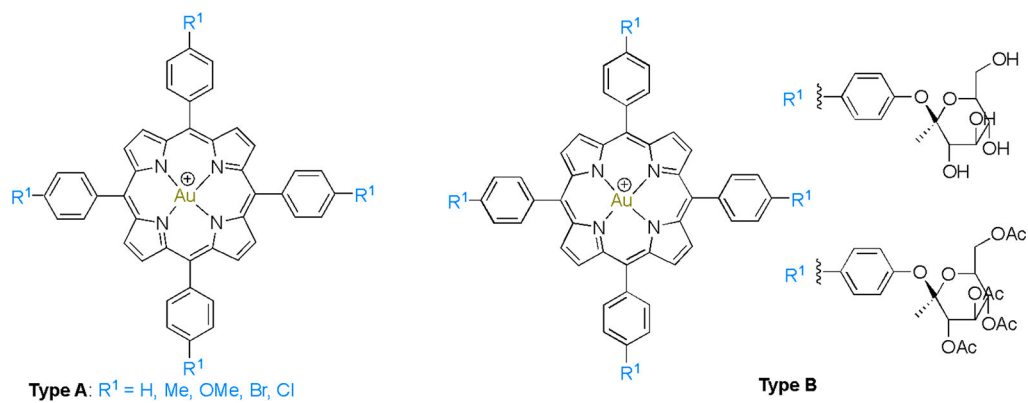




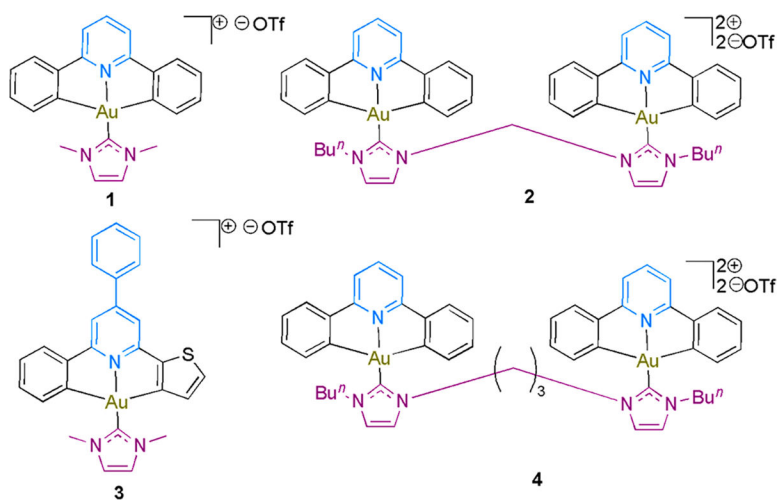
**Chart 2.**  
 Schematic Reaction for Bioconjugation of *meso*-Unsubstituted Gold(III) Porphyrins with GSH under Physiological Conditions



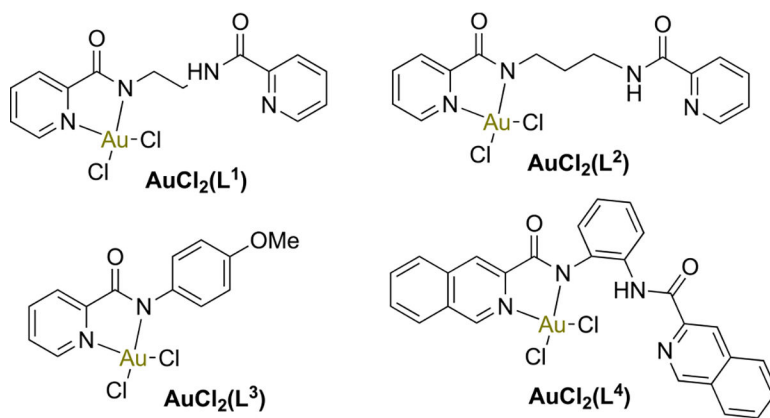
**Chart 3.**  
Chemical Structure of Au(I) Thiosemicarbazones



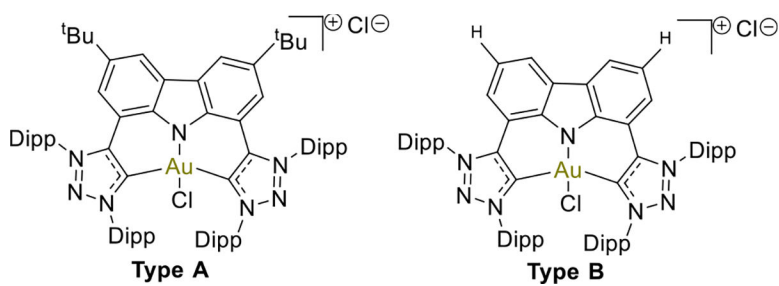
**Chart 4.**  
Chemical Structures of DNA Interfering Substituted Au(III) Tetraphenylporphyrin



**Chart 5.**  
Chemical Structures of  $[\text{Au}_n(\text{R}-\hat{\text{C}}\text{N}\hat{\text{C}})_n(\text{NHC})]^{n+}$  as Inhibitors of TopI

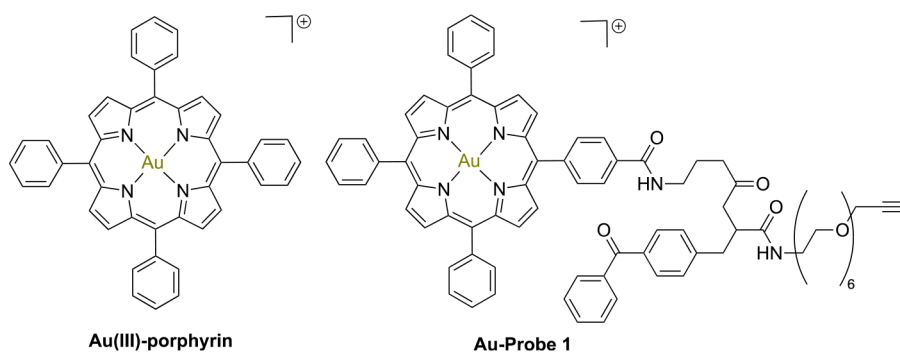


**Chart 6.**  
Chemical Structures of Pyridyl and Isoquinolylamido Au(III) Complexes

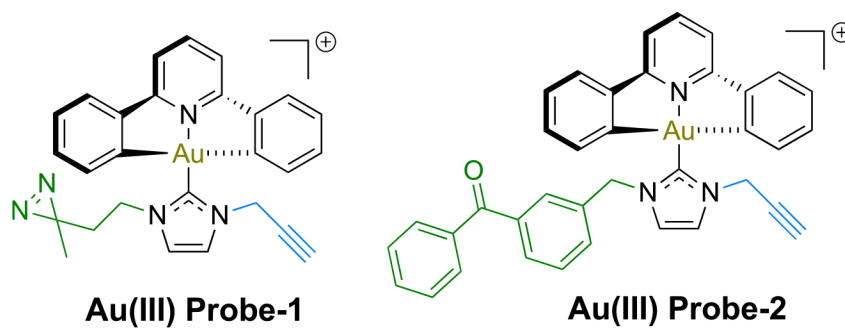


**Chart 7.**  
Chemical Structures of DNA Targeting Au(III) Pincer Complexes Supported by Carbazole Bis-carbene Ligands

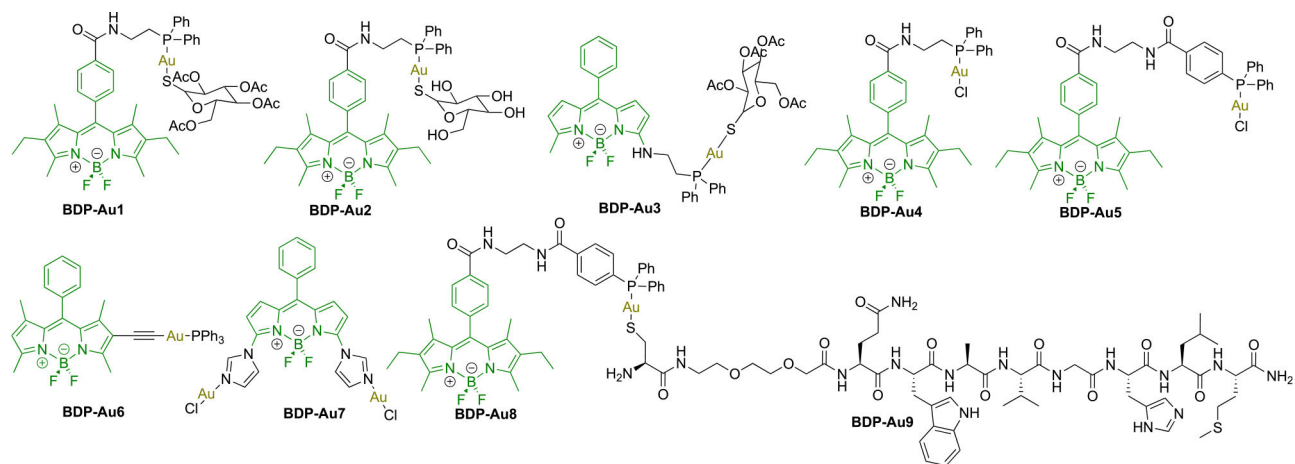




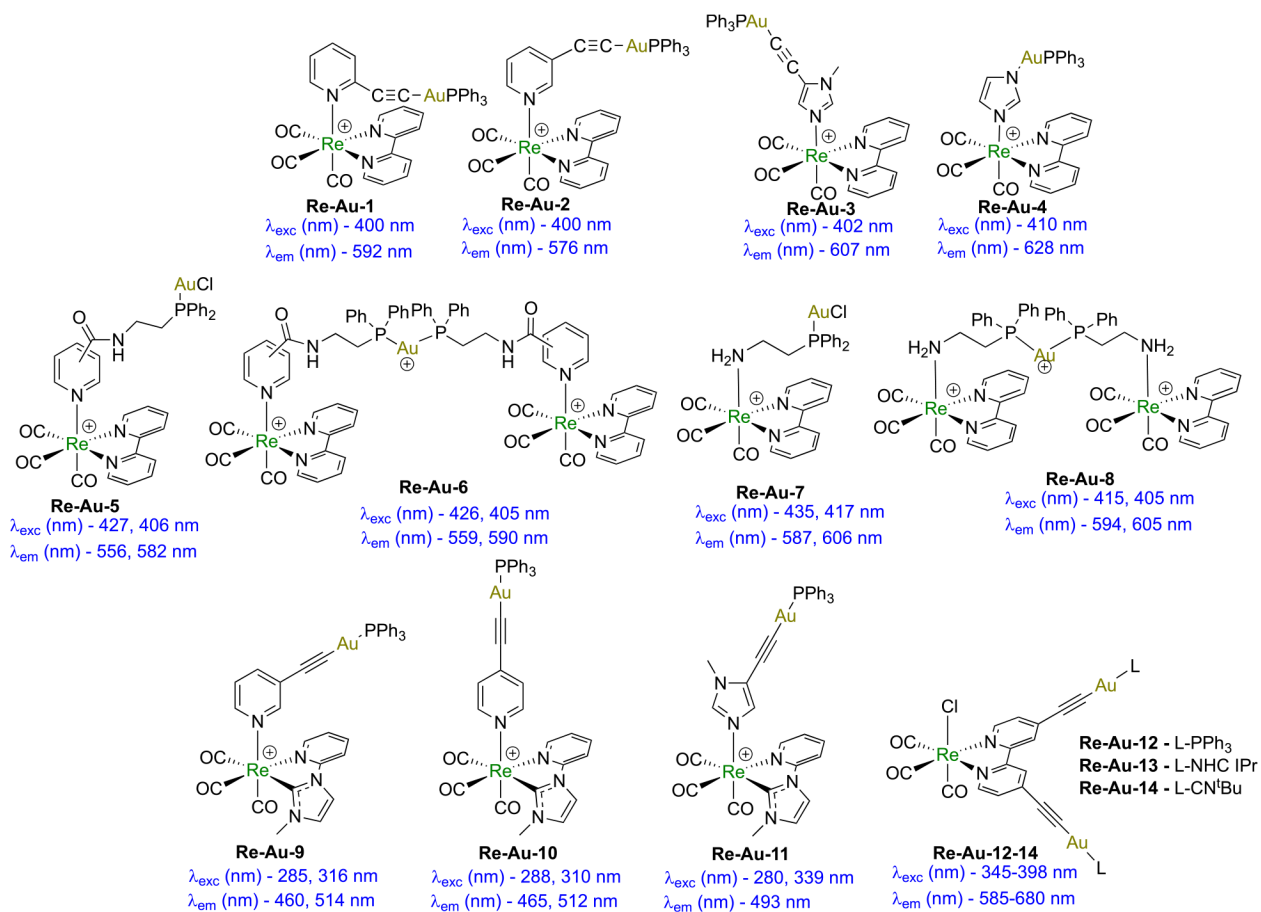
**Chart 8.**  
Benzophenone Photoaffinity Tag Au(III)-Porphyrin Probe



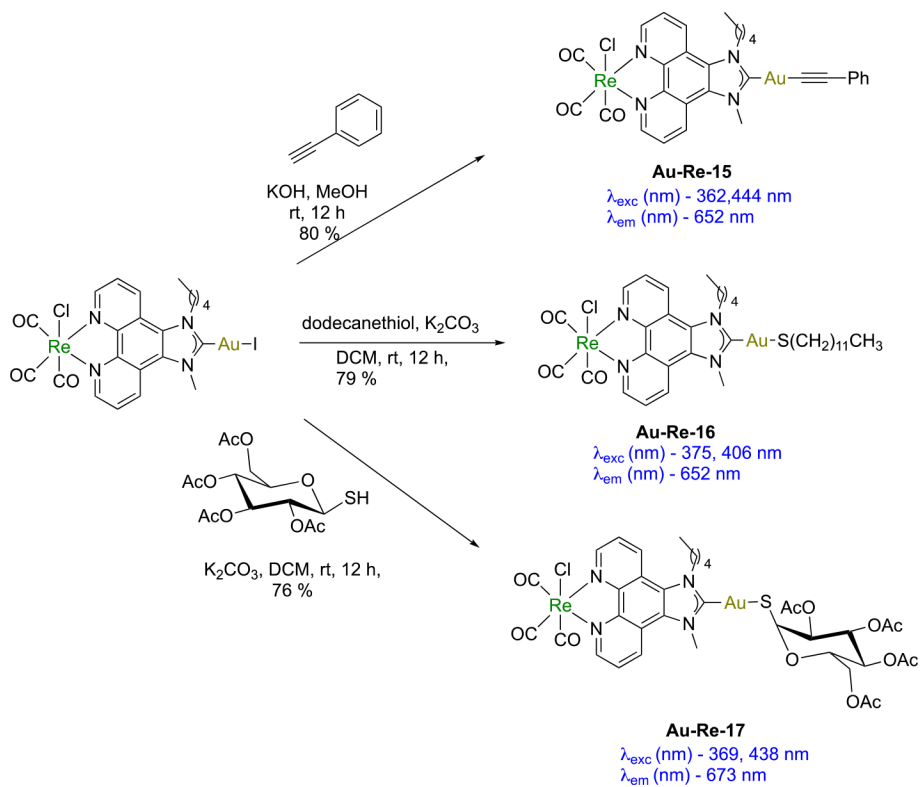
**Chart 9.**  
Chemical Structures of Some Au(III)-NHC Probes



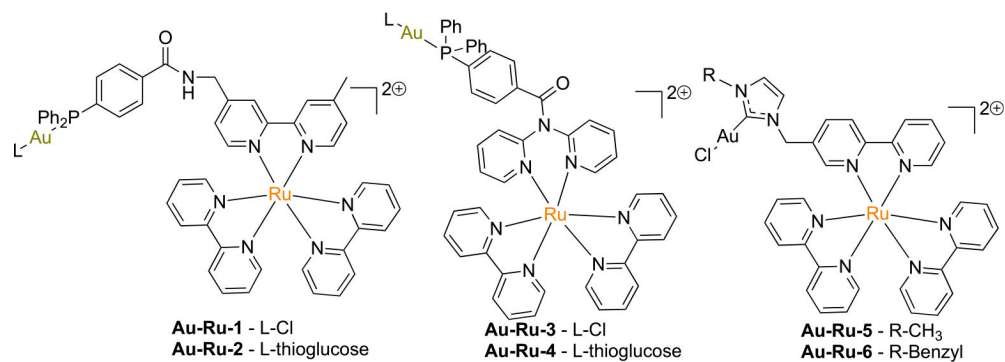
**Chart 10.**  
Chemical Structures of BODIPY Au(I) Probes



**Chart 11.**  
 Chemical Structures of Luminescent Re–Au Complexes

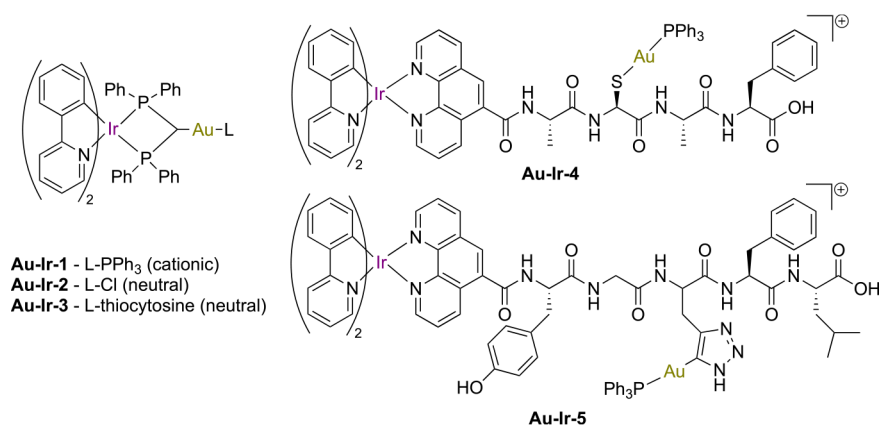


**Chart 12.**  
Reaction Scheme for Synthesis of Luminescent Re–Au Complexes Bearing NHC Ligands

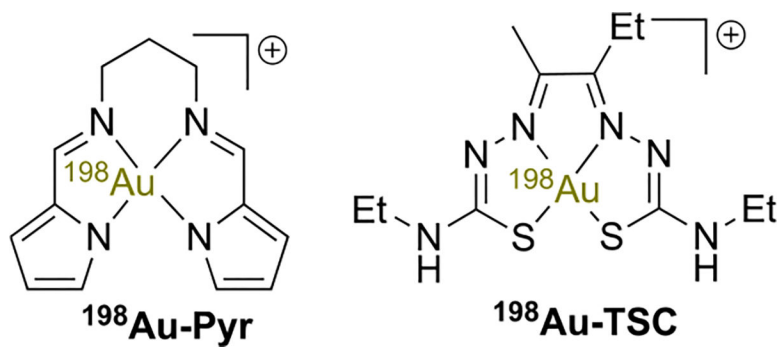


**Chart 13.**  
Chemical Structures of Luminescent Ru–Au Complexes

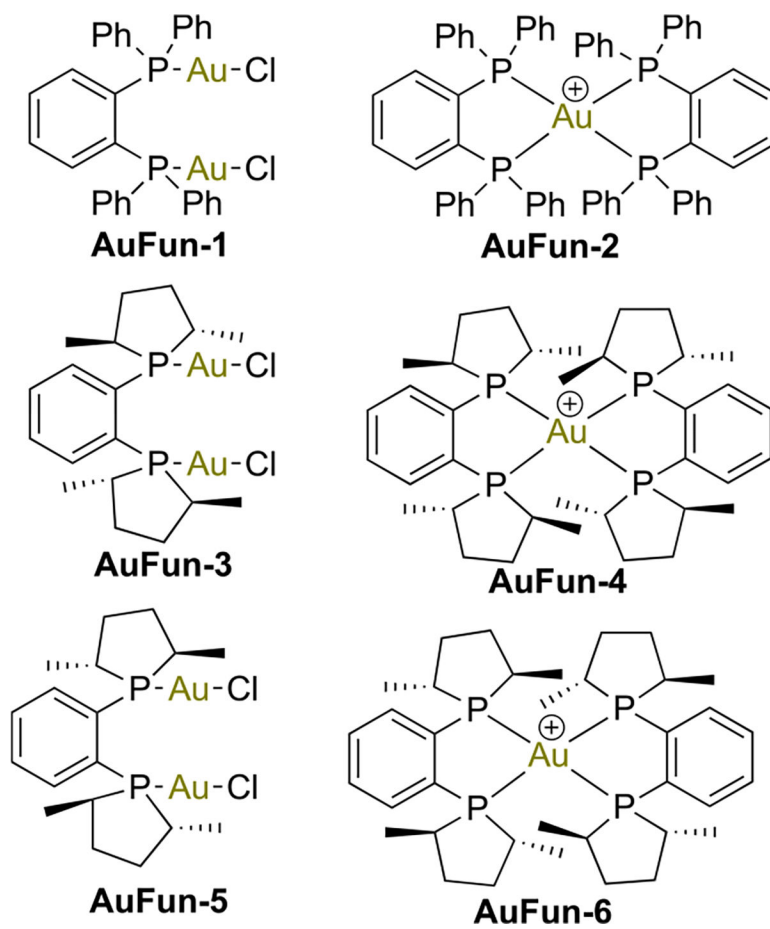




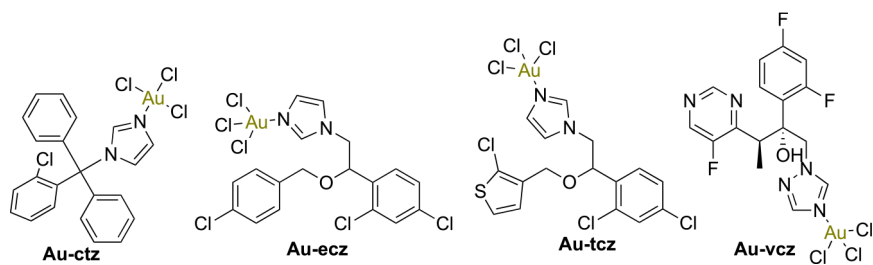
**Chart 14.**  
Chemical Structure of Phosphorescent Ir–Au Complexes



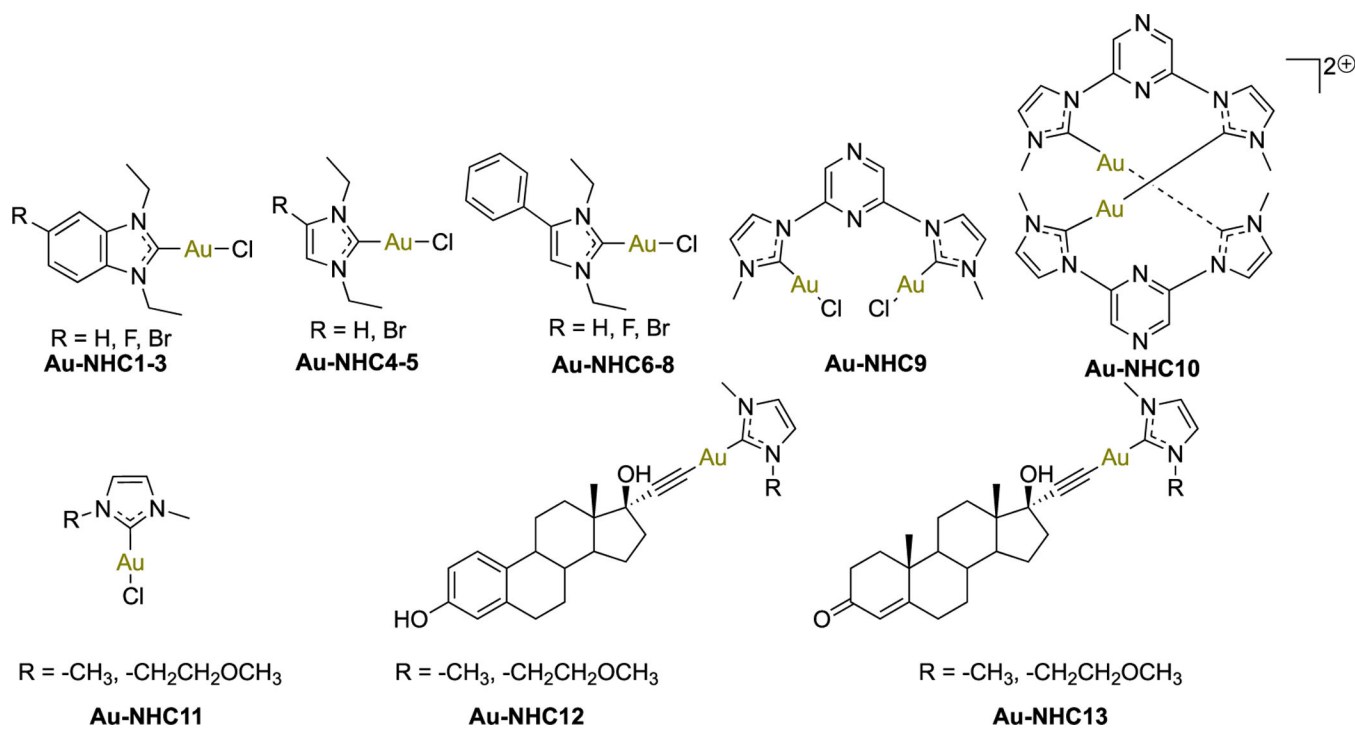
**Chart 15.**  
Chemical Structures of Some Radioactive Au(III) Complexes



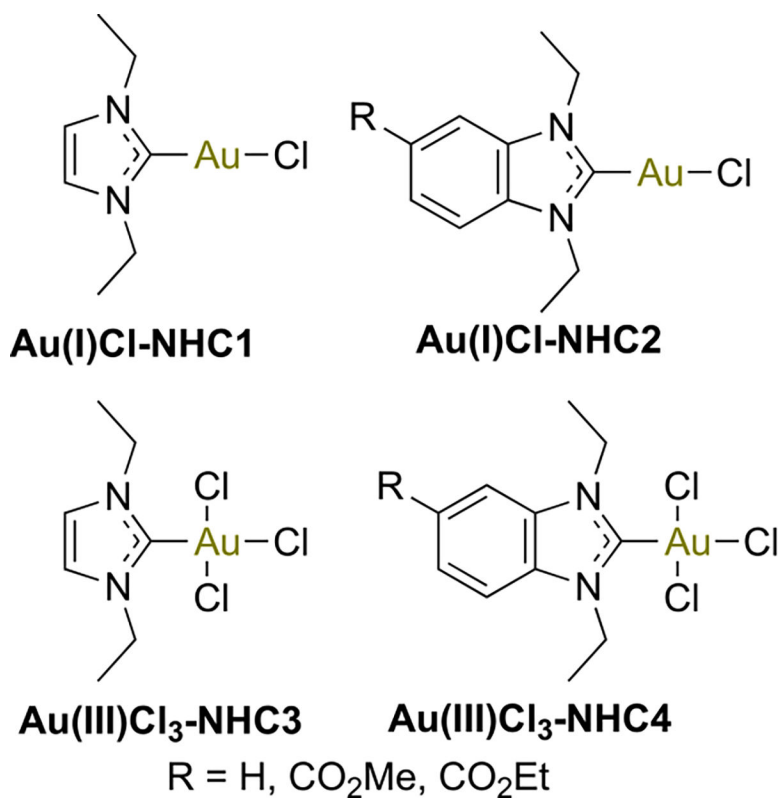
**Chart 16.**  
Chemical Structures of Bisphosphine-Au(I) Antifungal Complexes



**Chart 17.**  
Chemical Structures of Au(III)-Azoles

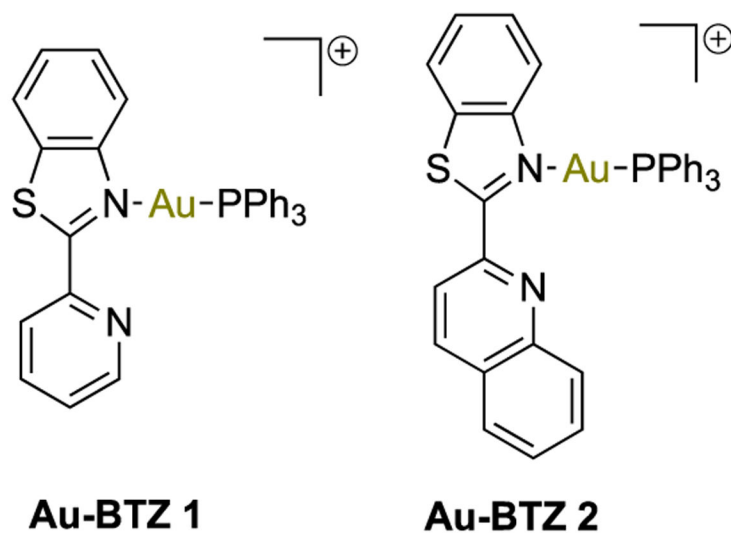


**Chart 18.**  
 Chemical Structures of Au(I)-NHC Complexes Studied for Their Antibacterial Activities

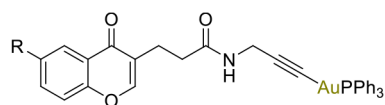


**Chart 19.**  
Chemical Structures of Au(I)/(III)-NHC Complexes Studied for Their Antibacterial Activities





**Chart 20.**  
Chemical Structures of Au(I) Benzothiazoles

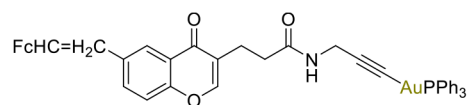
**Au-Chromone-1**

*S. aureus* subsp. *aureus* ATCCr 29213™ (MSSA) = 4 µg/mL

*S. aureus* subsp. *aureus* ATCCr 43300 (MRSA) = 2 µg/mL

*E. coli* ATCCr 25922 = > 256 µg/mL

*E. coli* ATCCrBAA-198 = > 256 µg/mL

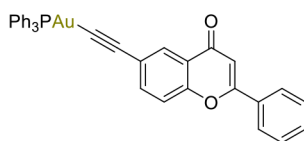
**Au-Chromone-2**

*S. aureus* subsp. *aureus* ATCCr 29213™ (MSSA) = 4 µg/mL

*S. aureus* subsp. *aureus* ATCCr 43300 (MRSA) = 2 µg/mL

*E. coli* ATCCr 25922 = > 256 µg/mL

*E. coli* ATCCrBAA-198 = > 256 µg/mL

**Au-flavone-3**

*S. aureus* subsp. *aureus* ATCCr 29213™ (MSSA) = 32 µg/mL

*S. aureus* subsp. *aureus* ATCCr 43300 (MRSA) = 2 µg/mL

*E. coli* ATCCr 25922 = > 256 µg/mL

*E. coli* ATCCrBAA-198 = > 256 µg/mL

**Cl-Au-PPh<sub>3</sub>****Au(I)TPP**

*S. aureus* subsp. *aureus* ATCCr 29213™ (MSSA) = 2 µg/mL

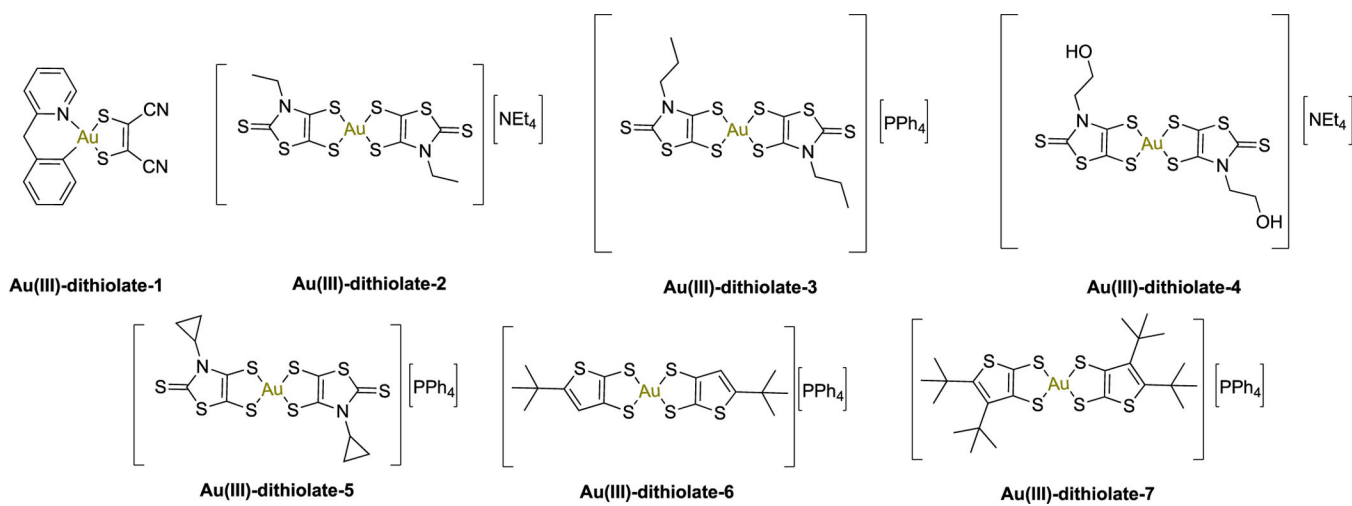
*S. aureus* subsp. *aureus* ATCCr 43300 (MRSA) = 1 µg/mL

*E. coli* ATCCr 25922 = 16 µg/mL

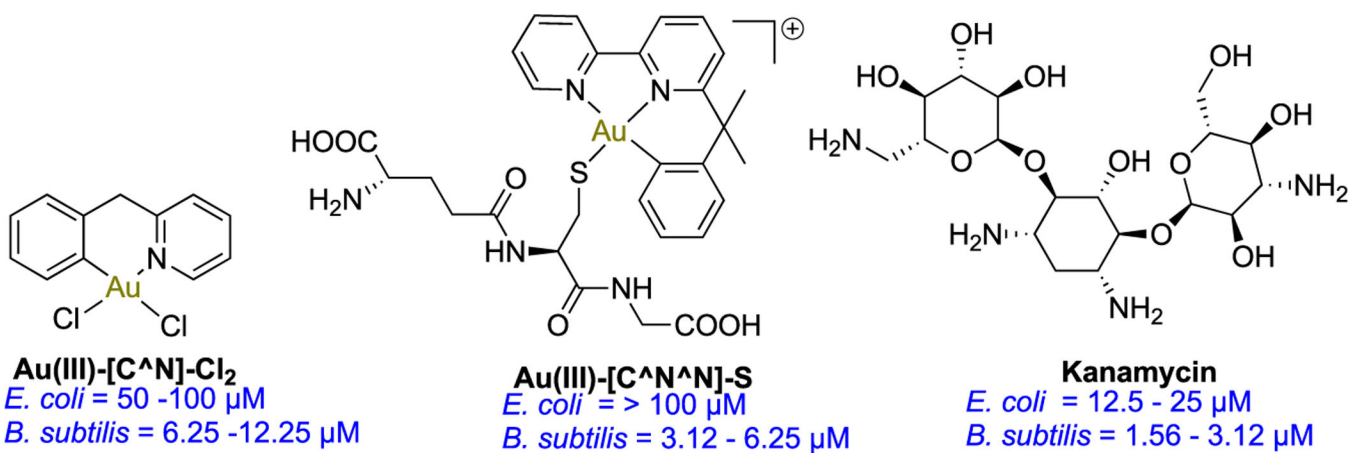
*E. coli* ATCCrBAA-198 = 32 µg/mL

**Chart 21.**

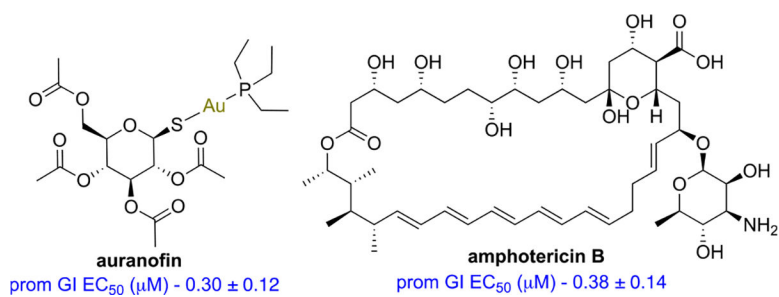
Chemical Structure of Alkynyl Au(I) Complexes and Their Antibacterial Activity

**Chart 22.**

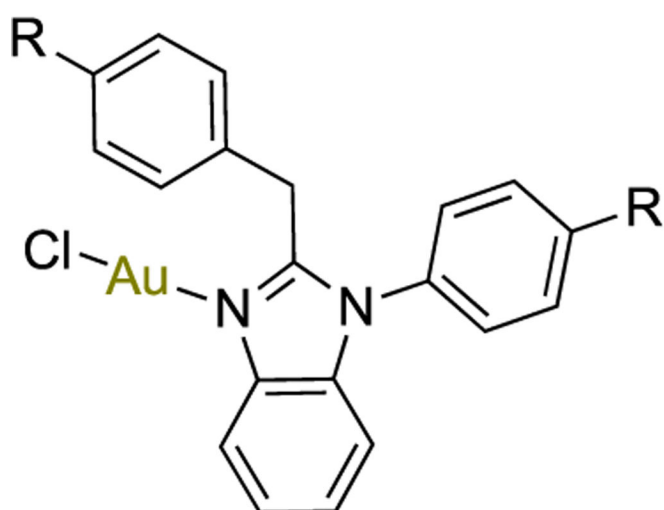
Chemical Structures of Au(III)-Dithiolate Studied for Their Antibacterial Activity



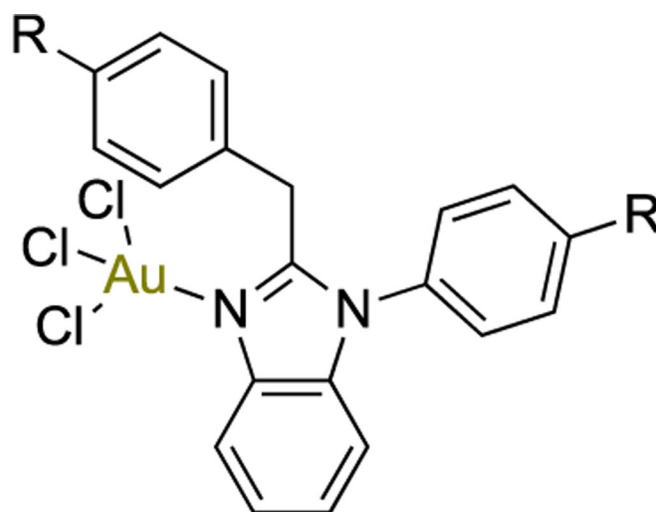
**Chart 23.**  
 Chemical Structure of Cyclometalated Au(III) Complexes and Kanamycin with Their Bactericidal Activity

**Chart 24.**

Chemical Structures and Antileishmanial Activity of Auranofin and Amphotericin B

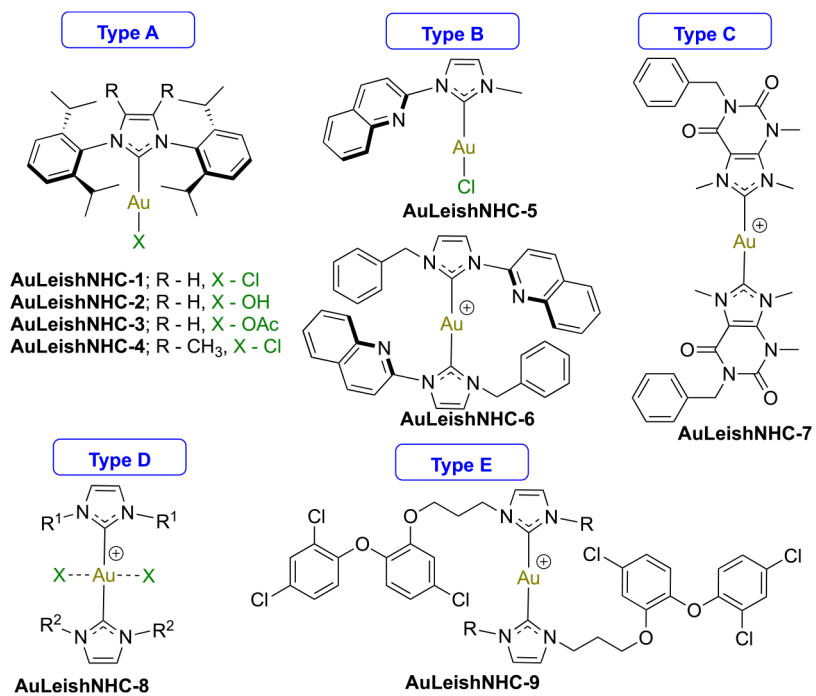


**AuBnz-1; R - H**  
**AuBnz-2; R - OCH<sub>3</sub>**



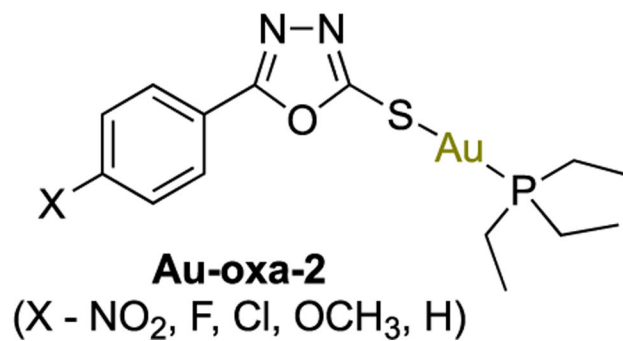
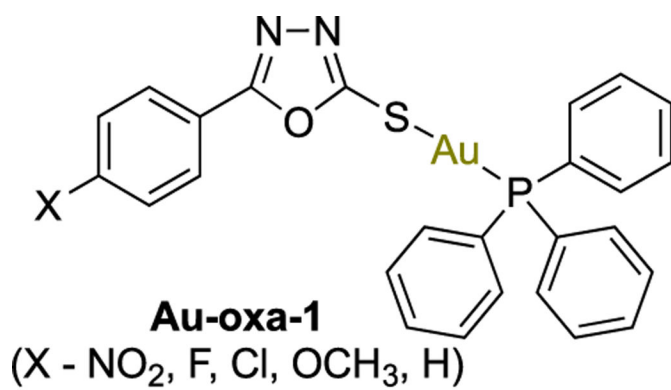
**AuBnz-3; R - H**  
**AuBnz-4; R - OCH<sub>3</sub>**

**Chart 25.**  
Chemical Structures of Benzimidazole Supported Au(I)/Au(III) Antileishmanial Agents

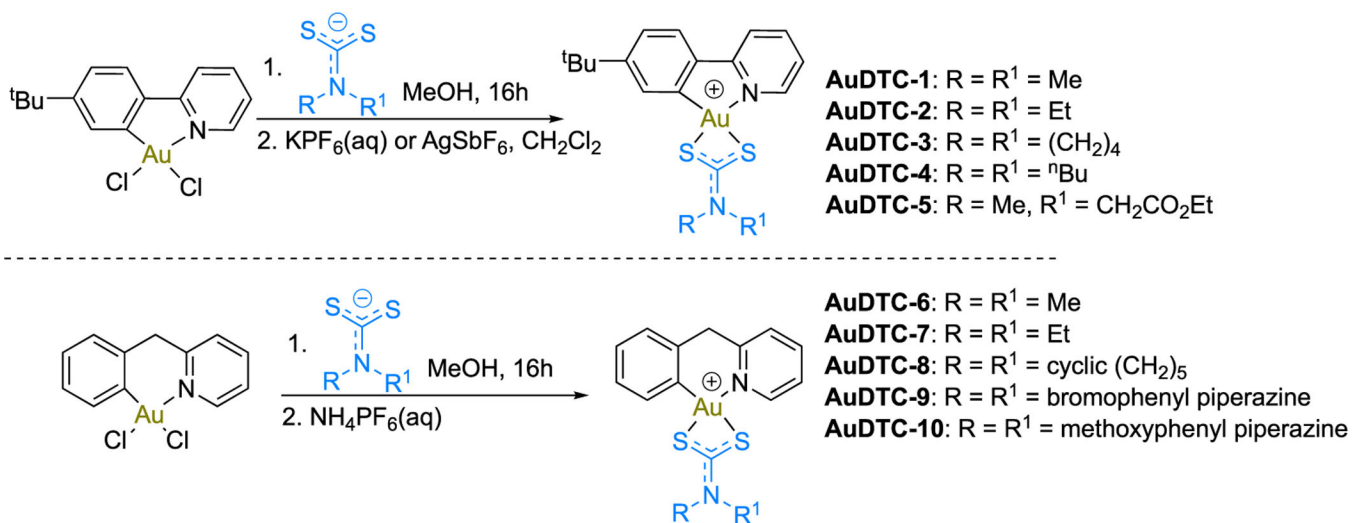


**Chart 26.**  
 Chemical Structures of Au(I)/Au(III)-NHC Antileishmanial Complexes

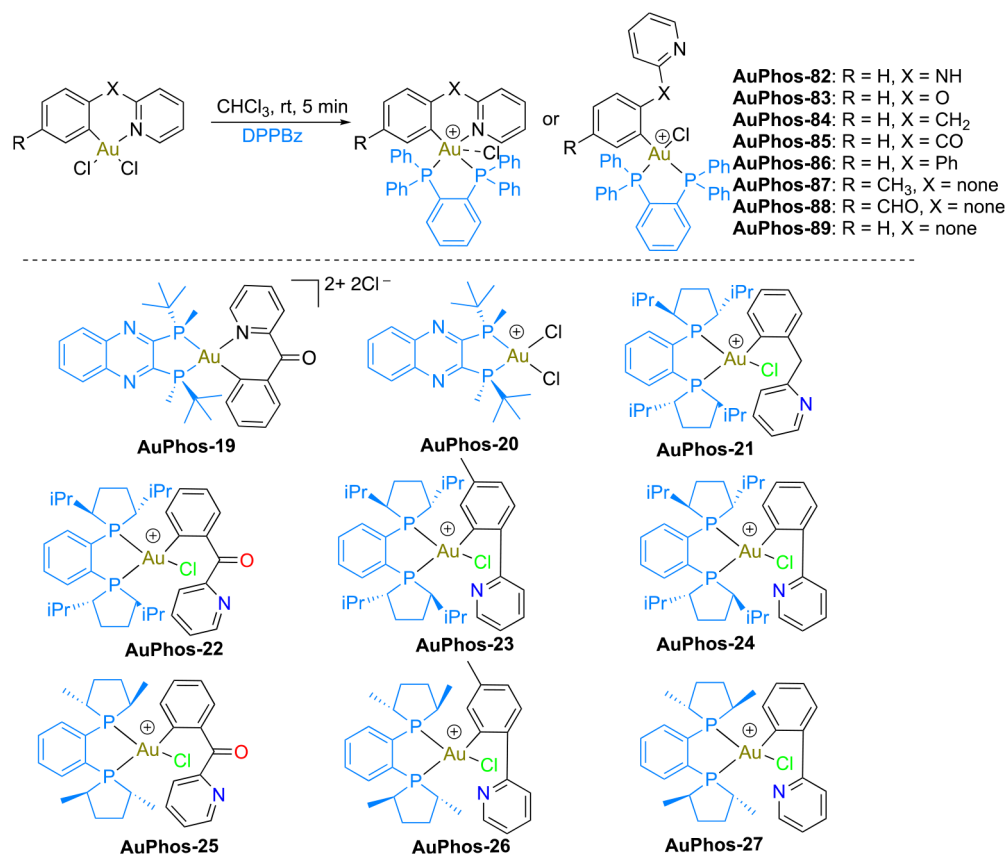




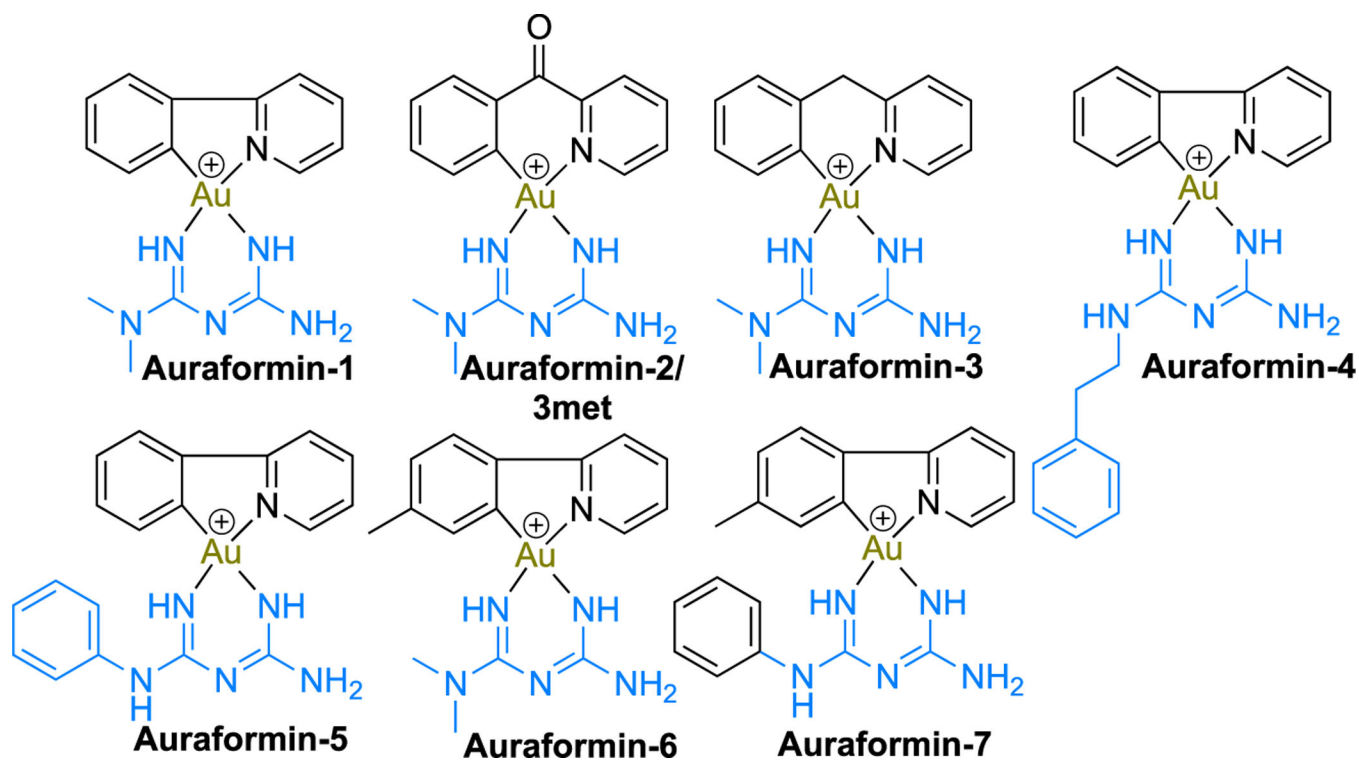
**Chart 27.**  
Chemical Structures of Au(I) Oxazole Complexes

**Chart 28.**

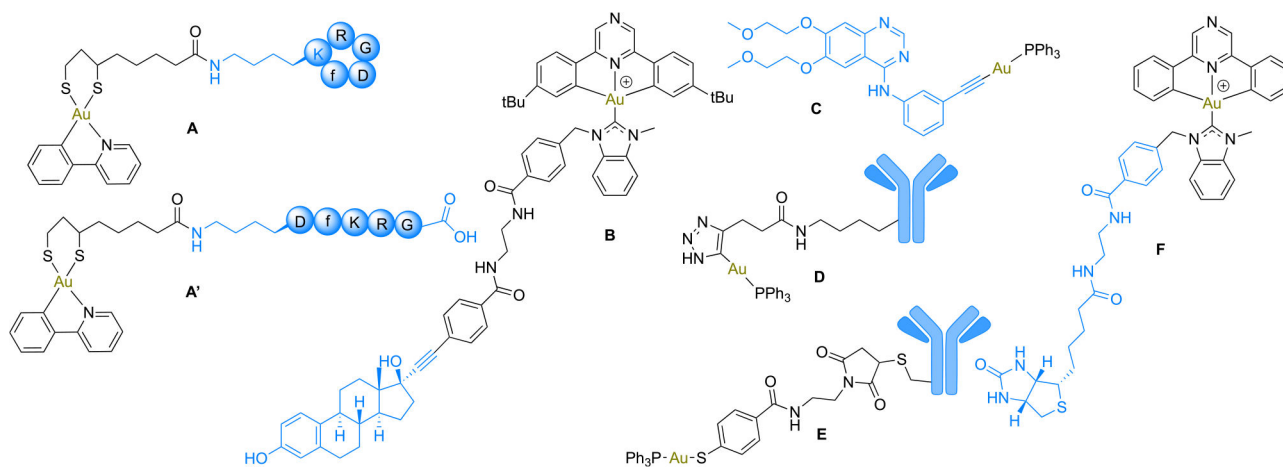
Synthetic Scheme to Obtain a Library of Gold(III) Dithiocarbamate Complexes



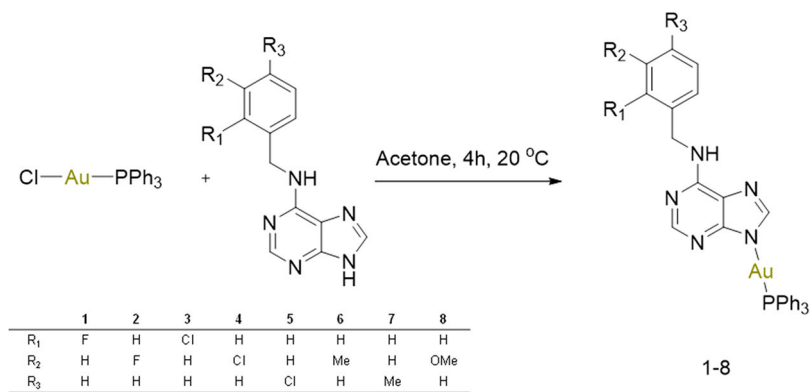
**Chart 29.**  
Synthetic Scheme and SAR Depicted Library of Cyclometalated Gold(III) Phosphine Complexes



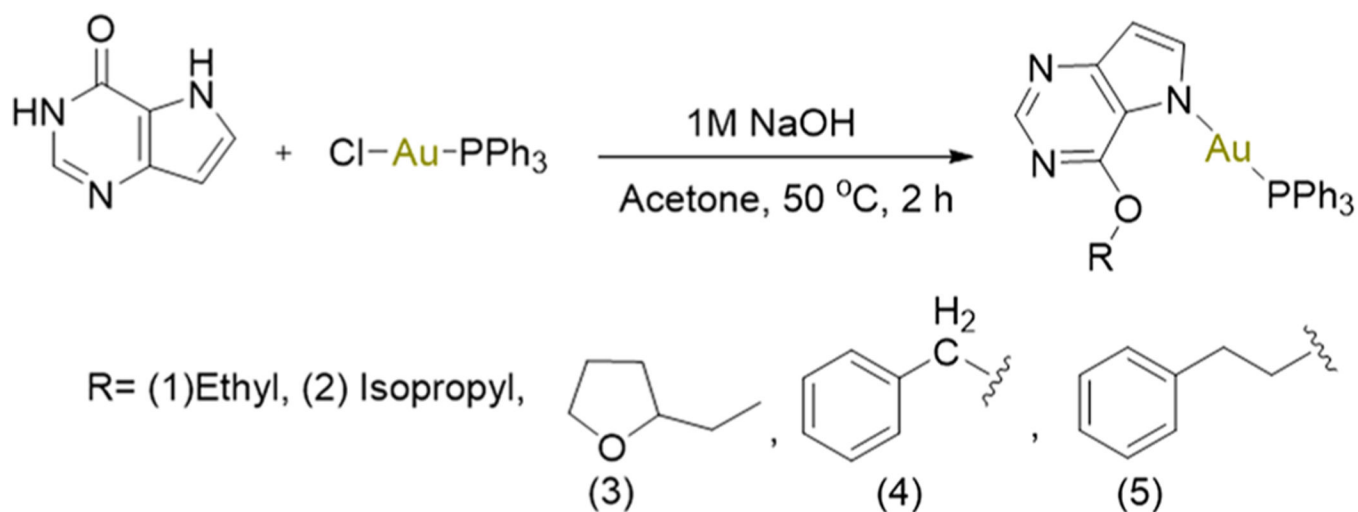
**Chart 30.**  
Cyclometalated Gold(III) Complexes Ligated to Metformin and Derivatives Thereof



**Chart 31.**  
Chemical Structures of Targeting Ligand Tethered Gold Agents



**Chart 32.**  
Synthetic Scheme and Structures of Gold Complexes Investigated for Anti-inflammatory Effects in Several Cancer Cell Lines

**Chart 33.**

Synthetic Scheme and Depiction of Au(I) Complexes Used for Anti-inflammatory Purposes



## Clinical Use of Gold Agents

Table 1.

Generic Name	Trade Name	Approval Granted	Mode of Administration	Indication
Auranofin	Ridaura	FDA, 1985	Oral	Rheumatoid arthritis
Aurothiosulfate	Sanochrysin	Abandoned 1931 due to toxicity	Intramuscular injection	Rheumatoid arthritis, tuberculosis
Aurothiopropr	Allochrysin	Approved by EULAR, no longer recommended for use	Intramuscular injection	Rheumatoid arthritis
Aurothiomalate	Myochrysin	Phase I (USA), approved United Kingdom	Oral	PKC $\epsilon$ , NSCLCs
Aurothioglucose	Solganol	Not approved	Oral	Rheumatoid arthritis

Table 2.

## Results from Clinical Trials of Auranofin in Different Disease Conditions

Rank	Title	Status	Study Result	Conditions	Interventions	Locations	References
1.	Oral Auranofin for Reduction of Latent Viral Reservoir in Patients with HIV Infection	Withdrawn	No Results Available	HIV	Drug: Auranofin	University of Miami - AIDS Clinical Research Unit, Miami, Florida, United States	293
2.	Auranofin PK Following Oral Dose Administration	Completed	No Results Available	Amoebiasis	Drug: Auranofin	Quintiles Phase I Services - Overland Park, Overland Park, Kansas, United States	294
3.	Auranofin in Treating Patients with Recurrent Epithelial Ovarian, Primary Peritoneal, or Fallopian Tube Cancer	Completed	No Results Available	Recurrent Fallopian Tube Cancer, Recurrent Ovarian Epithelial Cancer, Recurrent Primary Peritoneal Cavity Cancer	Drug: auranofin Other: laboratory biomarker analysis	Mayo Clinic, Rochester, Minnesota, United States	295
4.	Phase I and II Study of Auranofin in Chronic Lymphocytic Leukemia (CLL)	Completed	No Results Available	Chronic Lymphocytic Leukemia (CLL) Small Lymphocytic Lymphoma Leukemia, Prolymphocytic	Drug: auranofin	University of Kansas Cancer Center, Westwood, Kansas, United States	60
5.	Auranofin and Sirolimus in Treating Participants with Ovarian Cancer	Active, not recruiting	Has Results	Ovarian Serous Tumor Recurrent Ovarian Carcinoma Drug: Sirolimus	Drug: Auranofin Other: Laboratory Biomarker Analysis	Mayo Clinic, Rochester, Minnesota, United States	62
6.	Auranofin in Decreasing Pain in Patients with Paclitaxel-Induced Pain Syndrome	Completed	Has Results	Pain	Drug: auranofin Other: placebo Other: questionnaire administration	Mayo Clinic, Rochester, Minnesota, United States	296
7.	Auranofin for Giardia Protozoa	Completed	No Results Available	Amoebic Dysentery Giardiasis	Drug: Auranofin Other: Placebo	International Center for Diarrheal Disease Research Bangladesh - Parasitology, Dhaka, Bangladesh Rajshahi Medical College Hospital, Rajshahi 6000, Bangladesh	297
8.	Auranofin and Sirolimus in Treating Patients with Advanced Solid Tumors or Recurrent Non-Small Cell Lung Cancer	Withdrawn	No Results Available	Recurrent Non-small Cell Lung Cancer Unspecified Adult Solid Tumor, Protocol Specific	Drug: auranofin Drug: sirolimus Other: laboratory biomarker analysis Other: pharmacological study	Mayo Clinic in Florida, Jacksonville, Florida, United States	298
9.	Sirolimus and Auranofin in Treating Patients with Advanced or Recurrent Non-Small Cell Lung Cancer or Small Cell Lung Cancer	Recruiting	No Results Available	Extensive Stage Small Cell Lung Carcinoma Lung Adenocarcinoma Recurrent Non-Small Cell Lung Carcinoma Recurrent Small Cell Lung Carcinoma Squamous Cell Lung Carcinoma Stage IIIA Non-Small Cell Lung Cancer	Drug: Auranofin Drug: Sirolimus Other: Laboratory Biomarker Analysis Other: Pharmacological Study	Mayo Clinic in Arizona, Scottsdale, Arizona, United States Mayo Clinic, Jacksonville, Florida, United States	299

Rank	Title	Status	Study Result	Conditions	Interventions	Locations	References
10.	Multi Interventional Study Exploring HIV-1 Residual Replication: A Step Toward HIV-1 Eradication and Sterilizing Cure	Completed	No Results Available	Stage IIIB Non-Small Cell Lung Cancer Stage IV Non-Small Cell Lung Cancer Chronic Infection HIV	Drug: Maraviroc Drug: Dolutegravir Biological: Dendritic Cell Vaccine Drug: Auranofin Drug: Sirtuin Histone deacetylase inhibitor	CCDI, Sao Paulo, SP, Brazil	300
11	TB Host Directed Therapy	Unknown status	No Results Available	Tuberculosis	Biological: Dendritic Cell Vaccine Drug: Auranofin Drug: Sirtuin Histone deacetylase inhibitor Drug: Everolimus 0.5 MG Drug: Auranofin 6 MG Drug: Vitamin D3l Drug: CC-110501 Drug: ZHR6ZE/ 4HRb	The Aurum Institute: Tembisa Clinical Research Centre, Tembisa, Gauteng, South Africa	301
12.	A Proof-of-concept Clinical Trial Assessing the Safety of the Coordinated Undermining of Survival Paths by 9 Repurposed Drugs Combined with Metronomic Temozolomide (CUSP9x3 Treatment Protocol) for Recurrent Glioblastoma	Completed	No Results Available	Glioblastoma	Drug: Temozolomide Drug: Aprepitant Drug: Minocycline Drug: Disulfiram Drug: Celecoxib Drug: Sertaline Drug: Captopril Drug: Itraconazole Drug: Ritonavir Drug: Auranofin	University of Ulm School of Medicine, Ulm, Baden-Wuerttemberg, Germany	302
13.	Comparative Analysis of Outcomes Among Patients Initiating Xeljanz in Combination with Oral MTX Who Withdraw MTX Versus Continue MTX	Completed	Has Results	Rheumatoid Arthritis		Pfizer, New York, New York, United States	303
14.	An Observational Study of MabThera/ Rituxan (Rituximab) and Alternative TNF-Inhibitors in Patients with Rheumatoid Arthritis and an Inadequate Response to a Single Previous TNF-Inhibitor	Completed	Has Results	Rheumatoid Arthritis		Winnipeg, Manitoba, Canada Saint John, New Brunswick, Canada Brampton, Ontario Canada, and 212 other locations	304

Table 3.

## SAR of Aurano-fin and Antibacterial Activity

	<i>A. baumannii</i> NCTC 13420	<i>P. aeruginosa</i> NCTC 13437	<i>S. aureus</i> JE2 (USA300)	<i>E. faecium</i> ATCC 700221	<i>E. coli</i> ATCC 25922
Aur-1	47 (47)	377 (377)	0.04 (0.09)	0.2/0.09 (0.4)	24 (24)
Aur-2	47 (94)	377 (377)	0.04 (0.09)	0.2/0.4 (0.4)	24 (24)
Aur-3	24 (47)	189 (189)	0.04/0.09 (0.09)	0.09 (0.4)	12 (12)
Aur-4	82 (164)	>328	0.01 (0.01)	0.08 (0.2)	21 (21)
Aur-5	33 (33)	132 (132)	0.008 (0.06)	0.03/0.06 (0.1)	17 (17)
Aur-6	66 (132)	132 (132)	0.03 (0.1)	0.1 (0.3)	33 (33)
Aur-7	12 (12)	>194	0.003/0.006 (0.006)	0.05 (0.09)	24 (24)
Aur-8	76/19 (19)	>303	0.04/0.009 (0.1)	0.04/0.07 (0.3)	152/323 (152)
Aur-9	63/16 (251)	502 (502)	0.06/0.1 (0.5)	0.1 (2)	31 (31)
Aur-10	31 (31)	251 (251)	0.02 (0.1)	0.1/0.2 (0.5)	16 (16)
Aur-11	31 (63)	502 (502)	0.02/0.06 (0.1)	0.1/0.06 (0.5)	16 (16)
Aur-12	15/29 (116)	464 (464)	0.02 (0.05)	0.05/0.1 (0.5)	7/4 (7)
Aur-13	24/48 (190)	381 (381)	0.02/0.05 (0.09)	0.09 (0.4)	24 (24)
Aur-14	24 (24)	381 (381)	0.09/0.04 (0.09)	0.09/0.2 (0.4)	12 (12)
Aur-15	19/75 (>603)	302 (302)	0.02 (0.6)	0.6 (1)	151 (151)
Aur-16	18/36 (18)	291 (291)	0.009 (0.6)	0.02 (0.1)	36 (36)
Aur-17	18(18)	146 (146)	0.07/0.02 (0.07)	0.02 (0.1)	9 (9)
Aur-18	35 (35)	282 (282)	0.02 (0.3)	0.02/0.1 (0.3)	35 (35)
Aur-19	>546	>546	0.0004/0.02 (0.02)	0.06/0.1 (0.5)	>546
Aur-20	520 (>520)	>520	0.02/0.1 (0.2)	0.02 (0.2)	>520
Aur-21	10 (82)	41 (41)	0.03 (0.03)	0.2/0.3 (0.6)	10 (10)
Aur-22	19 (76)	305 (305)	0.005/0.02 (0.02)	0.1/0.3 (0.6)	76 (76)
Aur-23	37/74 (149)	149 (149)	0.009 (0.1)	0.6 (1)	74 (74)
Aur-24	7/13 (13)	52 (52)	0.1/0.2 (1.6)	0.4 (3)	7 (7)
Aur-25	11/23 (23)	92 (183)	0.001/0.02 (0.2)	0.09/0.2 (0.7)	23 (23)
Aur-26	74/147 (147)	74 (74)	2 (4)	5 (5)	>589
Aur-27	16/129 (518)	>518	1/2 (4)	4 (4)	>518
Aur-28	>438	>438	2 (3)	3 (3)	>438
Aur-29	29/58 (233)	>467	1/ (4)	2/4 (4)	>467

Author Manuscript

Author Manuscript

Author Manuscript

Author Manuscript

	<i>A. baumannii</i> NCTC 13420	<i>P. aeruginosa</i> NCTC 13437	<i>S. aureus</i> JE2 (USA300)	<i>E. faecium</i> ATCC 700221	<i>E. coli</i> ATCC 25922
Aur-30	>366	>366	3/1 (11)	>366	>366
Aur-31	6/13 (101)	101 (101)	0.1 (0.2)	0.2/0.4 (0.8)	6 (6)
Aur-32	84 (>336)	>336	3 (3)	3/5 (3)	>336
Aur-33	>311	>311	1/2 (2)	5 (5)	>311
Aur-34	>281	>281	1 (2)	2/4 (4)	>281
Aur-35	>292	>292	1 (2)	2/5 (5)	>292
Aur-36	>249	>249	4 (8)	31 (62)	>249
Aur-31	6/13 (101)	101 (101)	0.09 (0.2)	0.2/0.4(0.8)	6 (6)
Aur-37	17/4 (17)	>547	0.3/0.5 (1)	0.3/0.5 (0.5)	9 (9)
Aur-38	17/9 (17)	>547	0.3 (0.3)	0.3/0.5 (0.5)	9 (9)
Aur-39	16/8 (16)	>503	0.5 (0.5)	0.2/0.5 (0.5)	8/31 (31)
Aur-40	6/3 (23)	23/91 (91)	0.3 (0.7)	0.3 (0.3)	1/6 (11)

Table 4.

## Antileishmanial Activity of Au(I) Complexes

Compound	structure Cl—Au—L, where L =	prom GI EC <sub>50</sub> (μM)	prom tox EC <sub>50</sub> (μM)	<i>L. amazonensis</i> CBA EC <sub>50</sub> (μM)
AuLeish-1	P( <i>t</i> -Bu) <sub>2</sub> ( <i>p</i> -(N(CH <sub>3</sub> ) <sub>2</sub> )Ph)	0.11 ± 0.02	10.6 ± 0.4	0.2 ± 0.1
AuLeish-2	P(Cy) <sub>2</sub> ( <i>t</i> -Bu)	0.18 ± 0.07	NT <sup>a</sup>	0.7 ± 0.3
AuLeish-3	P(Ph)(C <sub>5</sub> H <sub>12</sub> ) <sub>2</sub>	0.3 ± 0.1	8.9 ± 0.7	0.23 ± 0.17
AuLeish-4	P( <i>t</i> -Bu) <sub>2</sub> ( <i>o</i> -(3,5-diphenyl-1 <i>H</i> -pyrazole)Ph)	0.37 ± 0.04	6.0 ± 3.0	0.8 ± 0.1
AuLeish-5	P(Et) <sub>3</sub>	0.39 ± 0.04	2.7 ± 0.9	0.27 ± 0.08
AuLeish-6	P(Ph) <sub>2</sub> (cy)	0.5 ± 0.1	8.2 ± 0.5	0.27 ± 0.03
AuLeish-7	P(Ph)(Et) <sub>2</sub>	0.6 ± 0.1	6.8 ± 0.5	0.22 ± 0.08
AuLeish-8	P(Ph) <sub>2</sub> ( <i>t</i> -Bu)	0.7 ± 0.1	11.8 ± 0.2	0.3 ± 0.2
AuLeish-9	P(Ph) <sub>2</sub> ( <i>i</i> -Pr)	0.8 ± 0.3	6.5 ± 1.0	0.17 ± 0.05
AuLeish-10	P(Ph) <sub>2</sub> (Et)	0.8 ± 0.1	7.0 ± 0.5	0.3 ± 0.1
AuLeish-11	P(Ph) <sub>3</sub>	1.3 ± 0.1	NT	0.5 ± 0.2
AuLeish-12	P(Ph)(Me) <sub>2</sub>	1.4 ± 0.2	8.9 ± 1.1	0.14 ± 0.03
AuLeish-13	P(cy) <sub>2</sub> ( <i>N,N</i> -dimethylaminobiphenyl)	1.5 ± 0.5	NT	0.18 ± 0.02
AuLeish-14	P(Ph) <sub>2</sub> (Bz)	2.1 ± 0.3	NT	0.6 ± 0.1
AuLeish-15	P(Ph)(CH <sub>2</sub> CH <sub>2</sub> CN) <sub>2</sub>	2.4 ± 0.2	NT	0.13 ± 0.02
AuLeish-16	P(Ph) <sub>2</sub> (4-biphenyl)	2.5 ± 0.2	10.2 ± 0.4	0.12 ± 0.02
AuLeish-17	P( <i>p</i> -FPh) <sub>3</sub>	3.0 ± 0.3	13.7 ± 0.4	0.2 ± 0.1
AuLeish-18	P(Ph) <sub>2</sub> (2-pyridine)	3.5 ± 0.6	13.6 ± 0.4	0.46 ± 0.02
AuLeish-19	P( <i>p</i> -(OCH <sub>3</sub> )Ph) <sub>3</sub>	3.8 ± 1.0	15.0 ± 0.1	0.2 ± 0.1
AuLeish-20	P(Ph) <sub>2</sub> ( <i>p</i> -(N(CH <sub>3</sub> ) <sub>2</sub> )Ph)	3.9 ± 1.3	NT	0.4 ± 0.2
AuLeish-21	P(Ph) <sub>2</sub> (CH <sub>2</sub> CH <sub>2</sub> NCOCH <sub>2</sub> CH <sub>2</sub> Ph)	4.2 ± 1.2	NT	0.16 ± 0.05
AuLeish-22	P(cy) <sub>3</sub>	4.4 ± 2.1	NT	0.5 ± 0.1
AuLeish-23	P( <i>p</i> -(CH <sub>3</sub> )Ph) <sub>3</sub>	4.6 ± 1.1	NT	0.5 ± 0.4
AuLeish-24	P(Ph) <sub>2</sub> (CH <sub>2</sub> CHCH <sub>2</sub> )	5.3 ± 1.1	NT	0.50 ± 0.04
AuLeish-25	P(Ph) <sub>2</sub> ( <i>p</i> -(NH <sub>2</sub> )Ph)	5.5 ± 0.2	>20	0.21 ± 0.04
AuLeish-26	P(Ph) <sub>2</sub> (CH <sub>2</sub> CH <sub>2</sub> NCOCH <sub>2</sub> Ph)	5.6 ± 0.3	>20	0.14 ± 0.06
AuLeish-27	P(2-furan) <sub>3</sub>	6.0 ± 0.9	NT	0.5 ± 0.2
AuLeish-28	P( <i>p</i> -ClPh) <sub>3</sub>	6.9 ± 1.3	NT	0.30 ± 0.04
AuLeish-29	P(Ph) <sub>2</sub> ( <i>p</i> -(CO <sub>2</sub> H)Ph)	7.6 ± 2.0	NT	0.40 ± 0.15
AuLeish-30	P(3,5-(CF <sub>3</sub> ) <sub>2</sub> Ph) <sub>3</sub>	9.4 ± 0.6	NT	0.4 ± 0.1
AuLeish-31	P(1-naphthalene) <sub>3</sub>	10.5 ± 0.9	NT	0.9 ± 0.2
AuLeish-32	P( <i>p</i> -(CF <sub>3</sub> )Ph) <sub>3</sub>	16.8 ± 7.0	NT	0.3 ± 0.1
AuLeish-33	P(Ph) <sub>2</sub> ( <i>m</i> -(SO <sub>3</sub> H)Ph)	17.4 ± 3.5	NT	0.6 ± 0.2
AuLeish-34	P(Cy) <sub>2</sub> ( <i>o</i> -Tol)	>20	NT	0.7 ± 0.3
AuLeish-35	P(Ph) <sub>2</sub> ( <i>m</i> -(CO <sub>2</sub> H)Ph)	>20	NT	0.15 ± 0.05

Compound	structure Cl—Au—L, where L =	prom GI EC <sub>50</sub> (μM)	prom tox EC <sub>50</sub> (μM)	<i>L. amazonensis</i> CBA EC <sub>50</sub> (μM)
<b>AuLeish-36</b>	P(Ph)( <i>p</i> -(SO <sub>3</sub> H)Ph) <sub>2</sub>	>20	NT	0.3 ± 0.1
<b>AuLeish-37</b>	P(CH <sub>2</sub> CH <sub>2</sub> COOH) <sub>3</sub>	>20	NT	0.70 ± 0.01
<b>AuLeish-38</b>	P( <i>p</i> -(SO <sub>3</sub> H)Ph) <sub>3</sub>	>20	NT	0.15 ± 0.02

<sup>a</sup> Antileishmanial activity of gold(I) compounds in *L. amazonensis* promastigote growth inhibition assays. Cl, chloride; prom, promastigote; GI, growth inhibition; tox, toxicity; CBA, cell-based amastigote; NT, not toxic or growth inhibitory. Data are presented as mean ± SD.

Author Manuscript

Author Manuscript

Author Manuscript

Author Manuscript



**Table 5.**

Inhibitory Values of Benzimidazole-Based Gold Complexes against Replication of Spike-ACE2

Complex	Spike-ACE2 (IC <sub>50</sub> $\mu$ M)	PLpro SARS-CoV-1 (IC <sub>50</sub> $\mu$ m)	PLpro SARS-CoV-2 (IC <sub>50</sub> $\mu$ m)
benzimidazole	>100	>100	>100
Chloroquine	31.9 $\pm$ 5.4	n.d.	n.d.
Disulfiram	n.d.	6.5 $\pm$ 0.4	1.05 $\pm$ 0.34
Auranofin	22.2 $\pm$ 2.8	25.5 $\pm$ 1.2	0.75 $\pm$ 0.13
Au-1	19.4 $\pm$ 5.7	6.3 $\pm$ 1.6	1.04 $\pm$ 0.02
Au-2	20.0 $\pm$ 2.3	5.5 $\pm$ 0.5	1.44 $\pm$ 0.22
Au-3	23.1 $\pm$ 6.8	14.2 $\pm$ 0.3	>100
Au-4	25.0 $\pm$ 4.2	14.1 $\pm$ 2.1	>50
Au-5	16.2 $\pm$ 2.4	6.7 $\pm$ 0.9	0.96 $\pm$ 0.07